Fast Radio Bursts

Kunihito Ioka (YITP, Kyoto U.)

井岡 邦仁 (京大基研)

Takahashi, KI, Mori & Funahashi 21

Shirasaki, Takahashi, Osato & KI 21

YUKAWA INSTITUTE FOR THEORETICAL PHYSICS

Center for Gravitational Physics
Yukawa Institute for Theoretical Physics

Contents

Fast Radio Bursts (FRB)

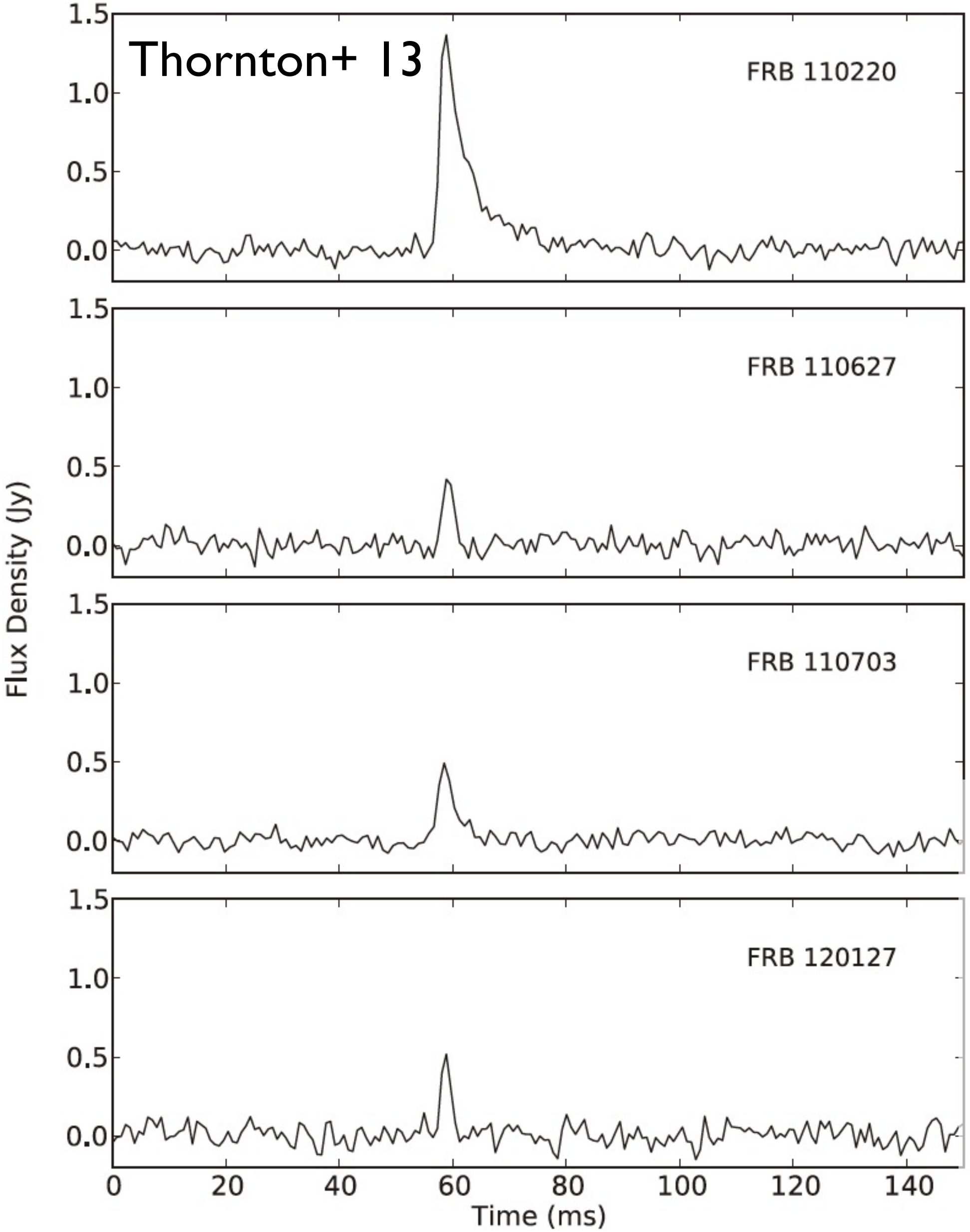

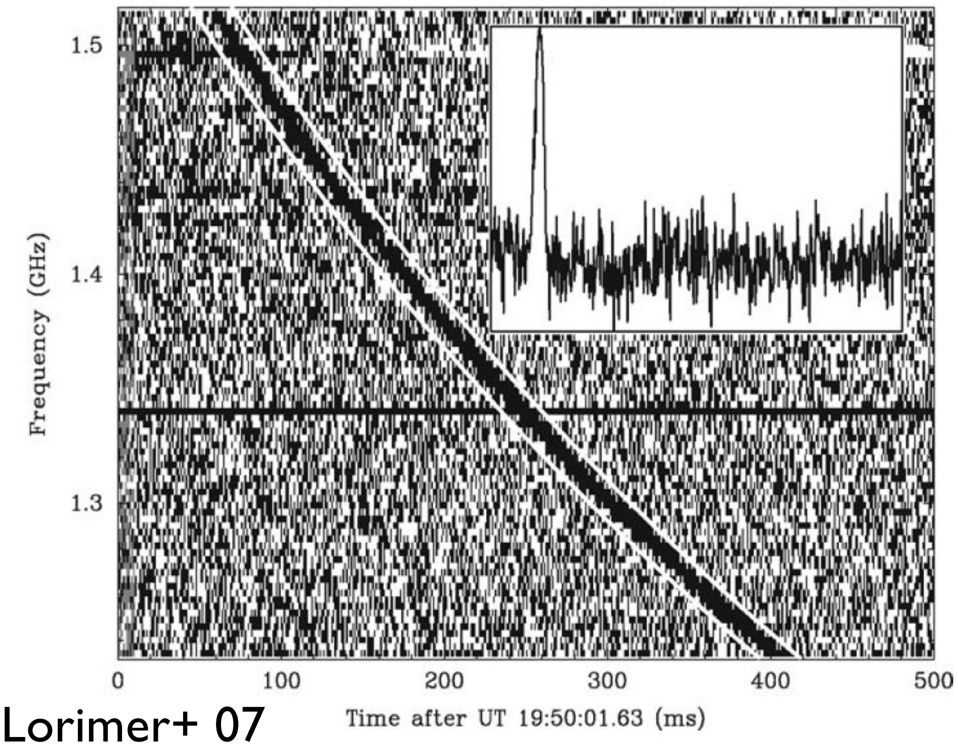

Lorimer+ 07

Most luminous radio transients discovered in 2007

Brightness Temperature

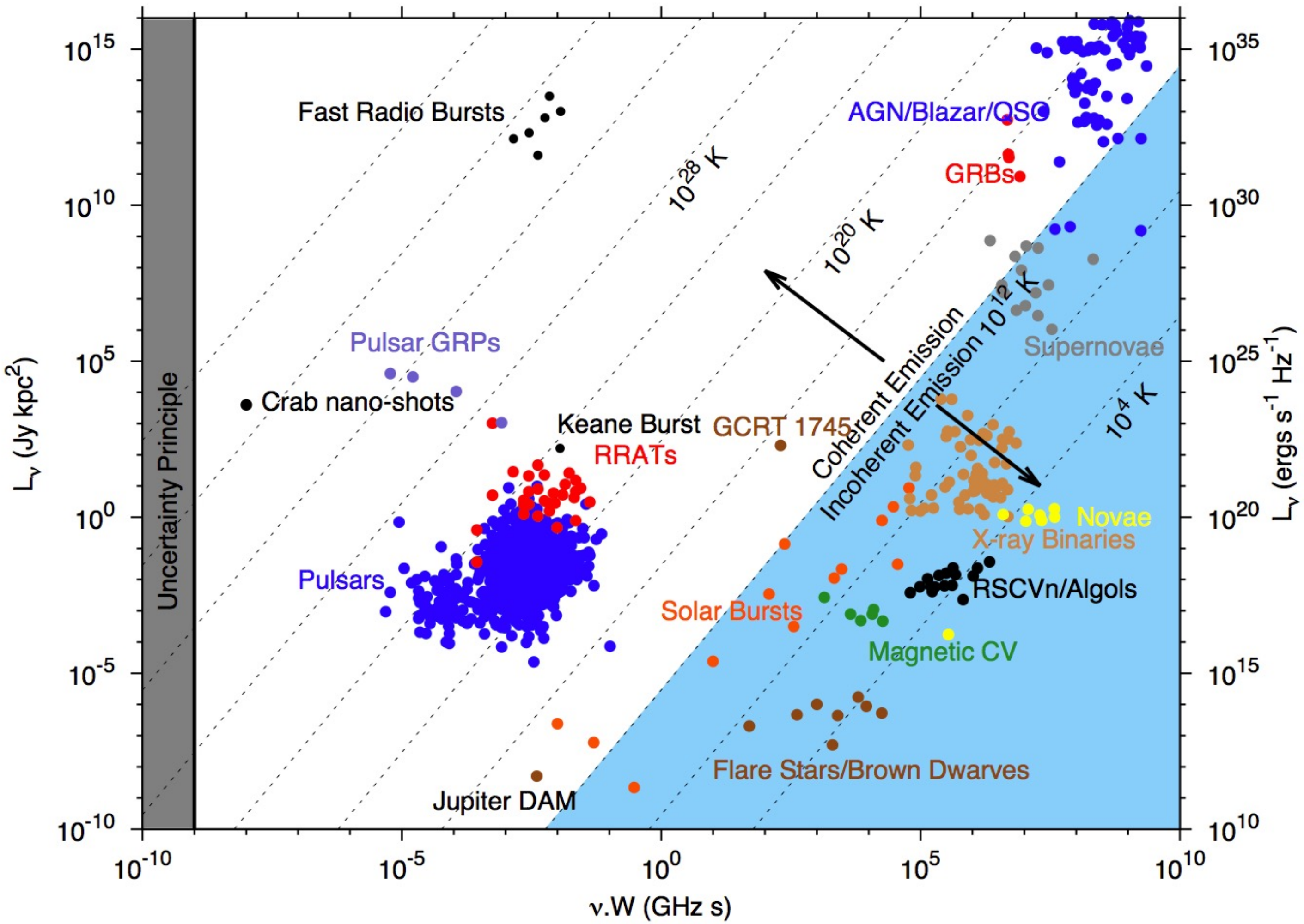

Pietka+ 14

$$T' = \frac{c^2 I_\nu}{2\nu^2 k\Gamma} > 10^{35}\,\mathrm{K}\,\frac{F_{\nu,\mathrm{Jy}}\, d_{\mathrm{Gpc}}^2}{\Delta t_{\mathrm{ms}}^2 \nu_{\mathrm{GHz}}^2 \Gamma^3}$$

Coherent ($T'>10^{12}$K) unless $\Gamma>10^8$

Coherent Emission

$$P_N = \left| \sum_{k=1}^{N} E_k e^{i\phi_k} \right|^2$$

$$= N\,|E|^2 + |E|^2 \sum_{k \neq j} e^{i(\phi_k - \phi_j)}$$

Incoherent

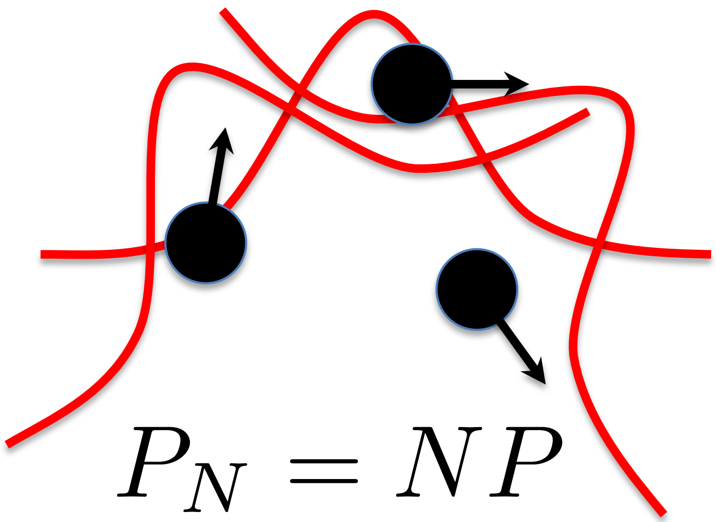

$$P_N = NP$$

Coherent

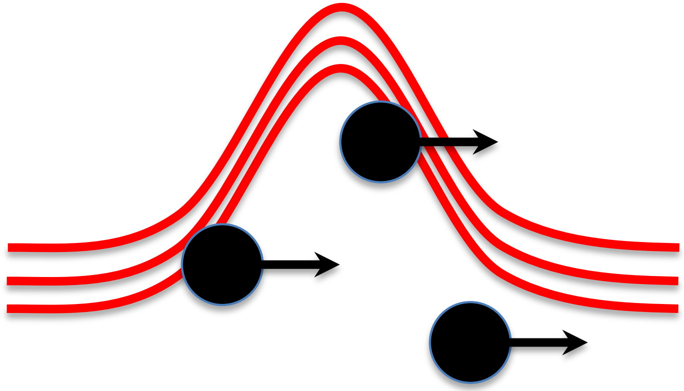

$$P_N = N^2 P$$

Possible Origins

- ***Perytons*** Burke-Spolaor+ 11; Kulkarni+ 14
- ***Galactic***
  - Nearby flaring star Loeb+ 13
  - RRAT (Rotating Radio Transient; intermittent pulsar)
- ***Extragalactic***
  - Magnetar giant flare Popov & Postnov 07; Thornton+ 13; Lyubarsky 14; Penn & Conner 15
  - NS-NS merger Hansen & Lyutikov 01; Totani 13
  - WD-WD merger Kashiyama+ 13
  - Collapse of hypermassive NS Falcke & Rezzolla 13; Zhang 13
  - Supernova into a nearby star Colgate+ 71,75; Egorov & Postnov 09
  - Supergiant pulse Cordes & Wasserman 15
  - Pulsar-orbiting bodies Mottez & Zarka 14

Possible Exotics

- Evaporation of BH Rees 77; Blandford 77; Kavic+ 08; Keane+ 12
- PBH to white hole Barrau+ 14
- Superconducting cosmic strings Cai+ 12;Yu+ 14
- Axion stars Iwazaki+ 14;Tkachev+ 14
- …

FRB Events are Growing

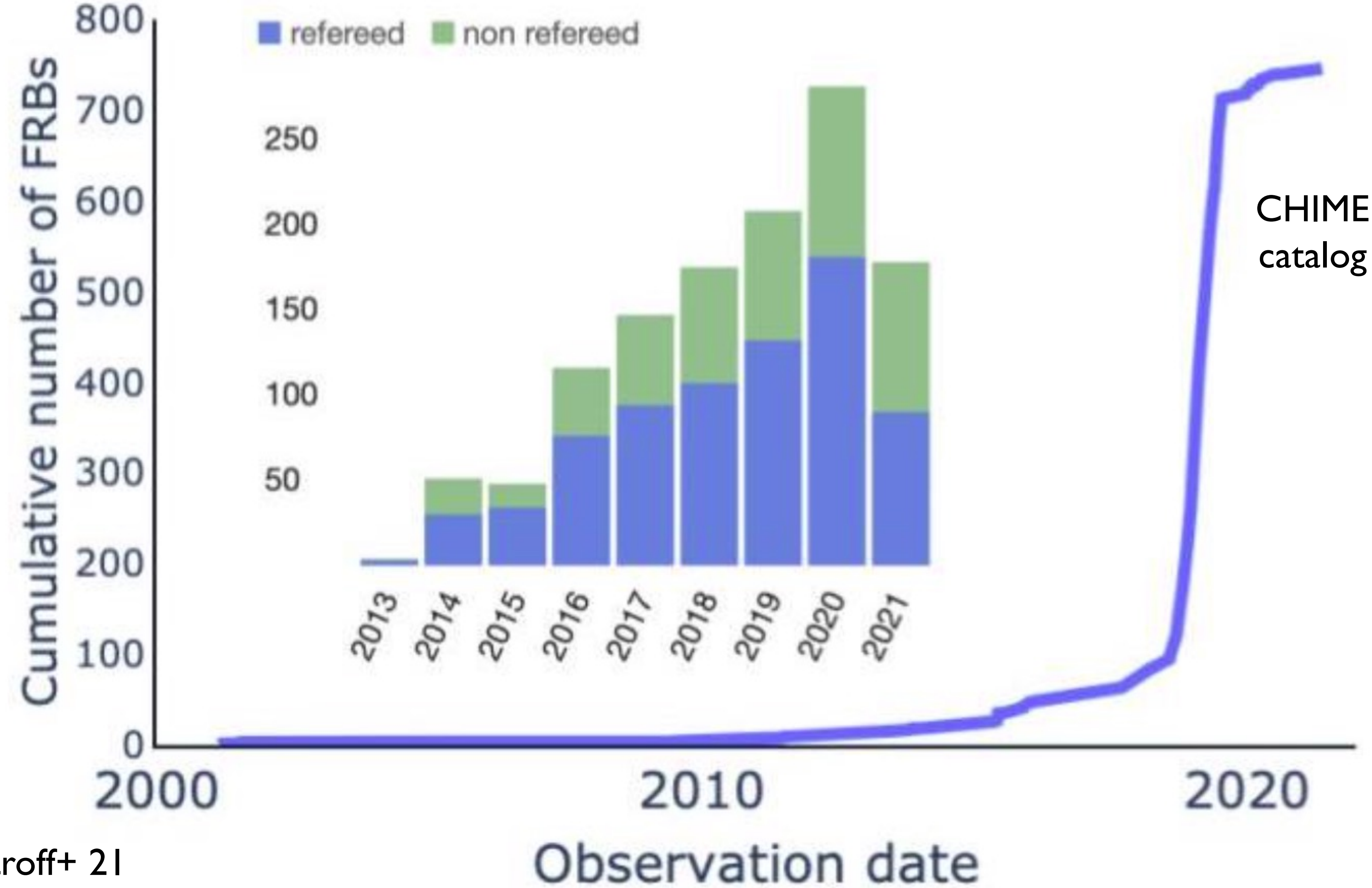

CHIME catalog

Petroff+ 21

FRB Science will Grow

CHORD (CHIME upgrade)

DSA-2000

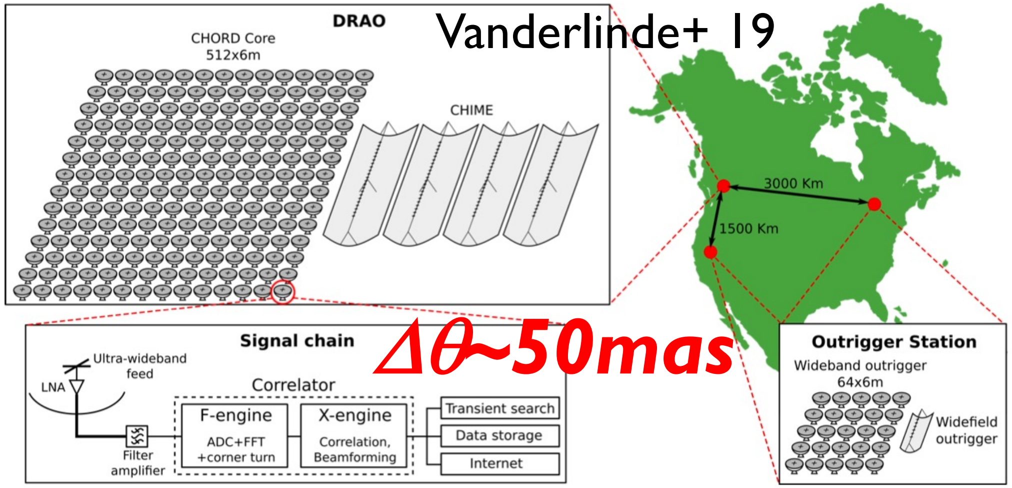

Δθ~50mas

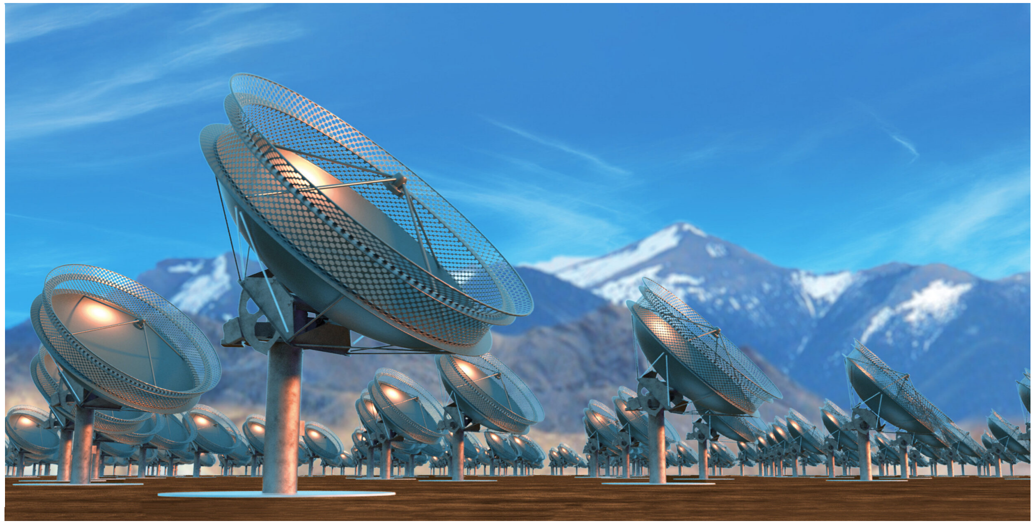

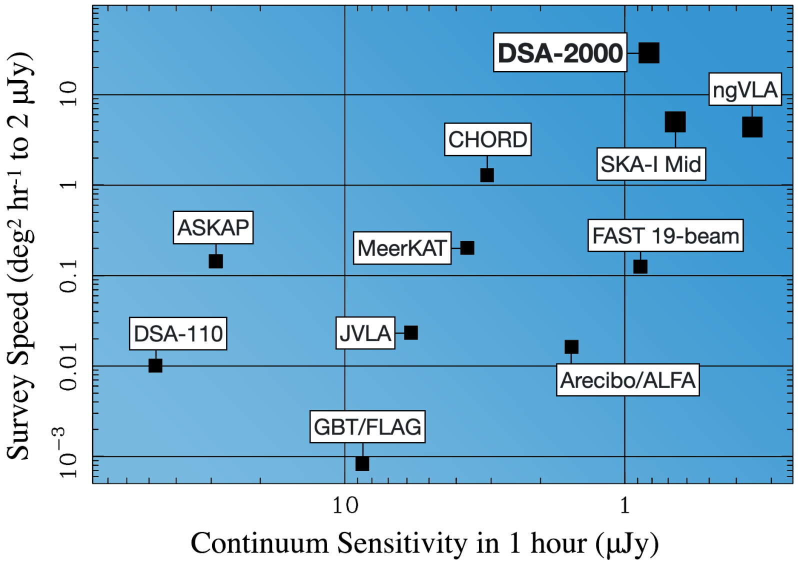

1000s FRBs/yr

Δθ~3.5 arcsec

→ FRB cosmology!

~18年前

GRB Cosmology

Massive star origin ⇒ High redshift GRBs

Like QSO
Like Supernova
Star formation
Reionization
Metal, Dust
Dark energy
…

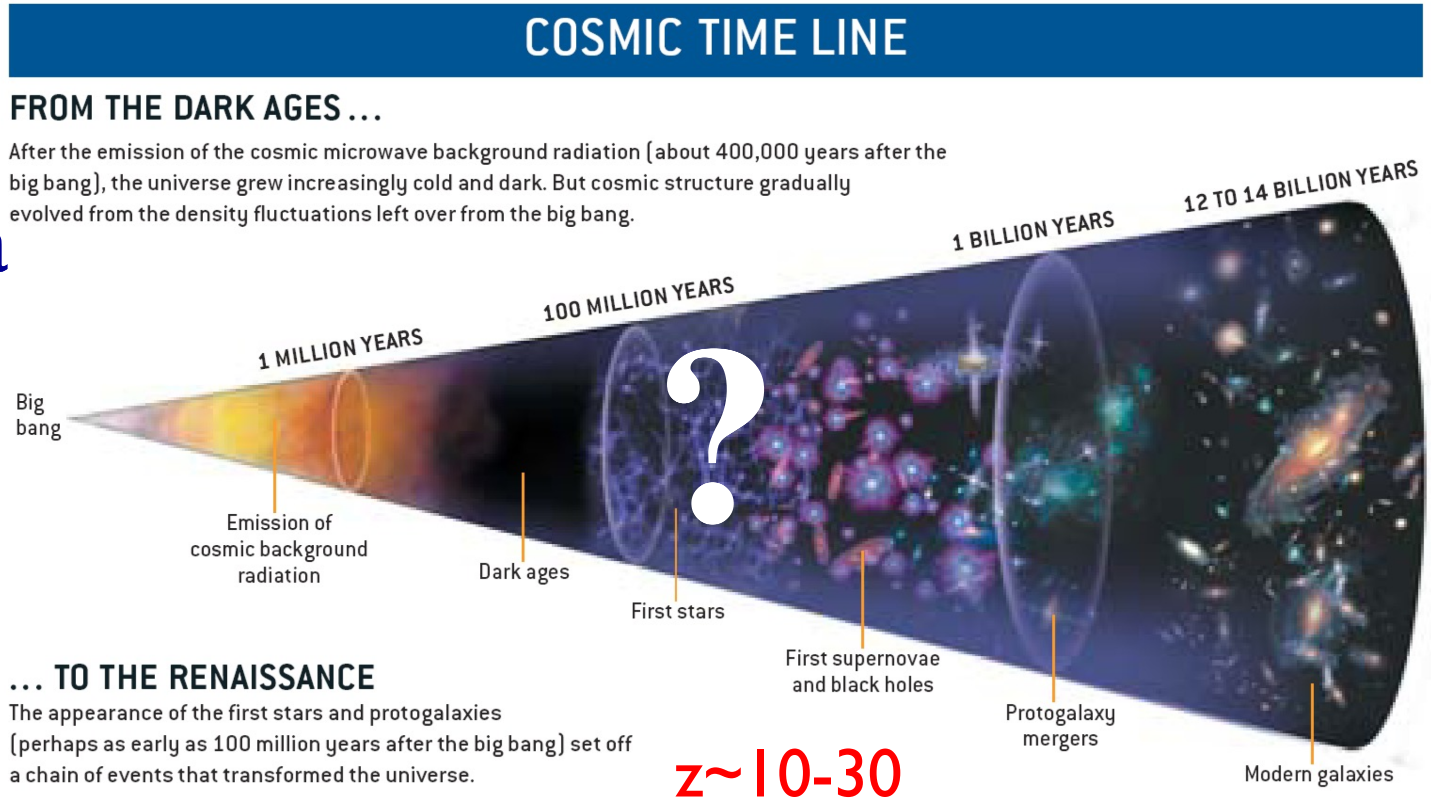

Larson & Bromm 02

z~10-30

GRB ⟷

z~8

QSO, galaxy ⟷

GRBs are useful for probing high-z

Radio Dispersion

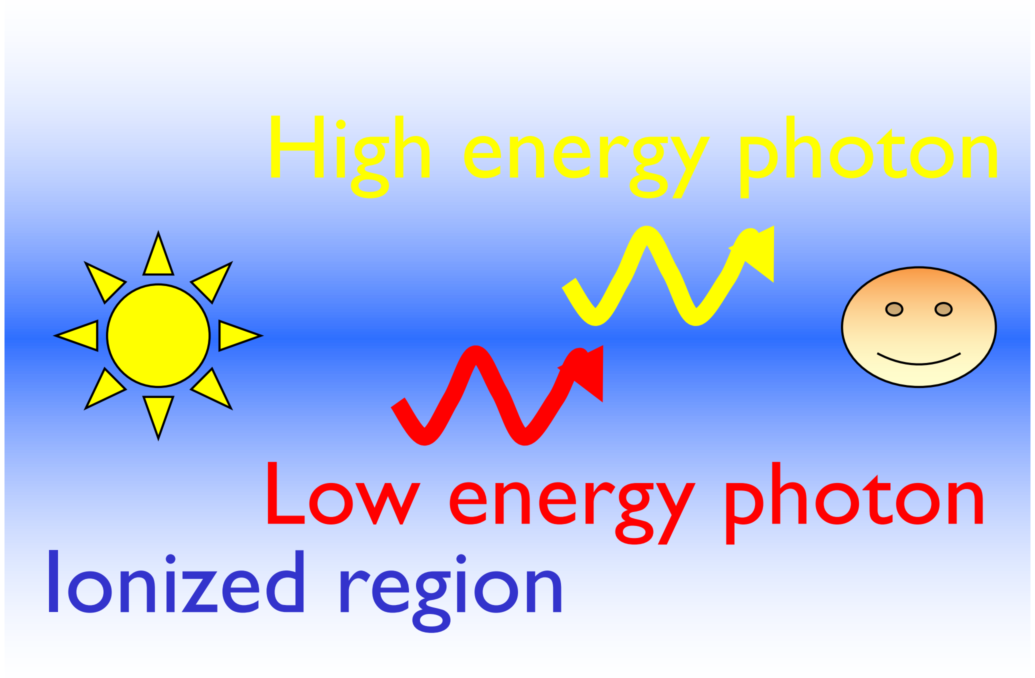

In a plasma, a light signal is delayed

$$\omega^2 = k^2 c^2 + \omega_p^2$$

plasma frequency

$$\omega_p = \sqrt{\frac{4\pi n e^2}{m}} = 5.63 \times 10^4 n^{1/2} \ \mathrm{s}^{-1}$$

$$\Delta t = 4.15 \ \mathrm{s} \left(\frac{\nu}{1 \ \mathrm{GHz}} \right)^{-2} \left(\frac{\mathrm{DM}}{10^3 \ \mathrm{pc \ cm}^{-3}} \right)$$

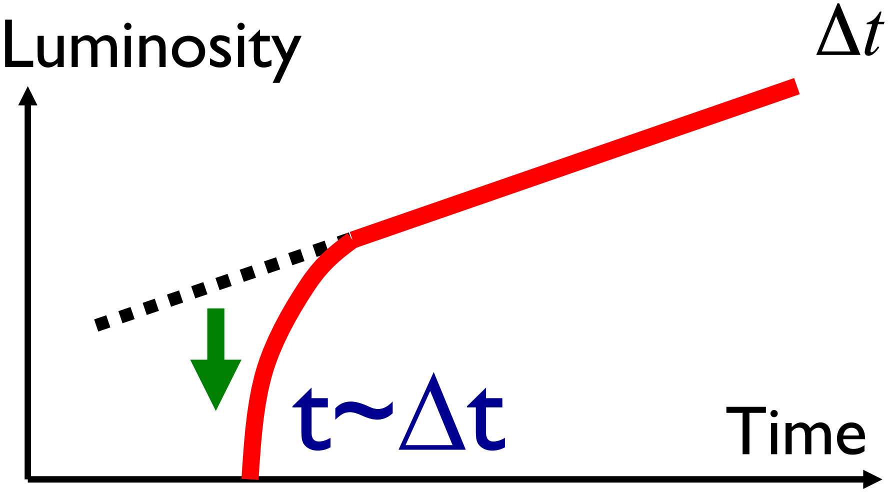

Distortion in light curve

⇒ DM

⇒ Reionization History

Dispersion Measure

is the column density of free electrons along light path

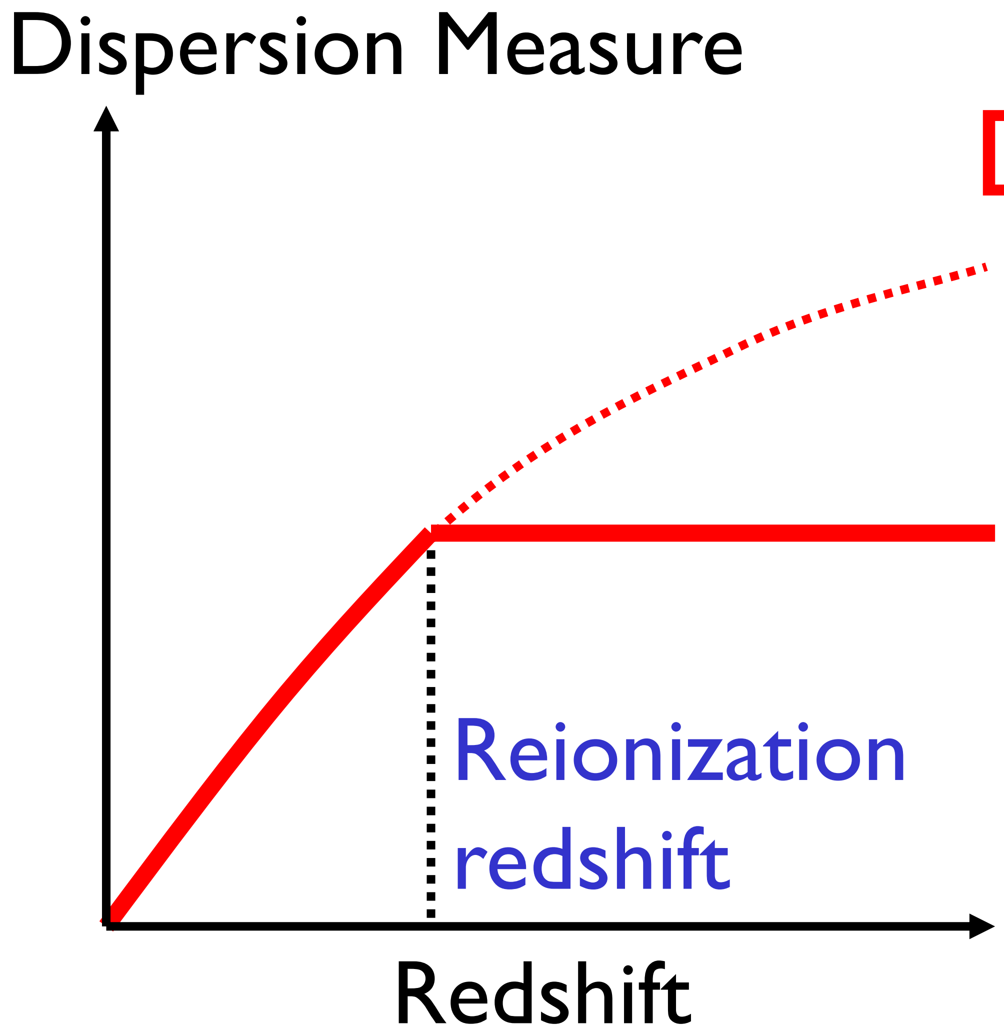

Dispersion Measure

↓

Reionization History

Recombined electrons provide no DM

KI 03, Inoue 04

Cosmic DM

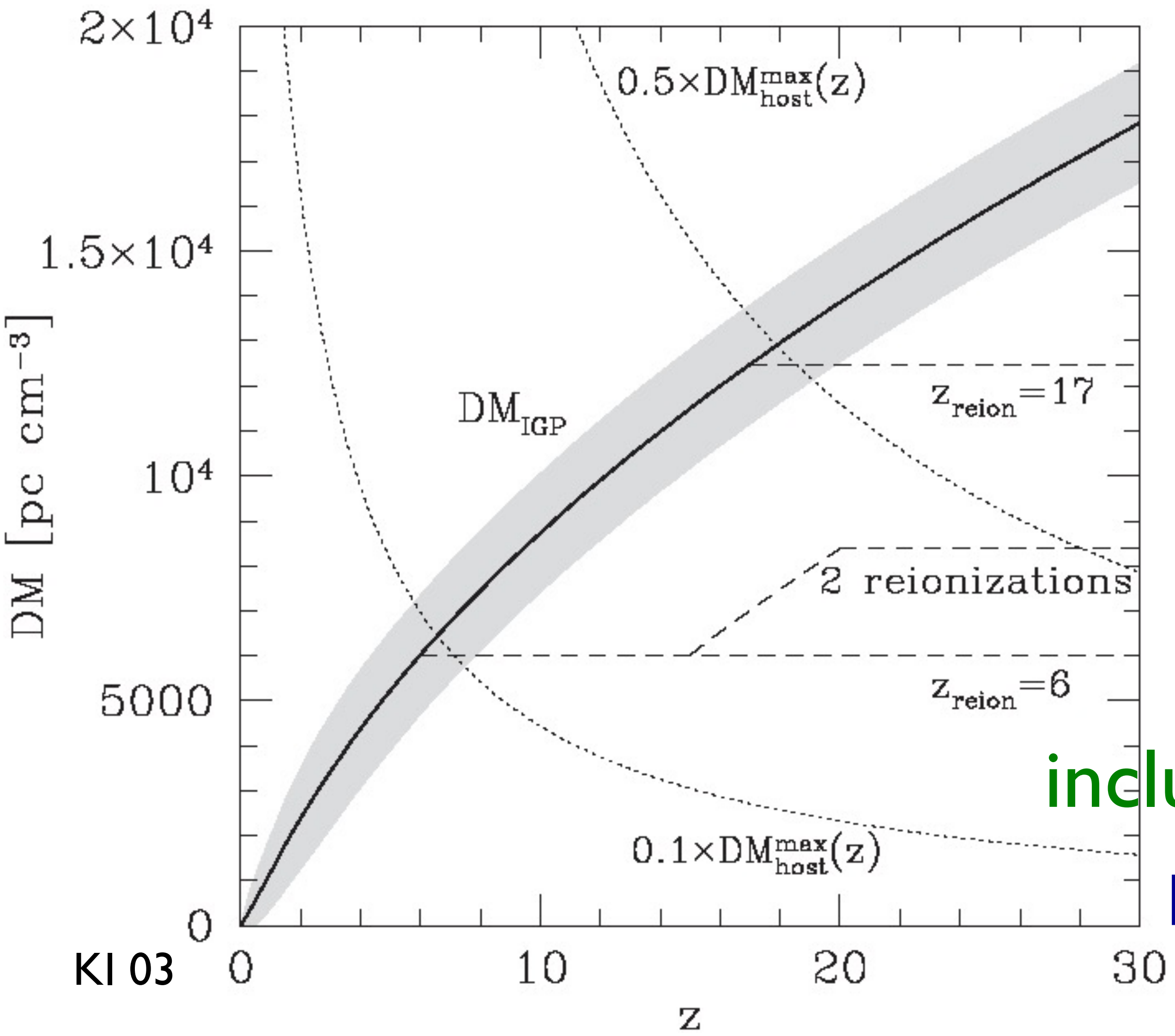

KI 03

$$\Delta t = \int_0^z dz \frac{dt}{dz} \frac{1}{2} \frac{(1+z)\nu_p^2}{[(1+z)\nu]^2}$$

$$= \frac{e^2}{2\pi m_e c} \frac{1}{\nu^2} \times$$

$$\frac{c n_0}{H_0} \int_0^z \frac{(1+z)\,dz}{\left[\Omega_m (1+z)^3 + \Omega_\Lambda\right]^{1/2}}$$

DM_{cosmic}

including missing baryon

DM_{Galaxy}~30-10^3 pc cm^{-3}

Dispersion Measure

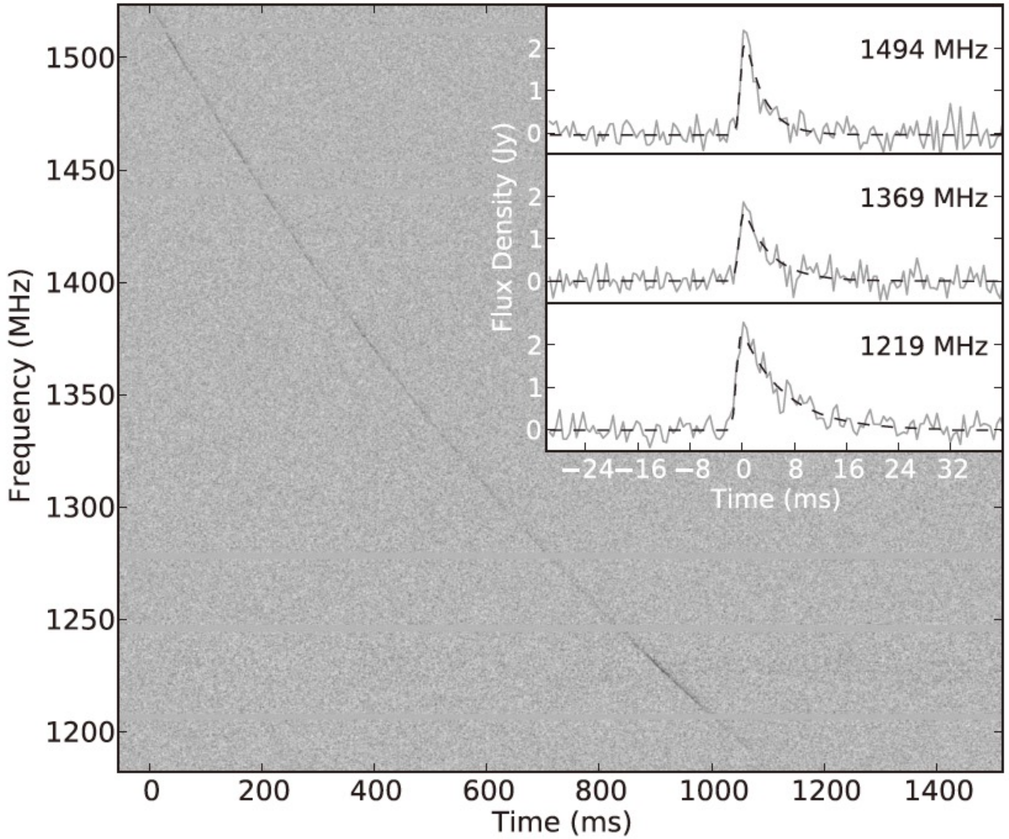

Thornton+ 13

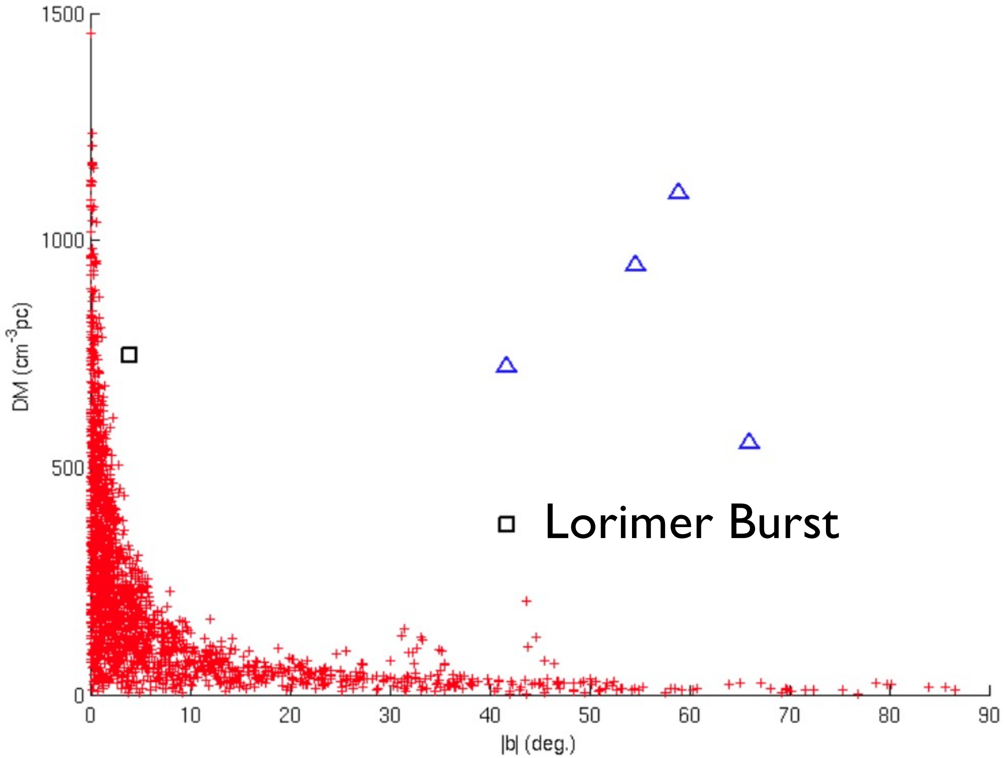

Galactic latitude

$\delta t \propto DM \cdot \nu^{-2}$

DM=500-1000 pc cm^{-3} ⇨ z~0.5-1?

PHYSICAL REVIEW LETTERS

VOLUME 14 21 JUNE 1965 NUMBER 25

PROPOSAL FOR THE DETECTION OF DISPERSION IN RADIO-WAVE PROPAGATION THROUGH INTERGALACTIC SPACE*

F. T. Haddock

Radio Astronomy Observatory, University of Michigan, Ann Arbor, Michigan

and

D. W. Sciama†

Department of Physics and Astronomy, University of Maryland, College Park, Maryland

(Received 20 April 1965)

Einstein-de Sitter

Steady-state model

$$\frac{1}{2}\frac{(\nu_p)_0^{\,2}}{v_0^{\,2}}\int_t^{t_0}\frac{1}{R(t)}dt,$$

NATURE VOL. 246 DECEMBER 14 1973 415

Possibility of Determining Intergalactic Gas Density by Radio Observations of Flares of Remote Sources

V. L. GINZBURG

P. N. Lebedev Physical Institute,
Academy of Sciences,
Moscow

$$\tau(\nu) = L/u - L/c = e^2 N_{mg} L/2\pi mc\nu^2 = 1.34 \times 10^{-3}\ (N_{mg} L/\nu^2)\ \mathrm{s}$$

THE ASTROPHYSICAL JOURNAL, 417:L25–L28, 1993 November 1

RADIO DISPERSION AS A DIAGNOSTIC OF GAMMA-RAY BURST DISTANCES

DAVID M. PALMER
Goddard Space Flight Center, Greenbelt, MD 20771
e-mail: palmer@tgrs.gsfc.nasa.gov
Received 1993 June 10; accepted 1993 August 17

ABSTRACT

If gamma-ray bursts sources emit even a small fraction of their energy in the radio spectrum, dispersion measurements of this emission would determine the distance to the source and thereby greatly constrain theoretical models. If a GRB is at $z \sim 1$, or is beyond the Galactic center and in the Galactic plane, the signal at low frequencies ($\sim$25 MHz) will be delayed by $\sim$1 hr, which is enough time to allow a radio telescope to be pointed toward the GRB location. Such a measurement could detect a GRB with $L_{\rm Radio}/L_{\gamma\text{-ray}} \gtrsim 10^{-7}$, while an observation at higher frequencies could detect a GRB with $L_R/L_\gamma \gtrsim 10^{-8}$, both of which are much more sensitive than the current upper limit of $L_R/L_\gamma \lesssim 10^{-3.5}$. A dispersion measurement for an extragalactic GRB would also observe for the first time the intergalactic plasma, which may be the dominant form of baryonic matter in the universe.

$$\mathrm{DM_{IGP}} = 2.64 \times 10^4 \Omega_{\rm IGP} \frac{h}{q_0} [(1 + 2q_0 z)^{1/2} - 1]\ \mathrm{pc\ cm^{-3}} \quad (2)$$

only for low z

Contents

Repeating FRB 121102

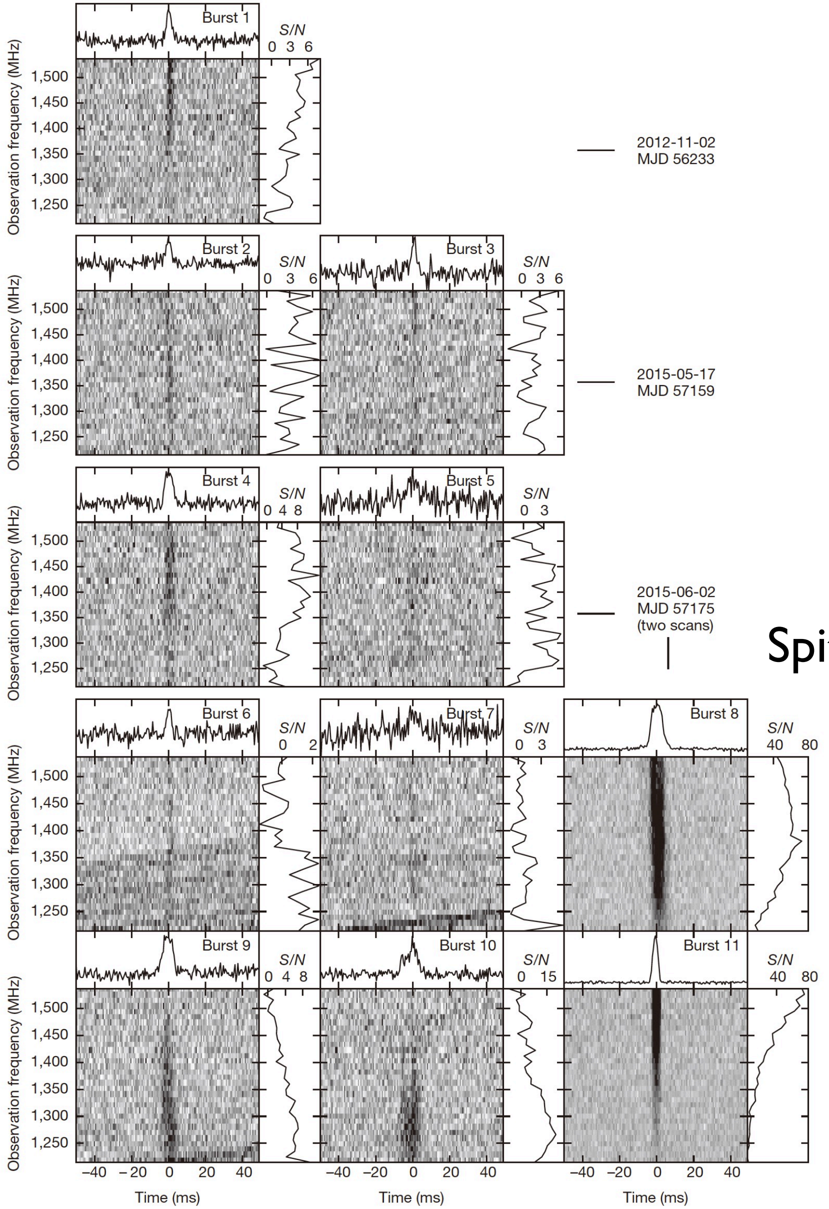

Spitler+ 16

Extended Data Table 1 | Arecibo FRB 121102 discovery and follow-up observations

UTC Date	Project	Position	Receiver	Frequency (GHz)	Backend	Dwell time (s)	# Bursts
Survey discovery observations presented in Spitler et al. (2014)							
2012-11-02	p2030	**FRBDISC**	ALFA	1.4	Mocks	200	**1 (Beam4)**
2012-11-04	p2030	FRBDISC	ALFA	1.4	Mocks	200	0
Follow-up observations presented in Spitler et al. (2014)							
2013-12-09	p2886	FRBGRID1a	ALFA	1.4	Mocks	2700	0
2013-12-09	p2886	FRBGRID2a	ALFA	1.4	Mocks	970	0
2013-12-09	p2886	FRBGRID2a	ALFA	1.4	Mocks	1830	0
2013-12-10	p2886	FRBGRID3a	ALFA	1.4	Mocks	2700	0
2013-12-10	p2886	FRBDISC	327-MHz	0.327	PUPPI	2385	0
Follow-up observations presented here for the first time							
2015-05-02	p2886	FRBDISC	L-wide	1.4	PUPPI	7200	0
2015-05-03	p2886	FRBGRID1b	ALFA	1.4	Mocks	1502	0
2015-05-03	p2886	FRBGRID2b	ALFA	1.4	Mocks	1502	0
2015-05-03	p2886	FRBGRID3b	ALFA	1.4	Mocks	343	0
2015-05-03	p2886	FRBGRID3b	ALFA	1.4	Mocks	1502	0
2015-05-03	p2886	FRBGRID1b	ALFA	1.4	Mocks	921	0
2015-05-05	p2886	FRBGRID1b	ALFA	1.4	Mocks	1002	0
2015-05-05	p2886	FRBGRID2b	ALFA	1.4	Mocks	1002	0
2015-05-05	p2886	FRBGRID3b	ALFA	1.4	Mocks	1002	0
2015-05-05	p2886	FRBGRID4b	ALFA	1.4	Mocks	1002	0
2015-05-05	p2886	FRBGRID5b	ALFA	1.4	Mocks	1002	0
2015-05-05	p2886	FRBGRID6b	ALFA	1.4	Mocks	1002	0
2015-05-09	p2886	FRBGRID1b	ALFA	1.4	Mocks	1002	0
2015-05-09	p2886	FRBGRID2b	ALFA	1.4	Mocks	1002	0
2015-05-09	p2886	FRBGRID3b	ALFA	1.4	Mocks	1002	0
2015-05-09	p2886	FRBGRID4b	ALFA	1.4	Mocks	1002	0
2015-05-09	p2886	FRBGRID5b	ALFA	1.4	Mocks	1002	0
2015-05-09	p2886	FRBGRID6b	ALFA	1.4	Mocks	1002	0
2015-05-09	p2886	FRBGRID6b	ALFA	1.4	Mocks	425	0
2015-05-17	p2886	FRBGRID1b	ALFA	1.4	Mocks	1002	0
2015-05-17	p2886	**FRBGRID2b**	ALFA	1.4	Mocks	1002	**2 (Beam6)**
2015-05-17	p2886	FRBGRID3b	ALFA	1.4	Mocks	1002	0
2015-05-17	p2886	FRBGRID4b	ALFA	1.4	Mocks	707	0
2015-05-17	p2886	FRBGRID4b	ALFA	1.4	Mocks	391	0
2015-05-17	p2886	FRBGRID5b	ALFA	1.4	Mocks	1002	0
2015-05-17	p2886	FRBGRID6b	ALFA	1.4	Mocks	1002	0
2015-06-02	p2886	FRBGRID1b	ALFA	1.4	Mocks	1002	0
2015-06-02	p2886	**FRBGRID2b**	ALFA	1.4	Mocks	1002	**2 (Beam6)**
2015-06-02	p2886	FRBGRID3b	ALFA	1.4	Mocks	1002	0
2015-06-02	p2886	FRBGRID4b	ALFA	1.4	Mocks	1002	0
2015-06-02	p2886	FRBGRID5b	ALFA	1.4	Mocks	1002	0
2015-06-02	p2886	**FRBGRID6b**	ALFA	1.4	Mocks	1002	**6 (Beam0)**
2015-06-02	p2886	FRBGRID6b	ALFA	1.4	Mocks	300	0

The observing setup of these observations is described in Methods. Data from ref. 4 and this study.

A FRB is Cosmological!

Repeating FRB 121102 ⇒ Radio interferometry

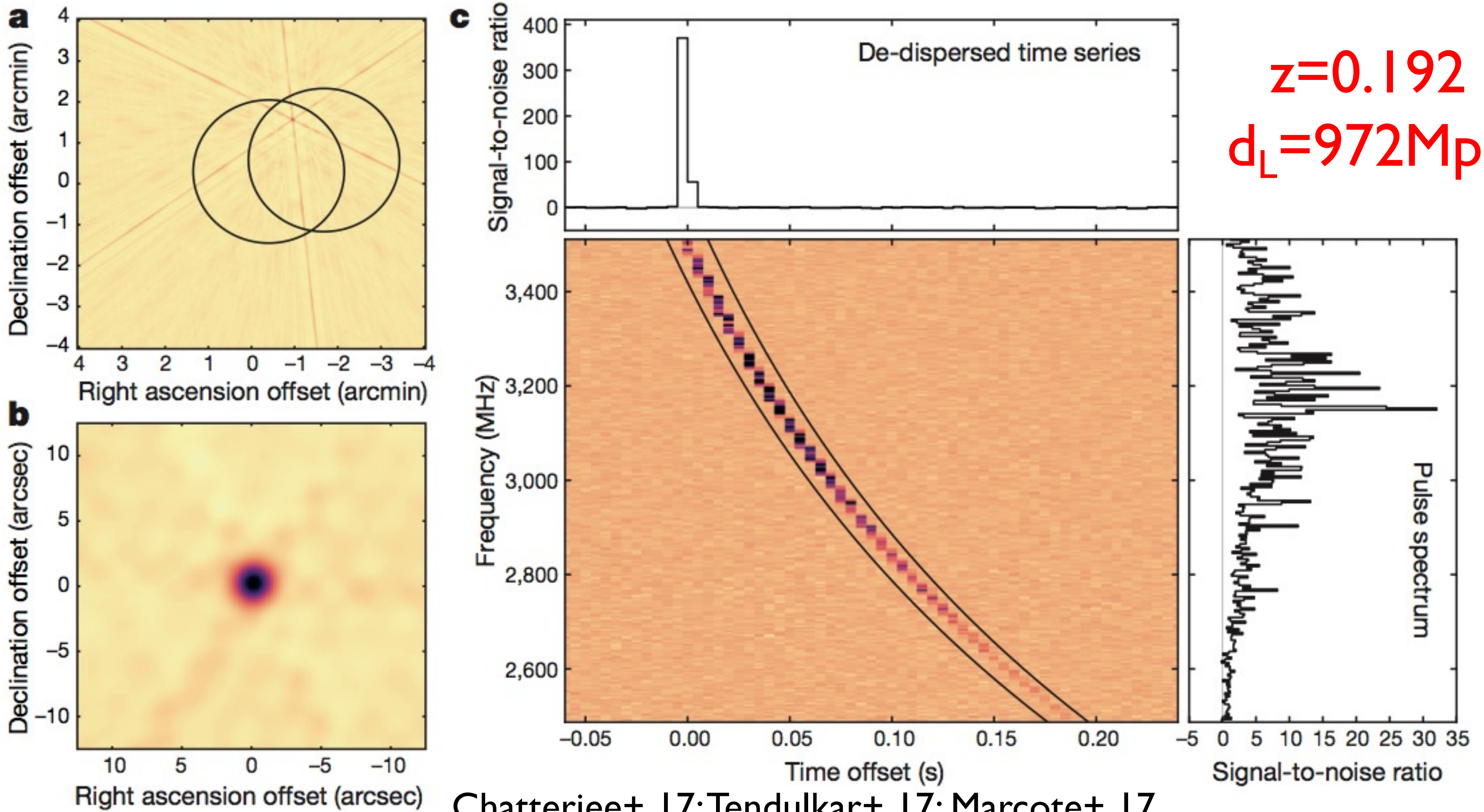

$z=0.192$

$d_L=972\mathrm{Mpc}$

Chatterjee+ 17; Tendulkar+ 17; Marcote+ 17

Hosts for Non-Repeaters

FRB 180924

z=0.3214

Old, clean galaxy

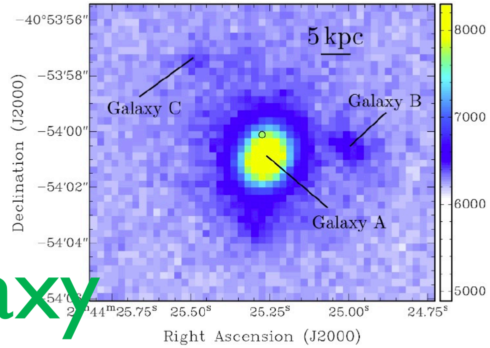

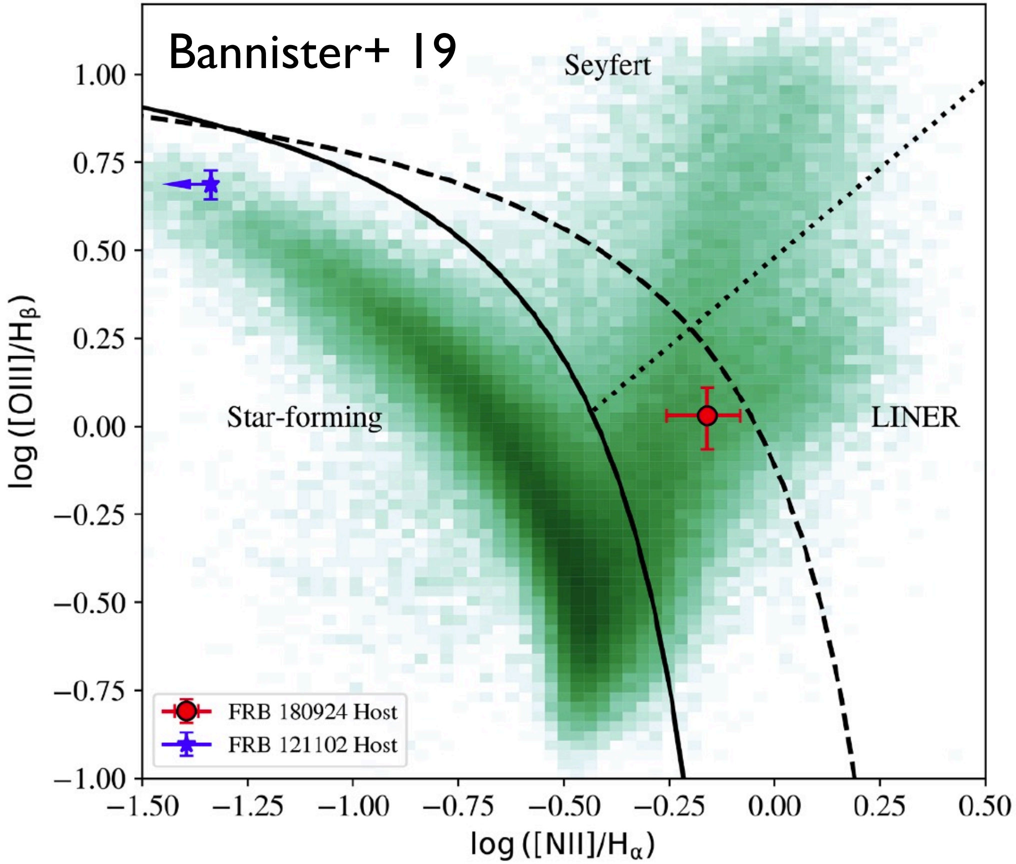

FRB 190523

z=0.66, old galaxy

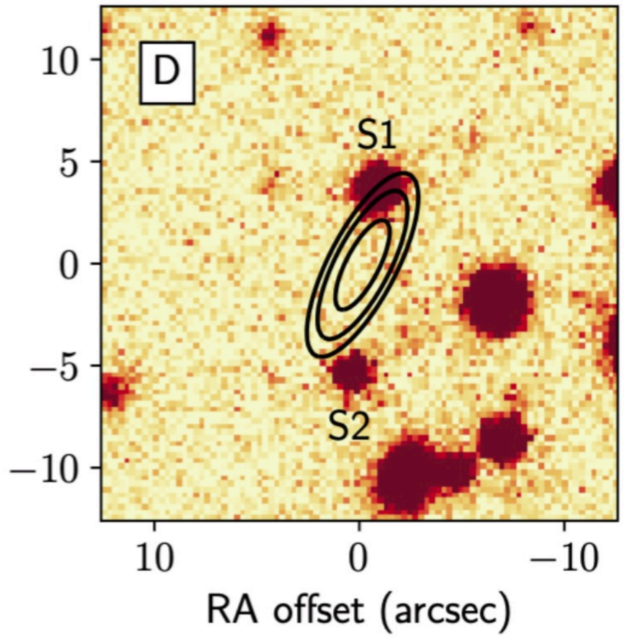

⇒ NS-NS?

WD→NS?

Ravi+ 19

Host galaxy redshift	0.660(2)
Host galaxy luminosity distance (Gpc)	4.08(1)
Burst energy (erg Hz^{-1})	5.6×10^{33}
Host galaxy stellar mass ($M_\odot$)	$10^{11.07(6)}$
Host galaxy star-formation rate ($M_\odot$ yr^{-1})	<1.3

Observed DM-z

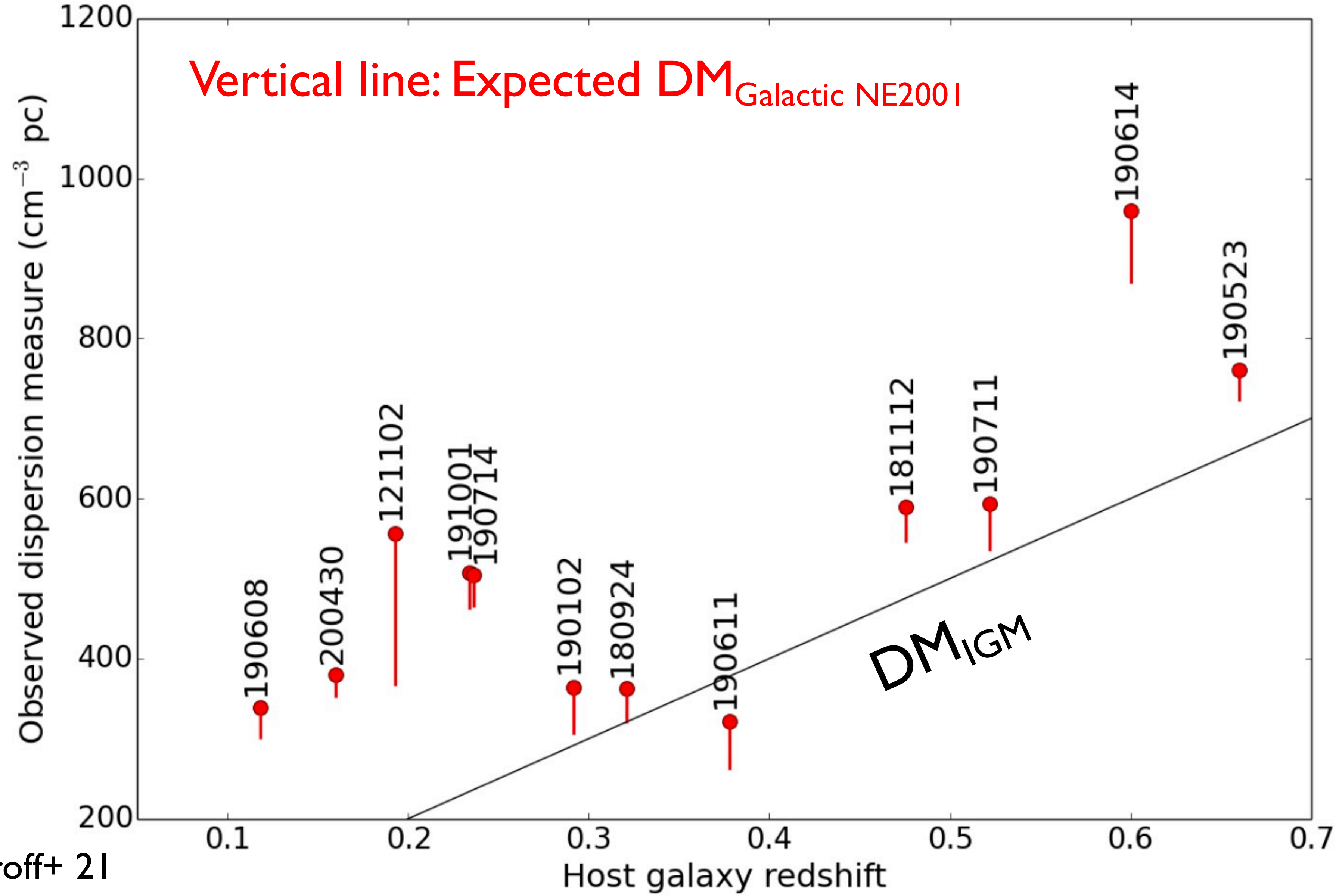

Petroff+ 21

Contents

- ***Introduction & History***
  - Dispersion measure
  - FRB repeaters & Host galaxies
  - Galactic FRB from a magnetar
- ***Host galaxies***
  - Diversity, Dwarf, Spiral, Globular cluster, …
- ***FRB cosmology***
  - DM, Cross-correlation, Lensing, RM, SM, …

Galactic FRB from Magnetar Bursts

A smoking gun! Magnetar: One of the origins

Mereghetti+ 20, Bochenek+ 20, CHIME/FRB+ 20, Li+ 20, Ridnaia+ 20, Tavani+ 20

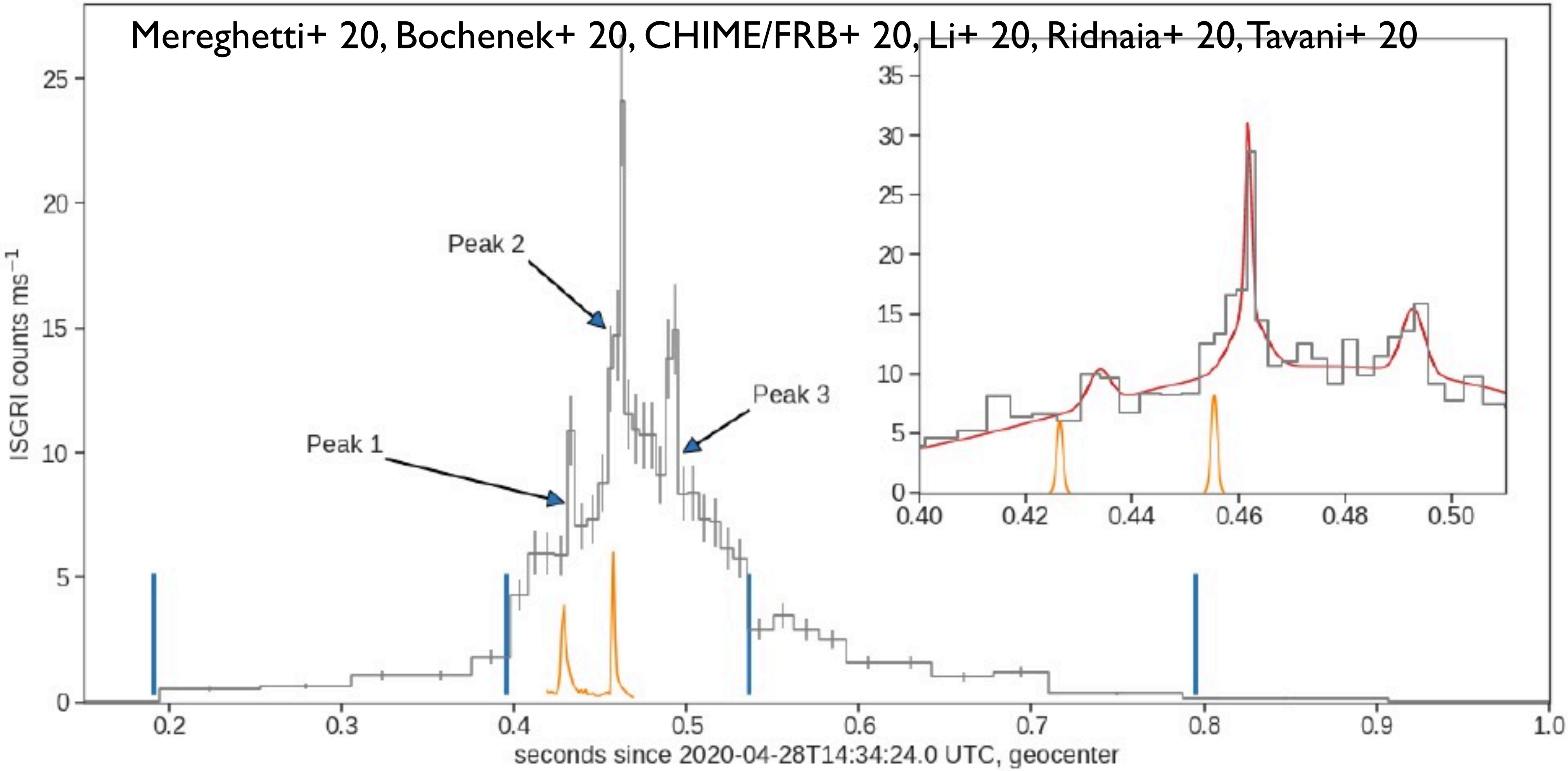

FRB 200428

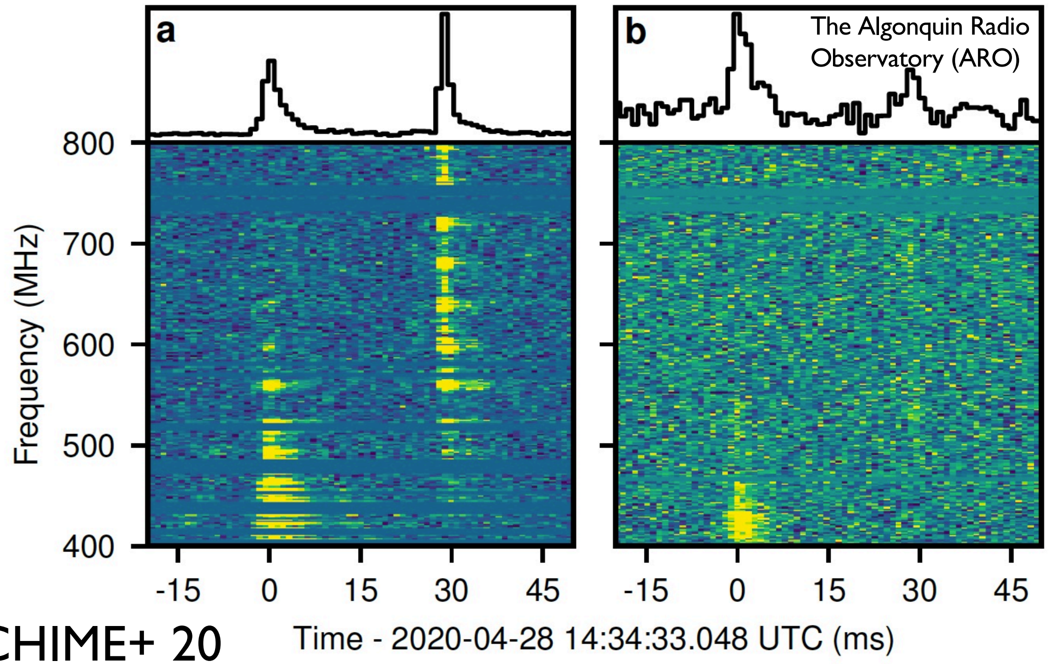

CHIME+ 20

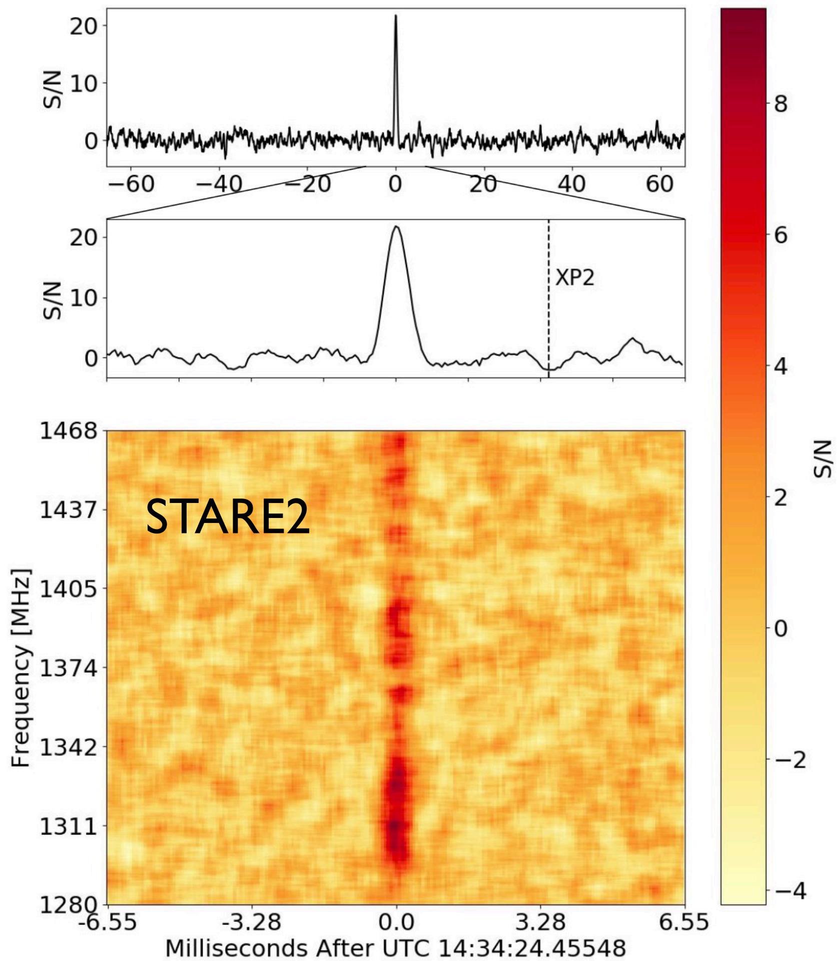

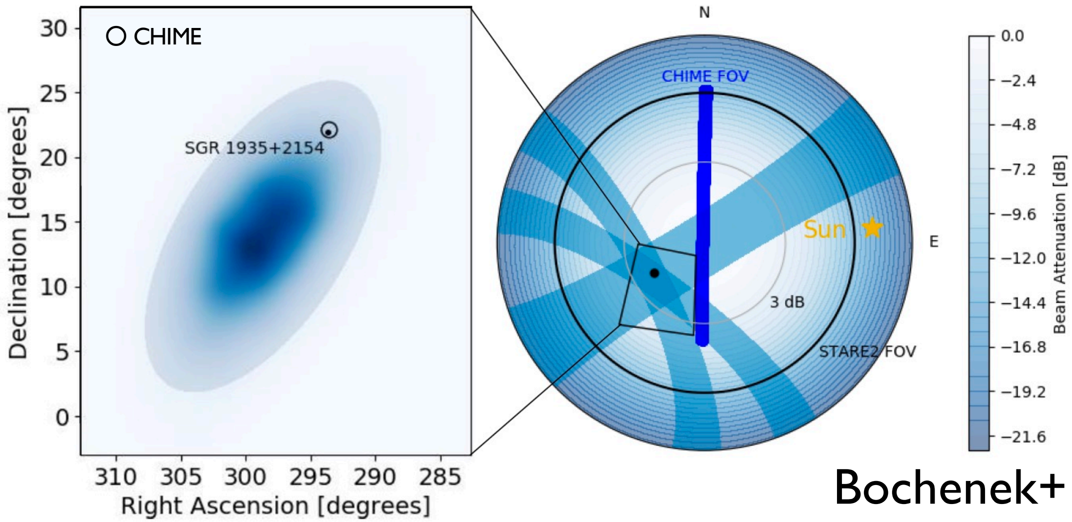

Bochenek+ 20

Mega Jy!!

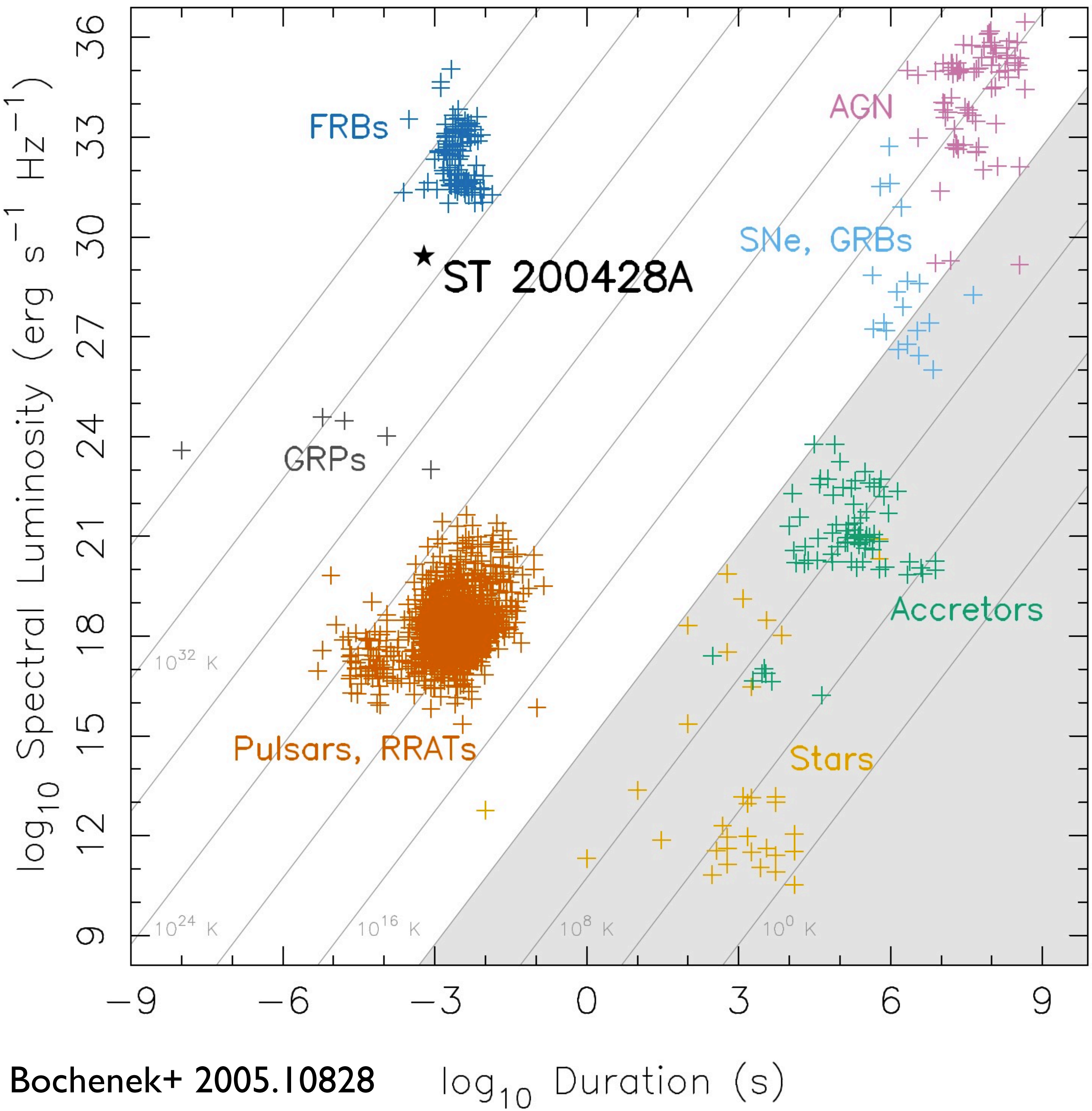

Bochenek+ 2005.10828

Assuming
d=6.5-12.5 kpc

Only FRBs detected
at 1-2GHz with known
distance

RRAT: rotating radio
transients

GRP: max ~ 3e4 Jy ms
~6e31 erg @430MHz

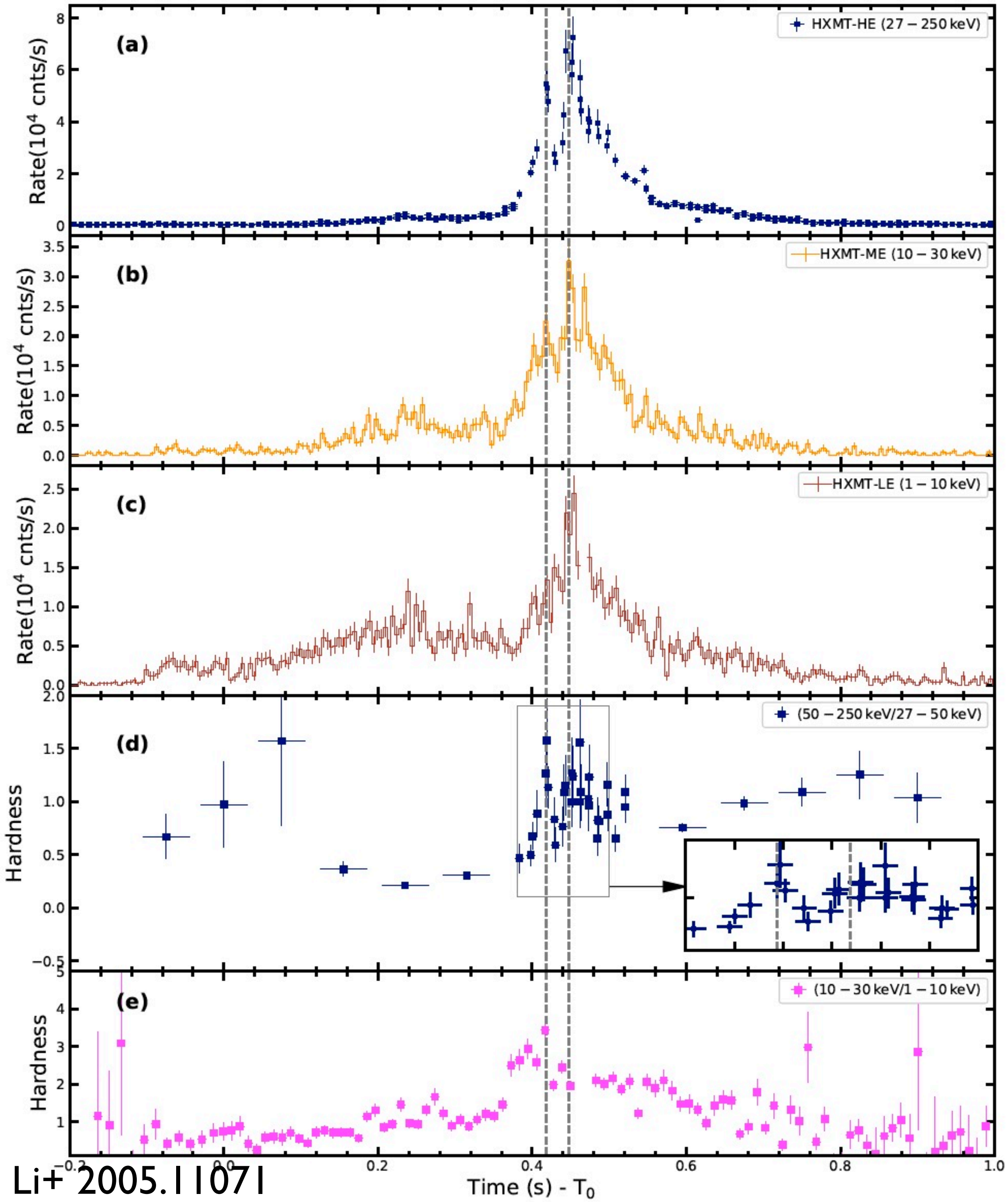

Li+ 2005.11071

Insight-HXMT
$7.14^{+0.41}_{-0.38}$e-7 erg/cm^2
~1e40 erg

HE: 1 ms resolution
near the peak
10 ms outside
ME & LE: 5 ms bin

Saturation near the peak
for HE & LE
Deadtime in ME

T0=14:34:24.0114UT
(geocentric time)

Contents

FRB 121102 Host Galaxy

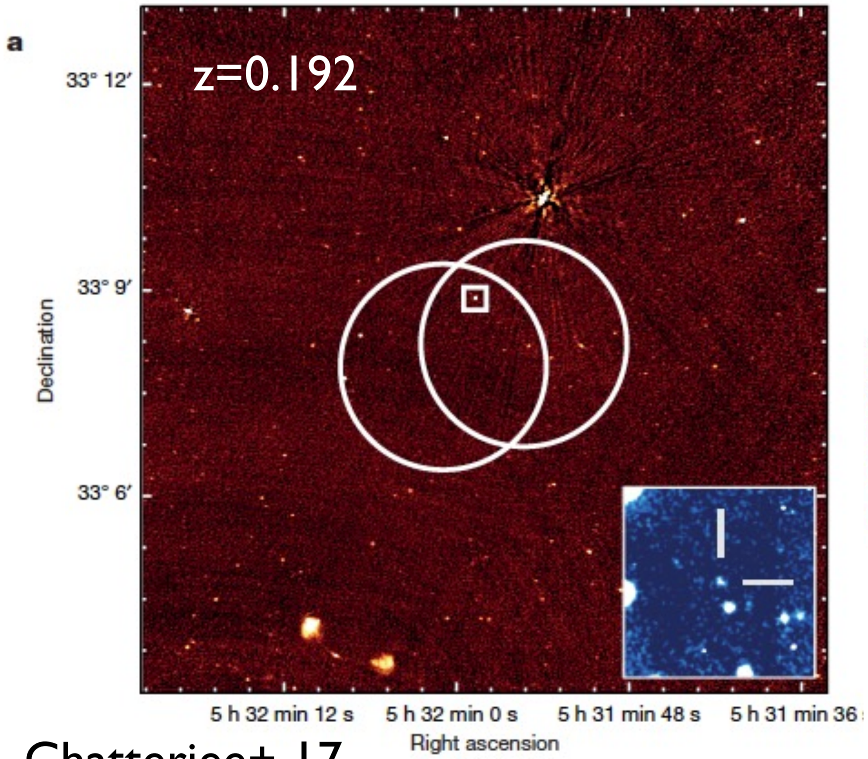

Chatterjee+ 17

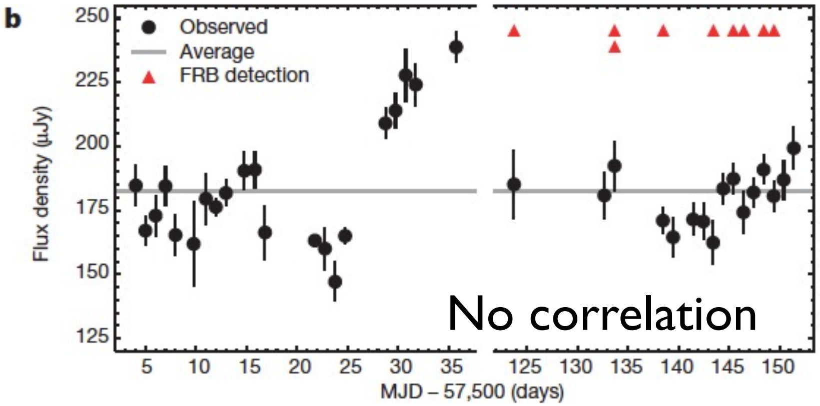

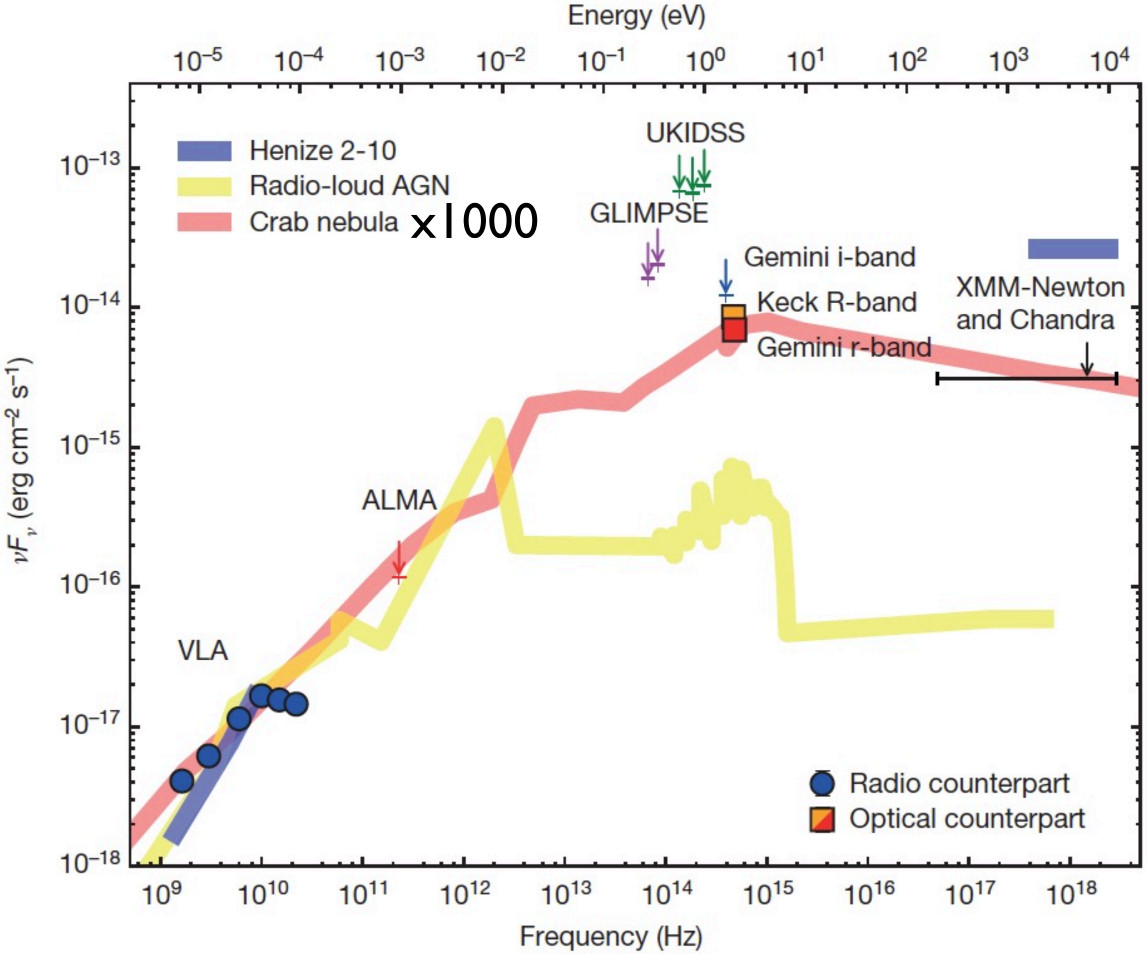

Low-Z *-forming dwarf ~(4-7)e7 $M_\odot$

Compact radio source < 0.7pc

L_{GHz}~10^{39} erg/s, off-center

Hosts for Non-Repeaters

FRB 180924

z=0.3214

Old, clean galaxy

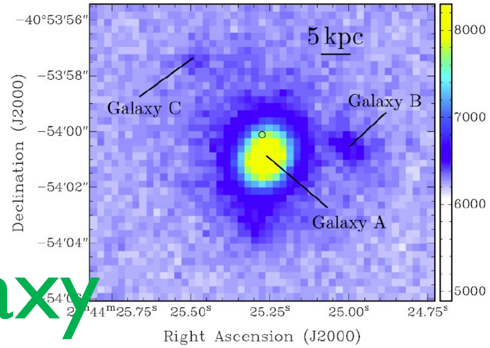

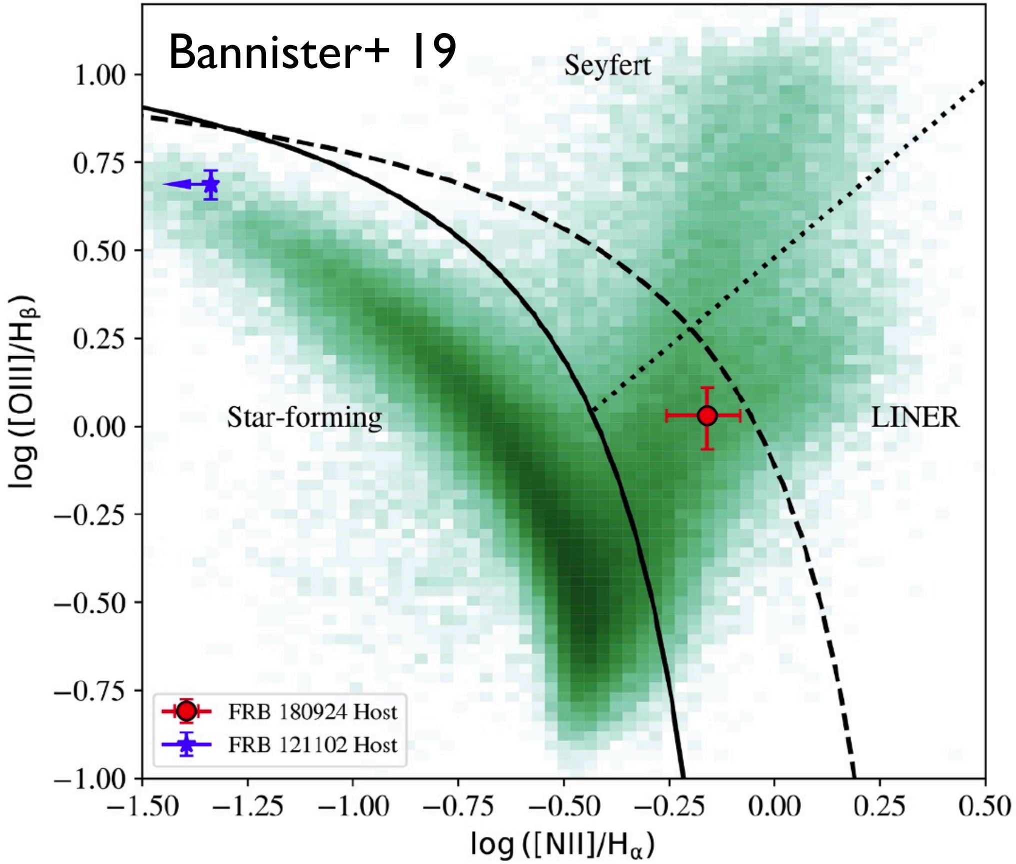

FRB 190523

z=0.66, old galaxy

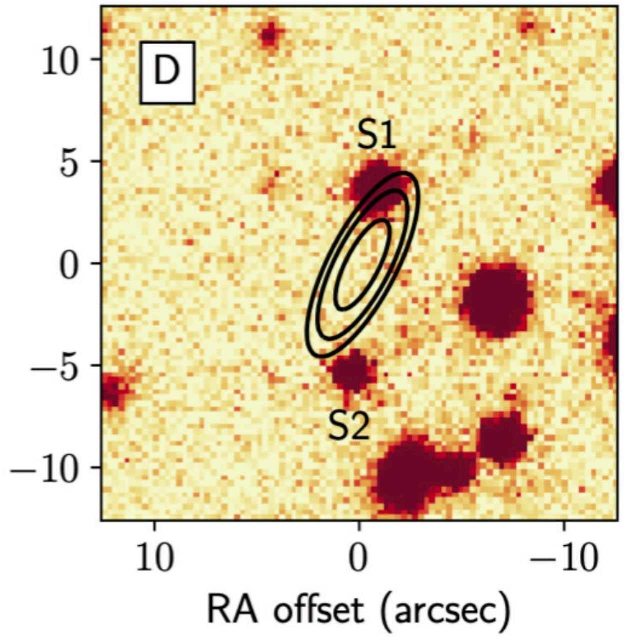

⇒ NS-NS?

WD→NS?

Ravi+ 19

Host galaxy redshift	0.660(2)
Host galaxy luminosity distance (Gpc)	4.08(1)
Burst energy (erg Hz^{-1})	5.6 x 10^{33}
Host galaxy stellar mass ($M_\odot$)	$10^{11.07(6)}$
Host galaxy star-formation rate ($M_\odot$ yr^{-1})	<1.3

Host of FRB 180916

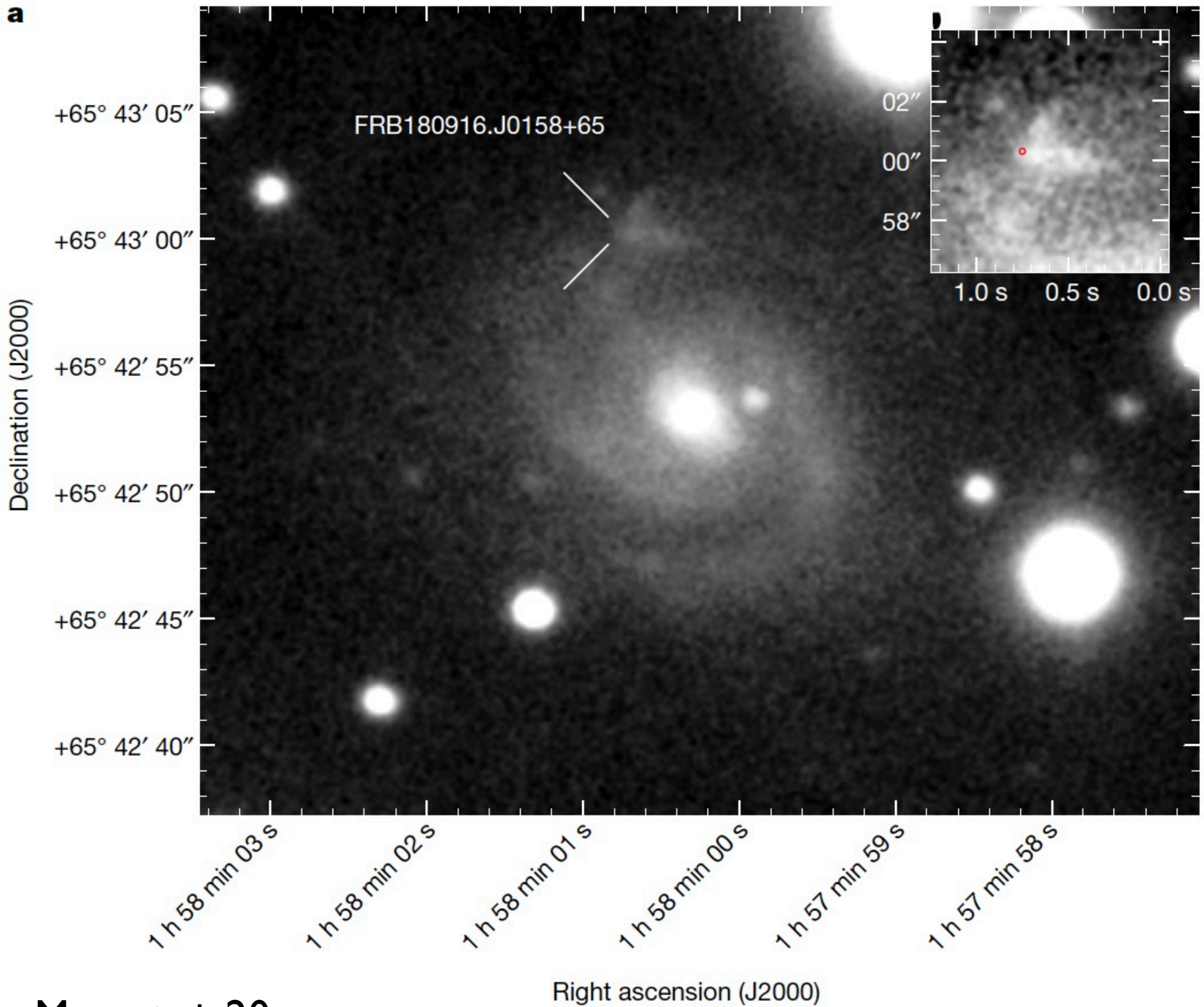

2nd host for repeater

z=0.0337

Massive spiral

Star-forming region

No luminous radio

Diverse host galaxies

Marcote+ 20

See also Li+ 19

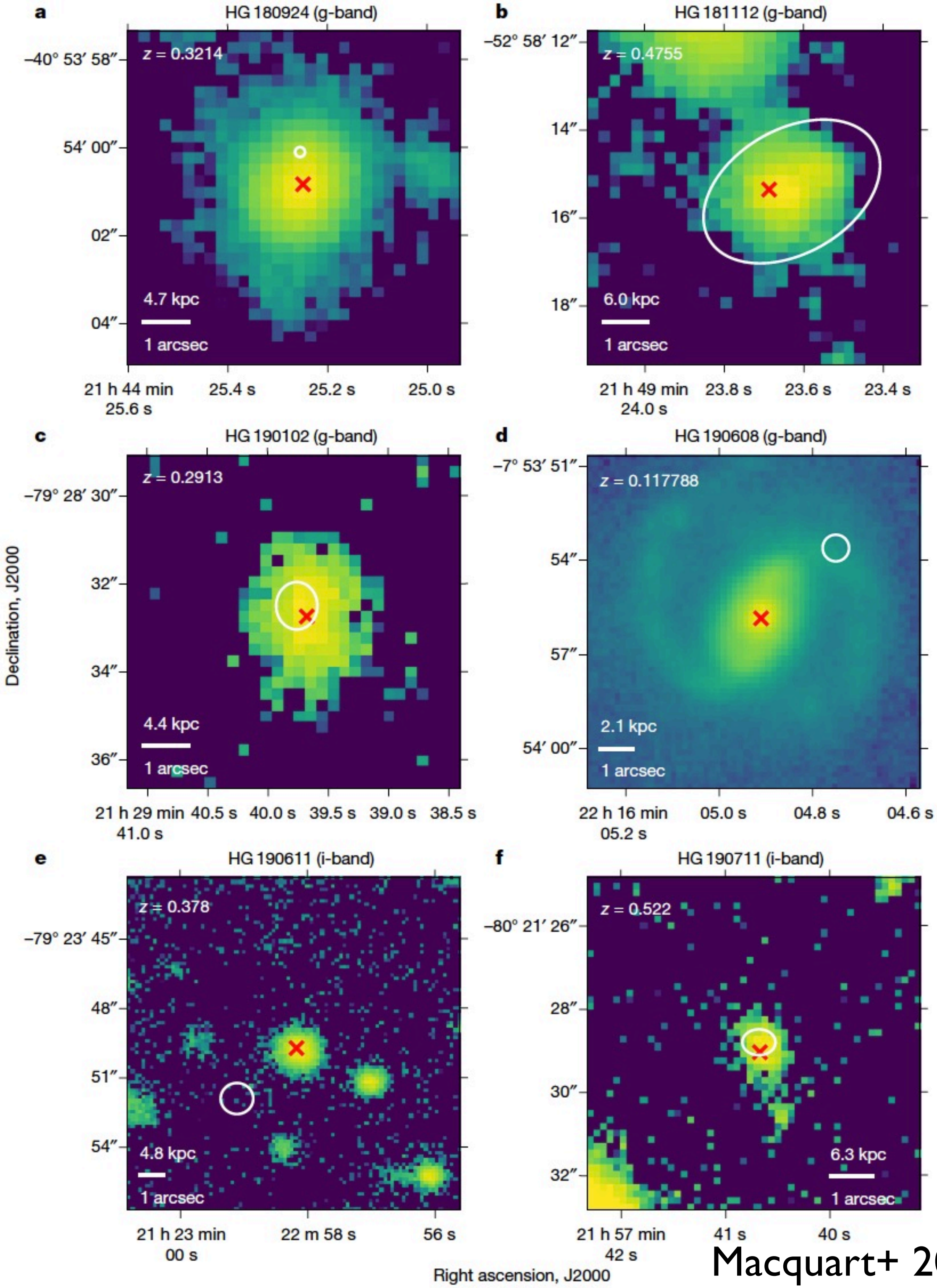

FRB	Time (UTC)[a]	DM (pc cm^{-3})	Rotation measure (rad m^{-2})	Fluence (Jy ms)[b]	Right ascension (h:min:s)[c]	Declination (degree:arcmin:arcsec)[c]	Host redshift	Offset from host nucleus (kpc)
180924	16:23:12.6265	361.42(6)	14(1)	16(1)	21:44:25.255 ± 0.006 ± 0.008	−40:54:00.10 ± 0.07 ± 0.09	0.3214	3.5 ± 0.9
181112	17:31:15.48365	589.27(3)	10.9(9)	26(3)	21:49:23.63 ± 0.05 ± 0.24	−52:58:15.4 ± 0.3 ± 1.4	0.4755	$3.1^{+15.7}_{-3.1}$
190102	05:38:43.49184	363.6(3)	110	14(1)	21:29:39.76 ± 0.06 ± 0.16	−79:28:32.5 ± 0.2 ± 0.5	0.291	$1.5^{+3.4}_{-1.5}$
190608	22:48:12.88391	338.7(5)	–	26(4)	22:16:04.75 ± 0.02 ± 0.02	−07:53:53.6 ± 0.3 ± 0.3	0.1178	7.0 ± 1.3
190611	5:45:43.29937	321.4(2)	–	10(2)	21:22:58.91 ± 0.11 ± 0.23	−79:23:51.3 ± 0.3 ± 0.6	0.378	17.2 ± 4.9
190711	01:53:41.09338	593.1(4)	–	34(3)	21:57:40.68 ± 0.051 ± 0.15	−80:21:28.8 ± 0.08 ± 0.3	0.522	$1.5^{+3.6}_{-1.5}$

The FRB detection pipeline makes use of the DBSCAN algorithm[25], as implemented by ref. [26], to mitigate RFI and reduce the frequency of false-positive FRB triggers.
[a]Burst arrival time referenced to a frequency of 1,152 MHz.
[b]Quoted errors on the last significant digit of the fluence represent a 90% confidence limit.
[c]Errors listed after the burst position represent the statistical and systematic uncertainties respectively, and are combined in quadrature for a final absolute positional uncertainty.

ASKAP

6km baseline, FOV=30 deg^2, $\Delta\theta$<0.5”

Diversity

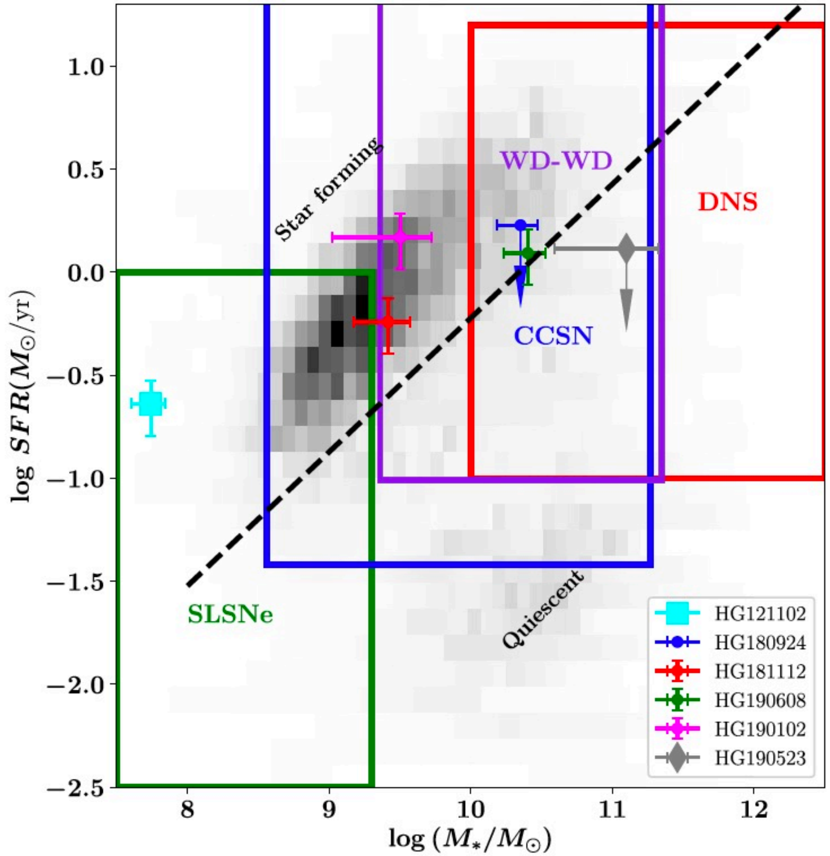

Macquart+ 20

Bhandari+ 20

Host Galaxy

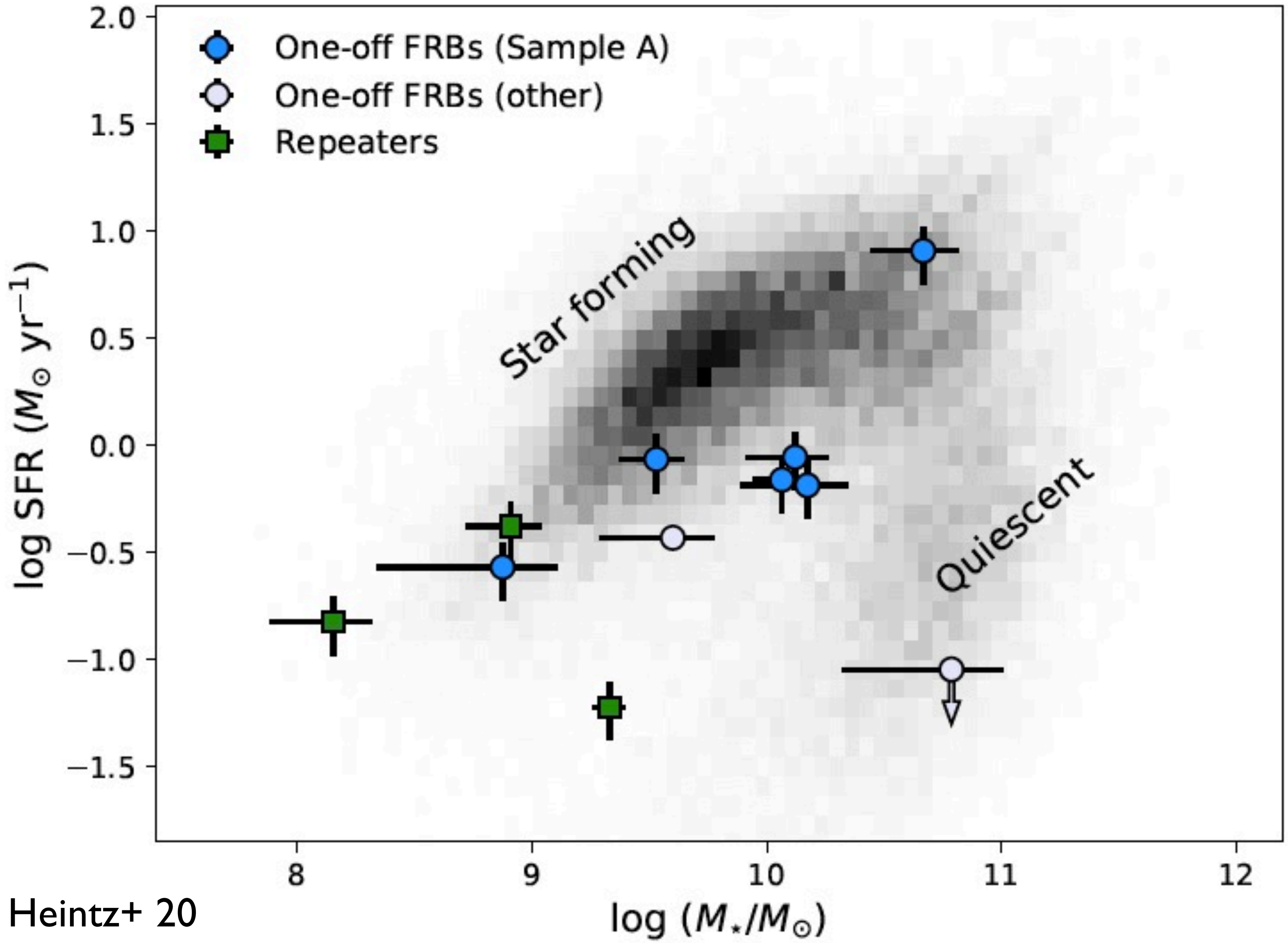

Broad range

green valley?

WD^2, NS^2, AIC WD, CCSN

not LGRB

not 121102

Heintz+ 20

see also Li & Zhang 20, Wang+ 20

Host Galaxies by HST

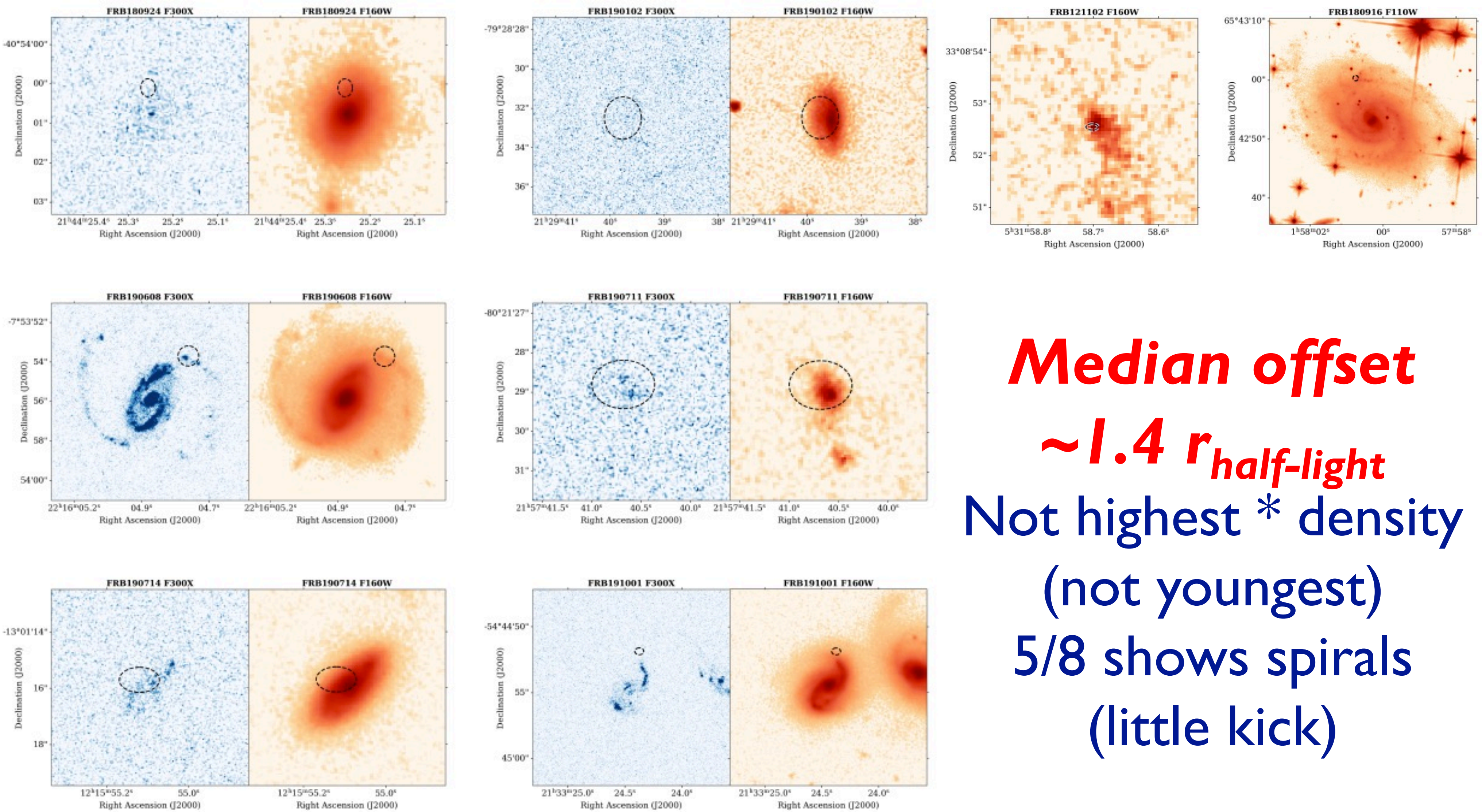

Median offset
~1.4 $r_{half\text{-}light}$

Not highest * density
(not youngest)
5/8 shows spirals
(little kick)

Mannings+ 21

DM for FRB 190608

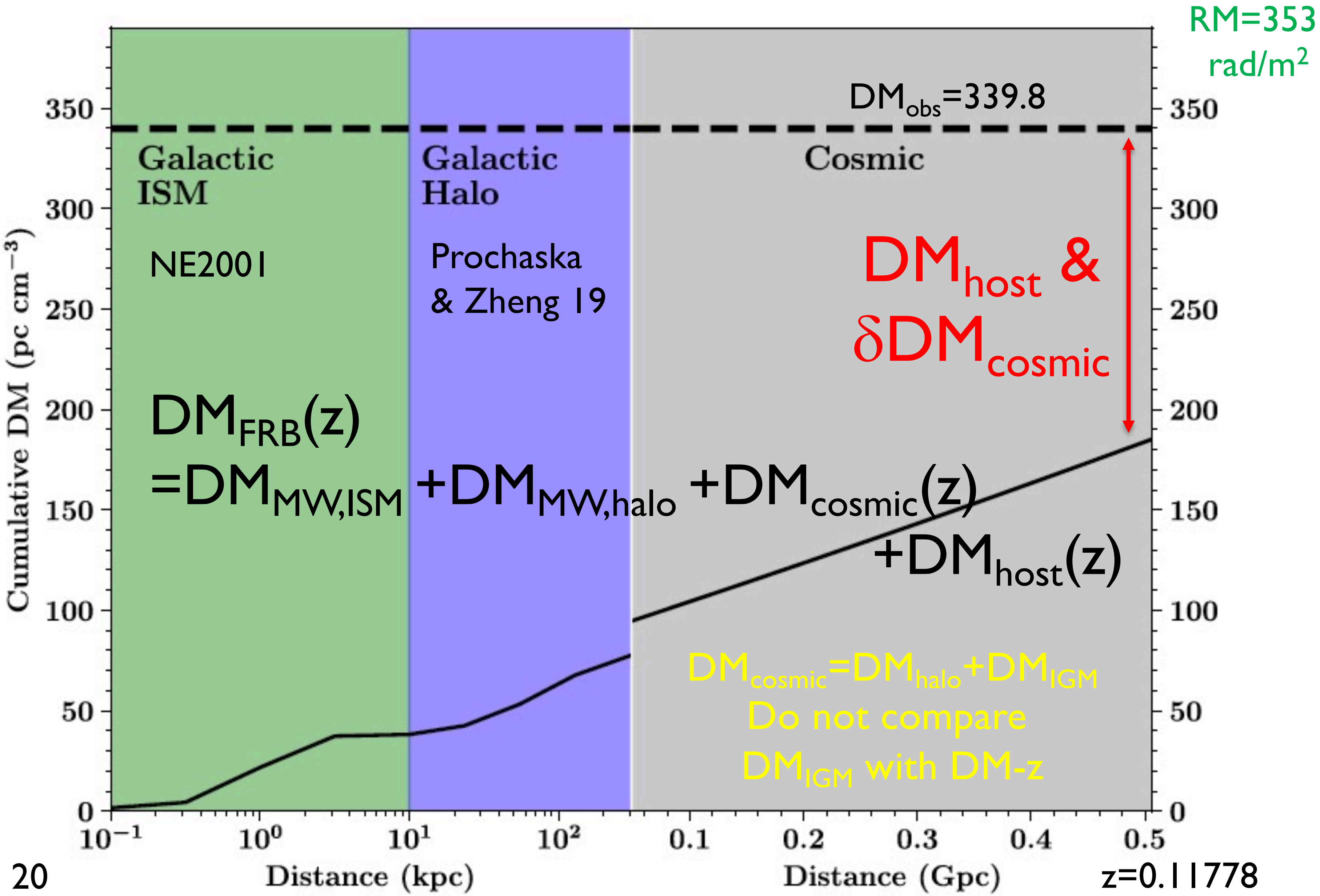

Simha+ 20

z=0.11778

Electron Distribution

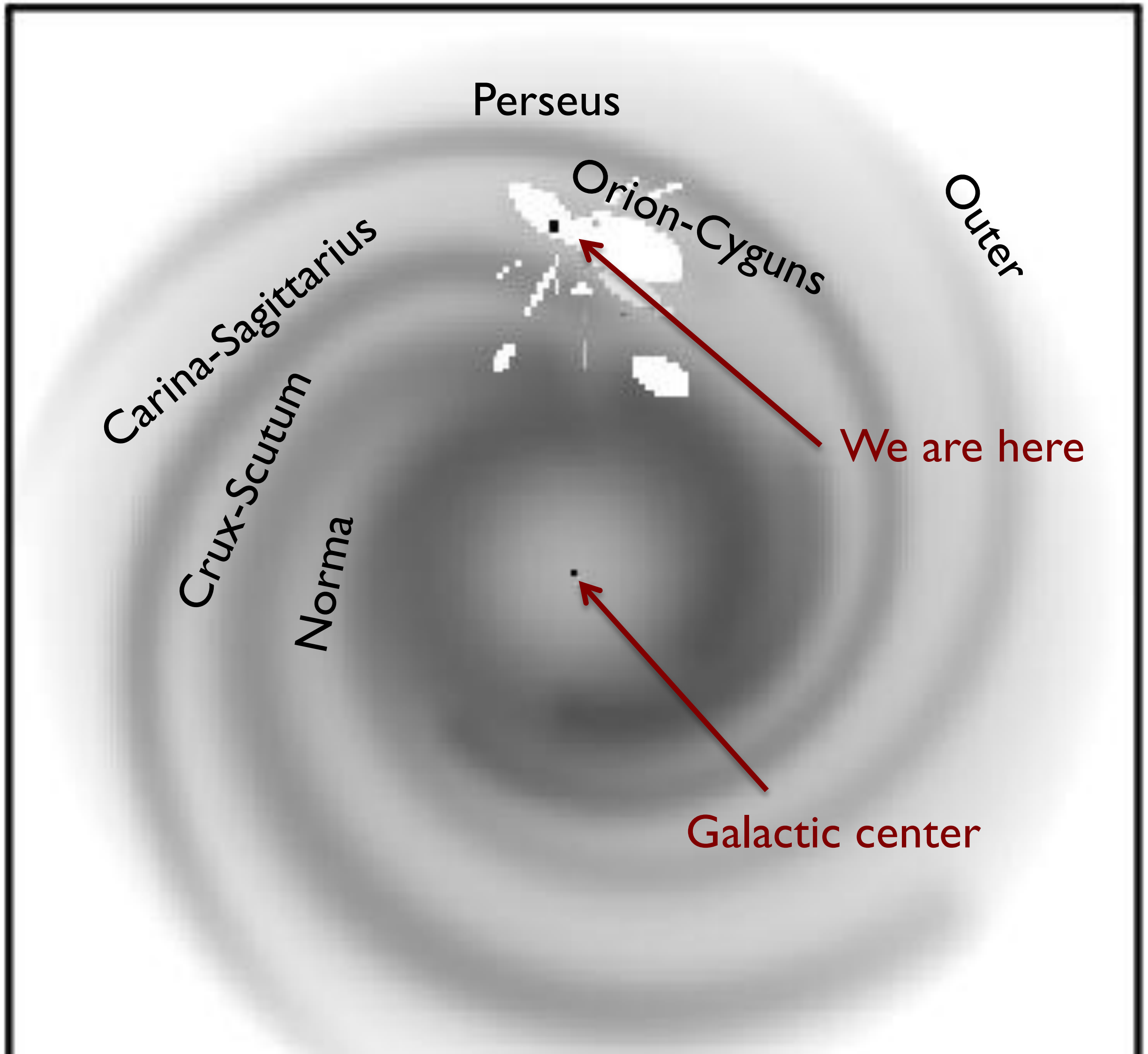

NE2001; Cordes & Lazio 03, see also Yao+ 17

Greyscale with log levels
30 × 30kpc at z=0

Structure components

- Thick & thin disks
- Spiral arms (incl. molec. ring)
- Galactic center comp.
- Local ISM
- Individual clumps & voids

Propagation effects

- Dispersion measure
- Pulse/Angular broadening
- Scintillation bandwidth
- Emission measure

Distance estimates

- HI absorption
- Parallax (interfero. or timing)
- Associations w/ GC or SNR

$DM_{\text{Milky Way, halo}}$

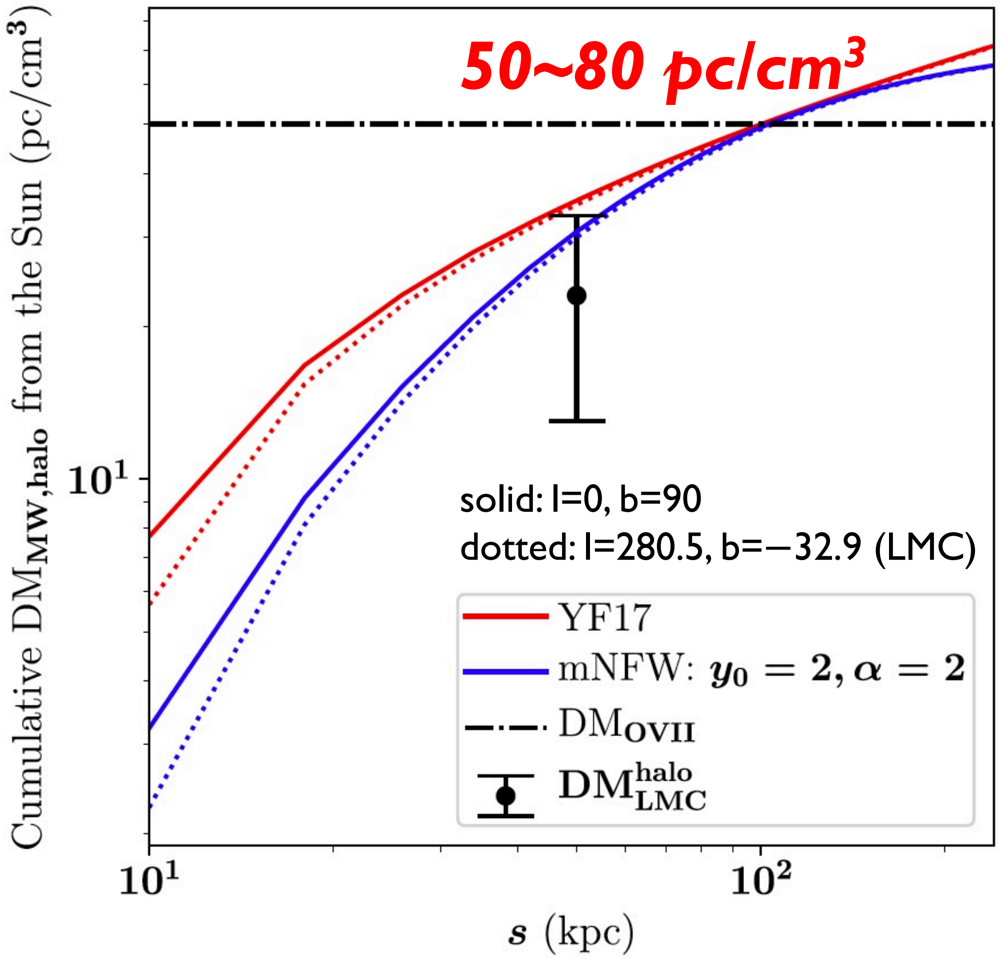

high-velocity clouds, O_{VII} abs., DM_{LMC}
hydrostatic gas

Prochaska & Zheng 19

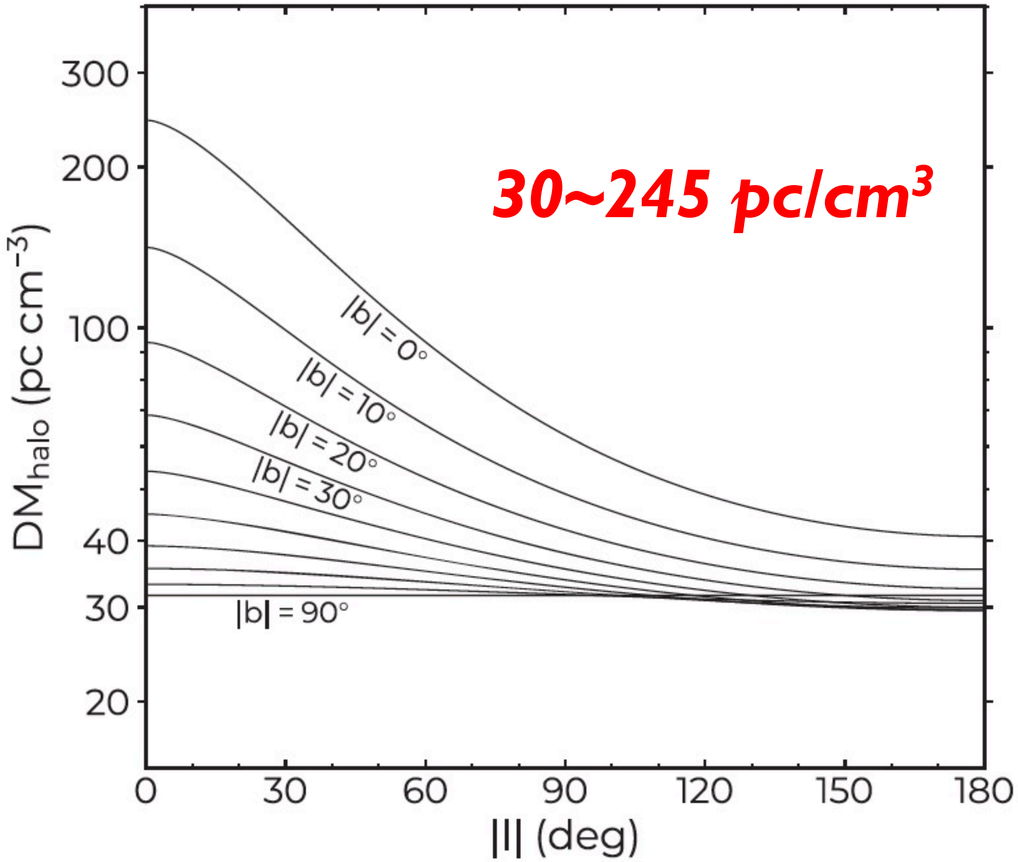

EM_X: spherical + disk-like hot gas

Yamasaki & Totani 20

see also Dolag+ 15, Platts+ 20

Observed DM-z

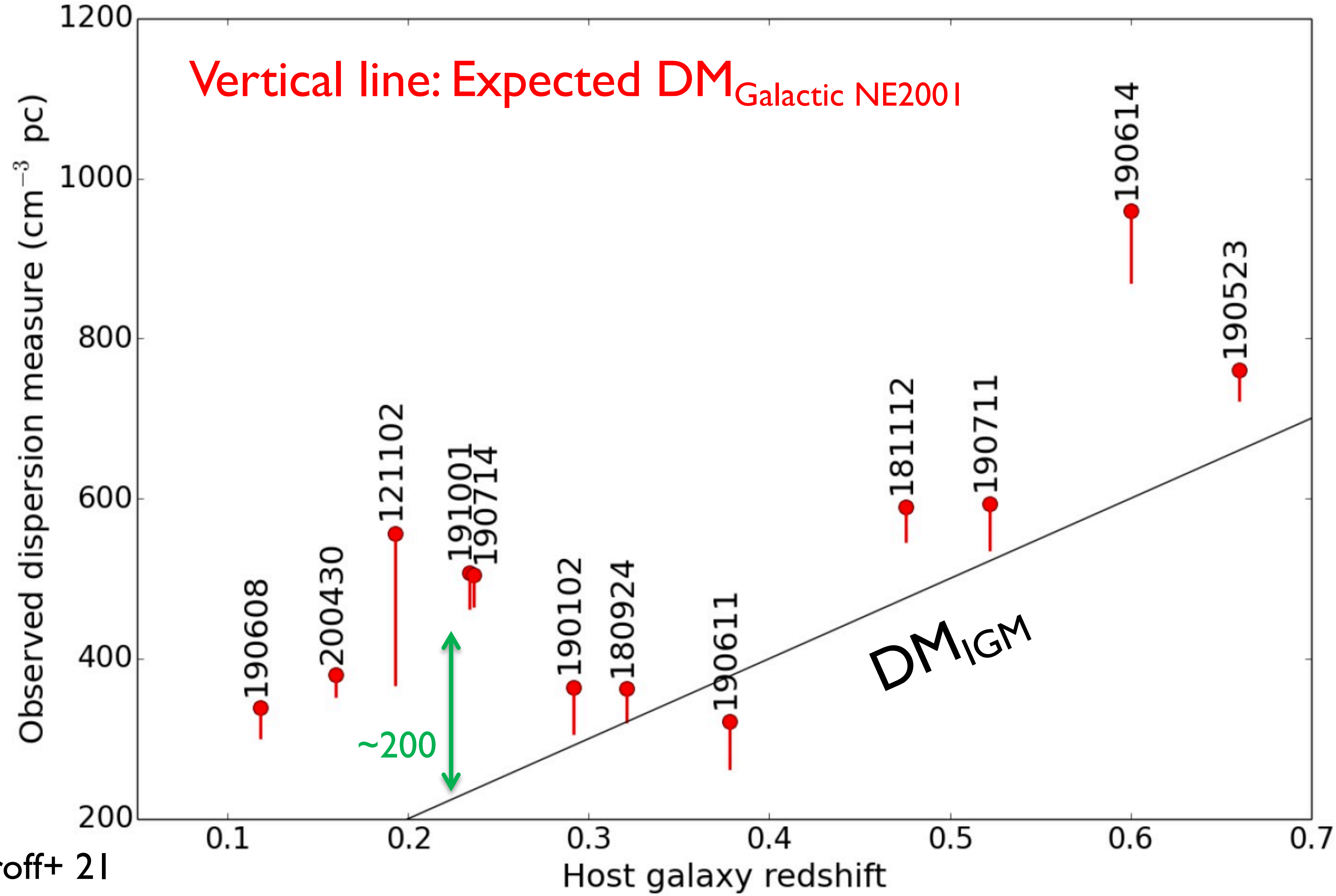

Petroff+ 21

FRB in a Globular Cluster

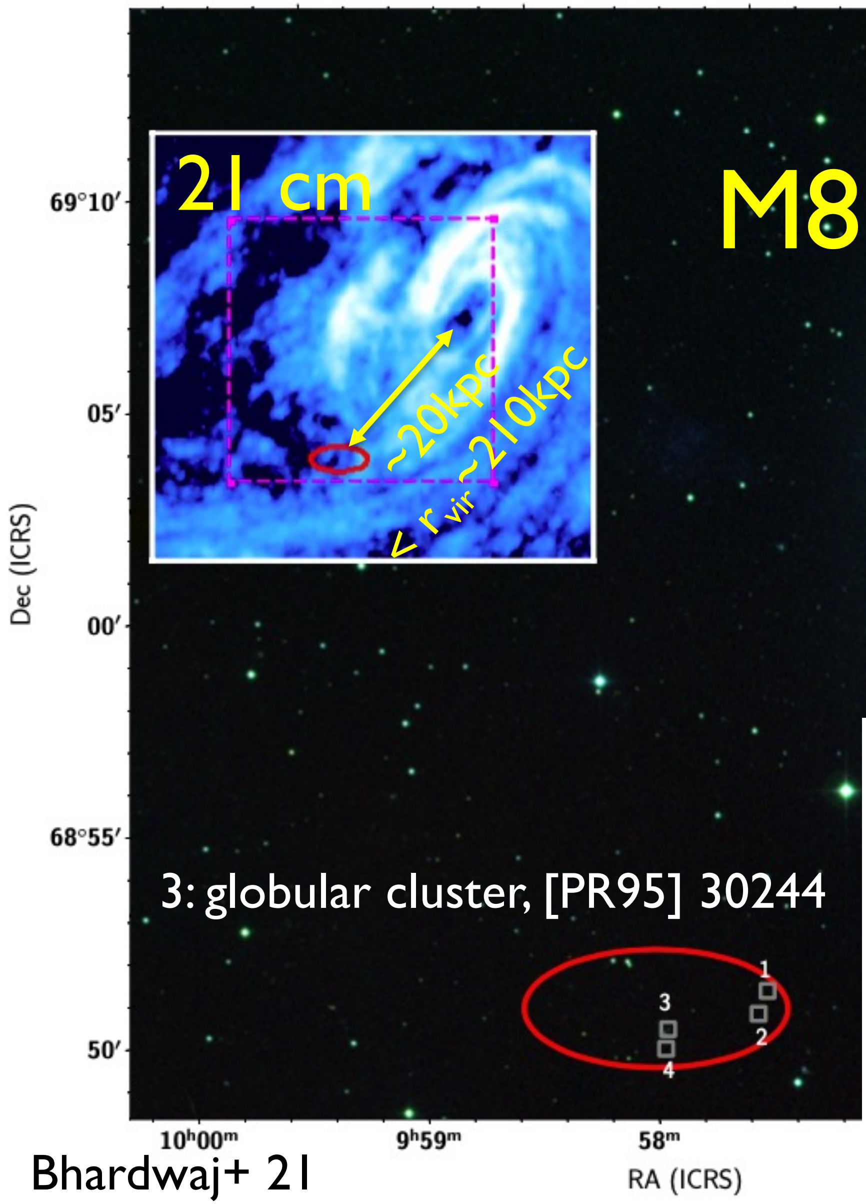

Bhardwaj+ 21

Not a magnetar?
or Accretion
-induced collapse?

Table 3. Notable properties of [PR95] 30244.

Property	Value	Reference
Metallicity $\log[Z/Z_\odot]$	$-1.79^{0.84}_{-0.85}$	this work
Metallicity [Fe/H]	$-1.83^{0.86}_{-0.87}$	this work
Stellar mass $\log[M/M_\odot]$	$5.78^{0.19}_{-0.22}$	this work
Effective radius (R_{eff}; kpc)	3.7	this work
Mass-weighted age (Gyr)	$9.13^{3.27}_{-4.18}$	this work
$(u-r)_0^a$ (AB mag)	1.96(2)	Alam et al. (2015a)
E(V-B)[b]	$0.19^{0.09}_{-0.10}$	this work
σ_r (km s^{-1})	22	this work
Absolute r-band mag. (AB)	−8.4	–
Luminosity distance (Mpc)	3.6	Karachentsev (2005)

[b] Milky Way extinction is corrected using the reddening map by Schlegel et al. (1998).
[c] Using $R_v = 3.1$.

Kirsten+ 21

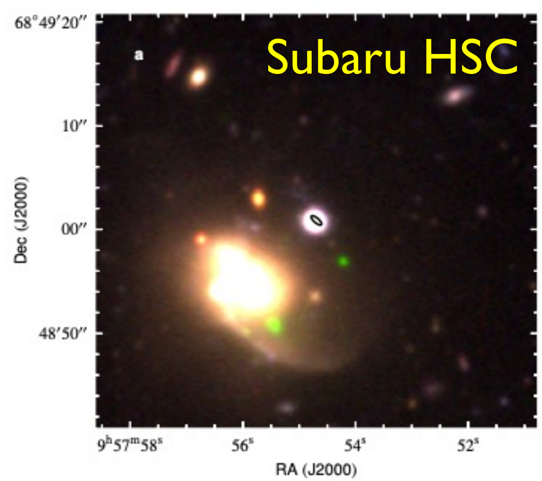

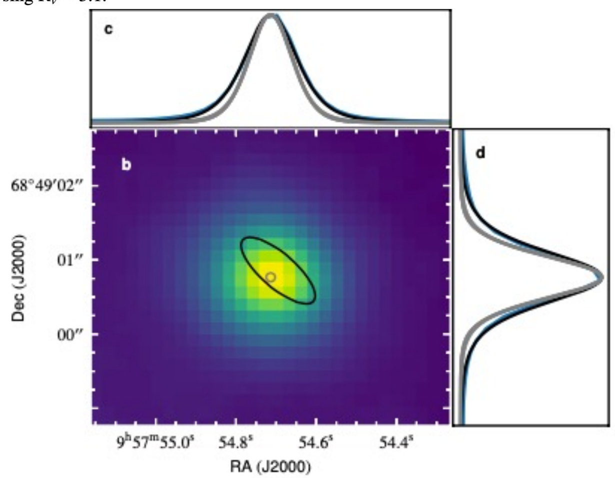

Low DM_{host}

DM_{M87} for $r \gg r_{M87}$

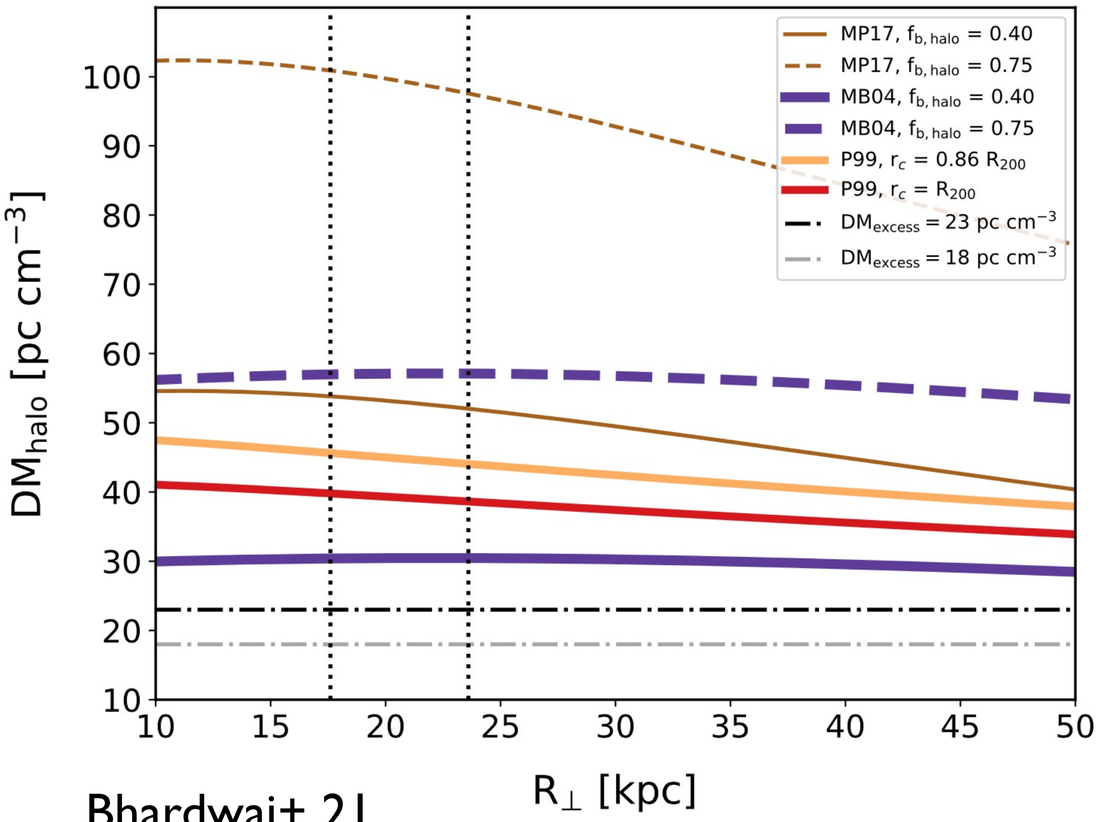

Bhardwaj+ 21

DM = 88 pc cm-3

$DM_{MW,ISM}$ = 35-40

$DM_{MW,halo}$ ~ 30

DM_{cosmic} ~ 1

DM_{M87} ~ 20

$DM_{MW,halo} < 55$

If we can select such FRBs, we can do better cosmology

M87 FRB is Nano Second

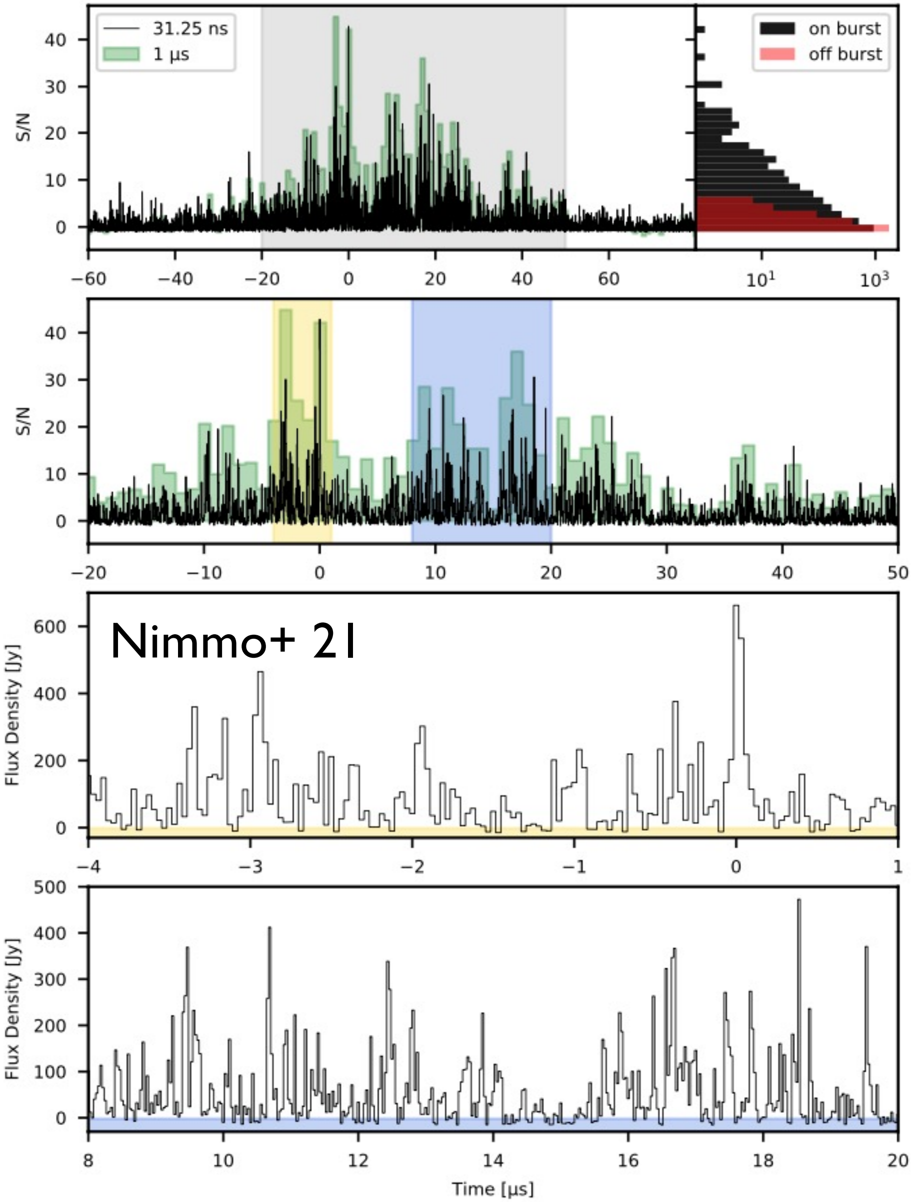

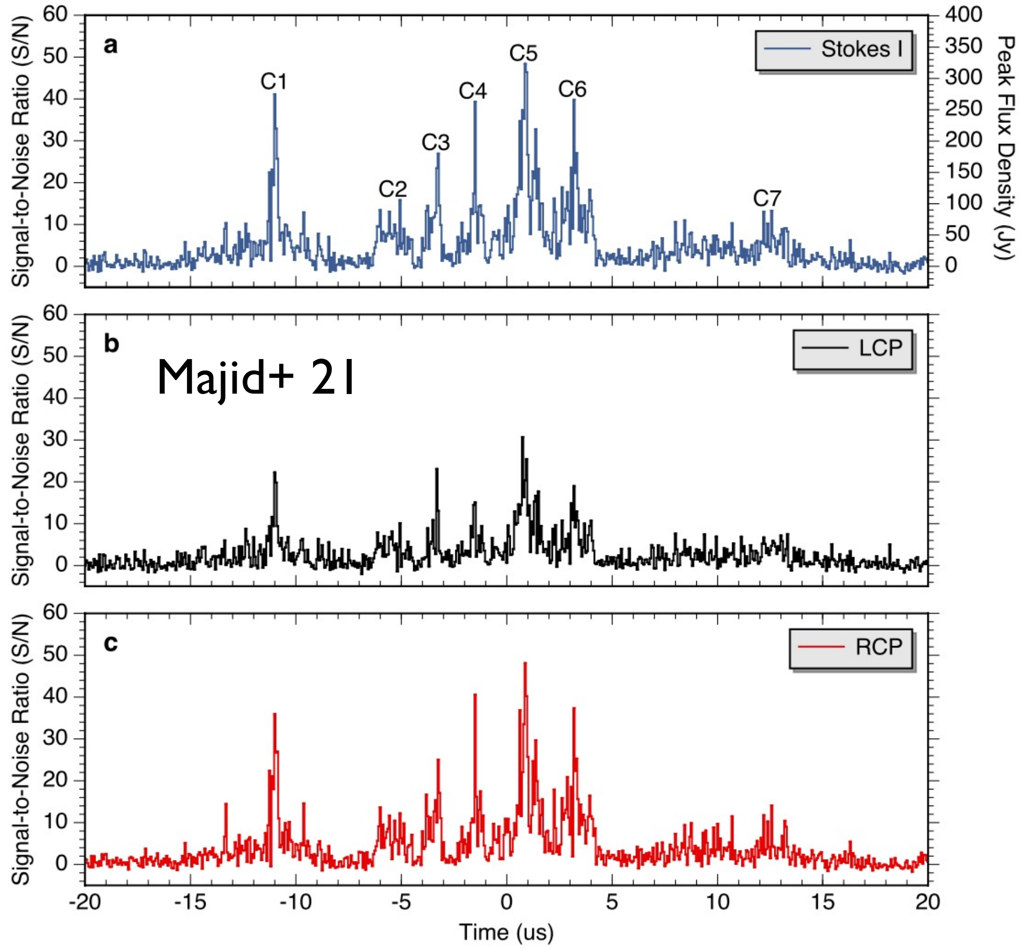

Δt < 62.5 ns!!

* CHIME abandons Δt<~ms

M87 FRB

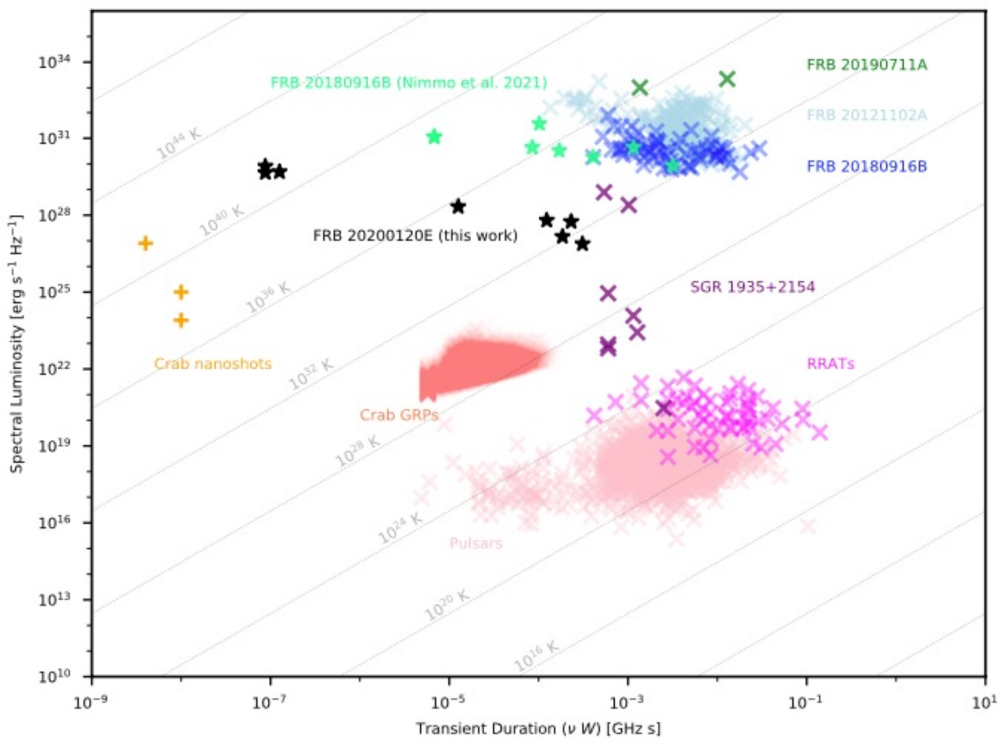

Nimmo+ 21

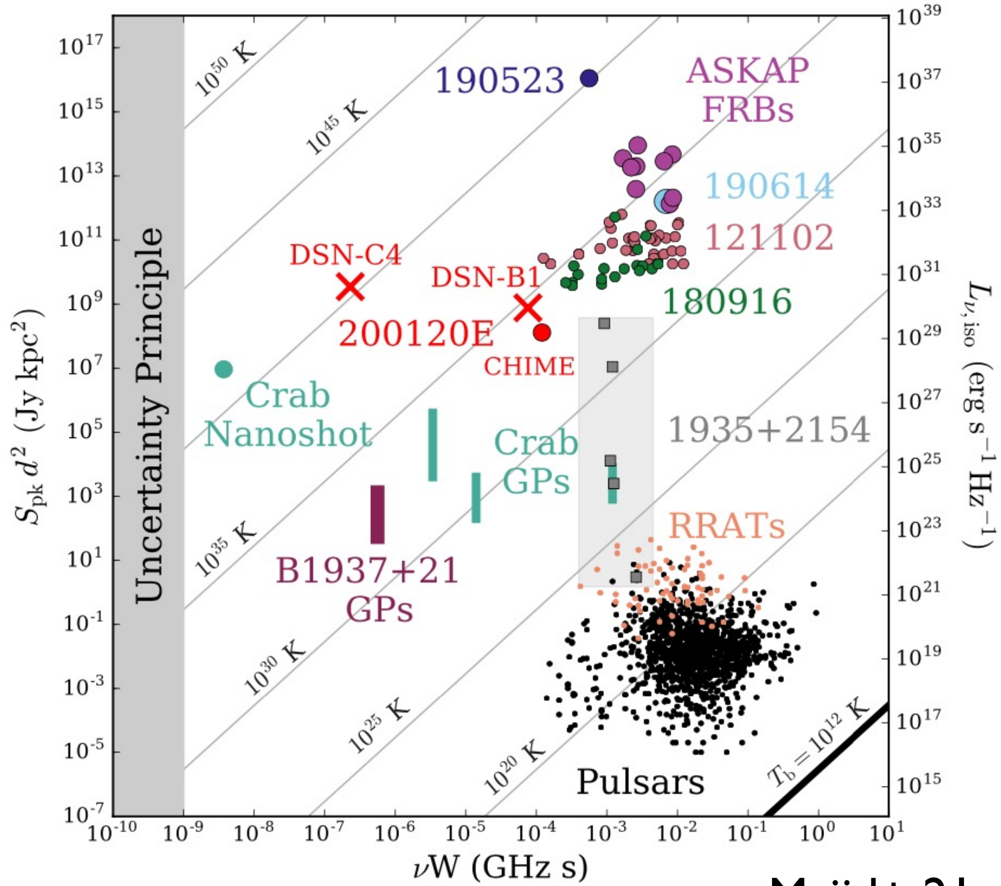

Majid+ 21

between ~Crab nanoshot & extragalactic FRBs?

* CHIME abandons Δt<~ms

Very High DM_{host}

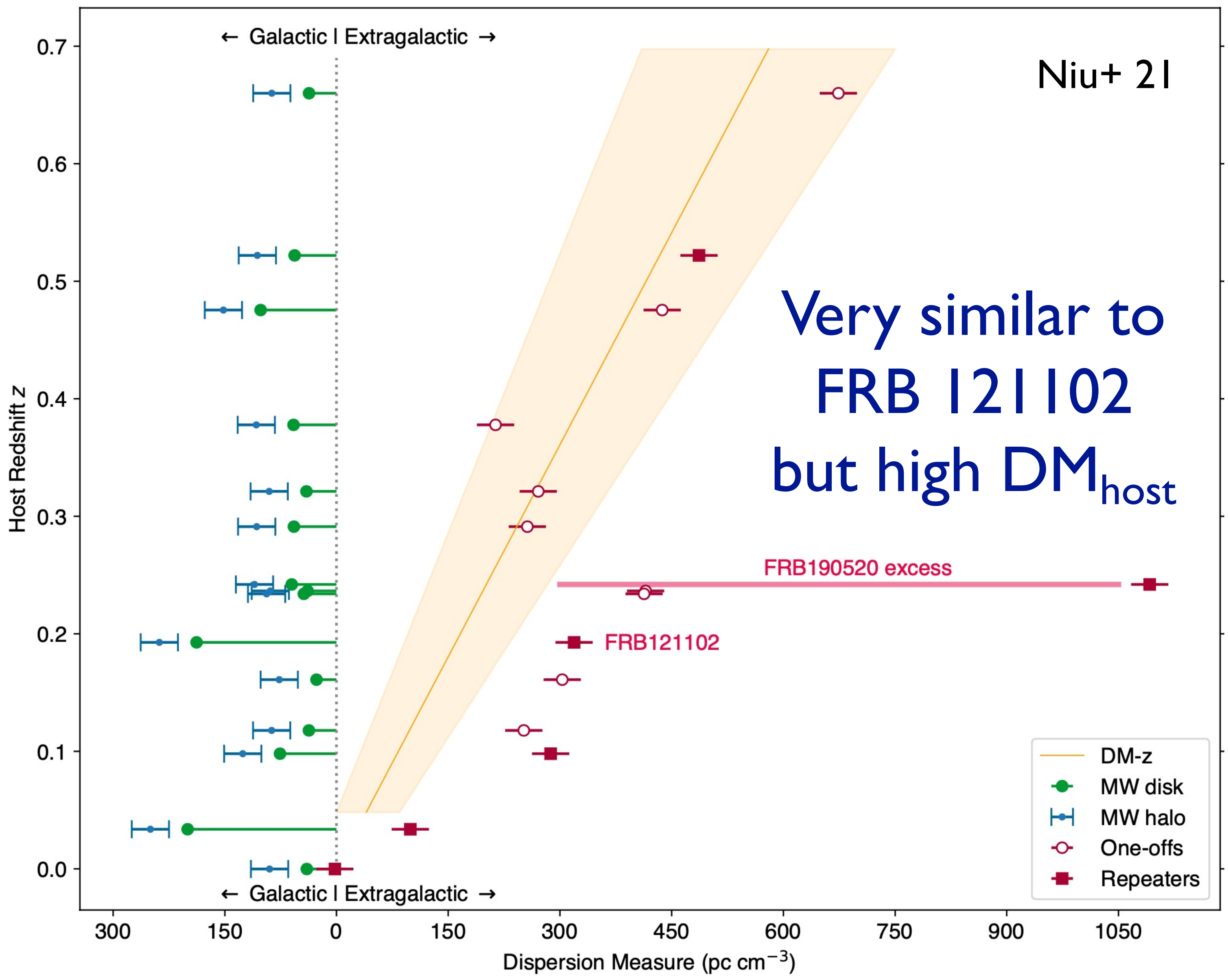

Table 1: Properties of FRB 190520B

Source name	FRB 190520B
Measured Parameters	
Right Ascension (J2000)	$16^h02^m04^s.266$
Declination (J2000)	$-11°17'17''.33$
Galactic Coordinates (l, b)	$359°.67, 29°.91$
Number of detections[a]	81
Dispersion Measure (pc cm^{-3})	1210.3±0.8
Measured width (ms)	13.5±1.2
Scattering timescale (ms) at 1.25GHz	9.8 ± 2
Scintillation bandwidth (MHz) at 1.4GHz	0.29 ± 0.15
Measured fluence (Jy ms)	0.03 to 0.33
DM_{MW} (pc cm^{-3})[b]	60 , 50
DM_{host} (pc cm^{-3})	902^{+88}_{-128}
Luminosity distance (Mpc)	1218
Isotropic energy (10^{37} erg)	3.6 to 40
Persistent Radio Source	
Right Ascension (J2000)	$16^h02^m04.259^s$
Declination (J2000)	$-11°17'17.38''$
Flux at 3.0 GHz (μJy)	202 ± 8
Host galaxy	
redshift (z)	0.241 ± 0.001
$M_\odot$ [c]	$\sim 6 \times 10^8$
Hα luminosity(10^{40} erg sec^{-1})	7.4 ± 0.2
SFR (yr^{-1}) [d]	~ 0.41 $M_\odot$

High z host dependence

$$\mathrm{DM_{host}} \propto (1+z) \times (1+z)^{-2}$$

Time dilation

Redshift

DM $\propto \nu^{-2}$

Negligible at high redshift

Contents

- ***Introduction & History***
  - Dispersion measure
  - FRB repeaters & Host galaxies
  - Galactic FRB from a magnetar
- ***Host galaxies***
  - Diversity, Dwarf, Spiral, Globular cluster, …
- ***FRB cosmology***
  - DM, Cross-correlation, Lensing, RM, SM, …

FRB Cosmology

KI 03, Inoue 04

- Missing baryon Ω_b
- Reionization
- Cosmological parameters, H_0, Ω_m, Ω_Λ

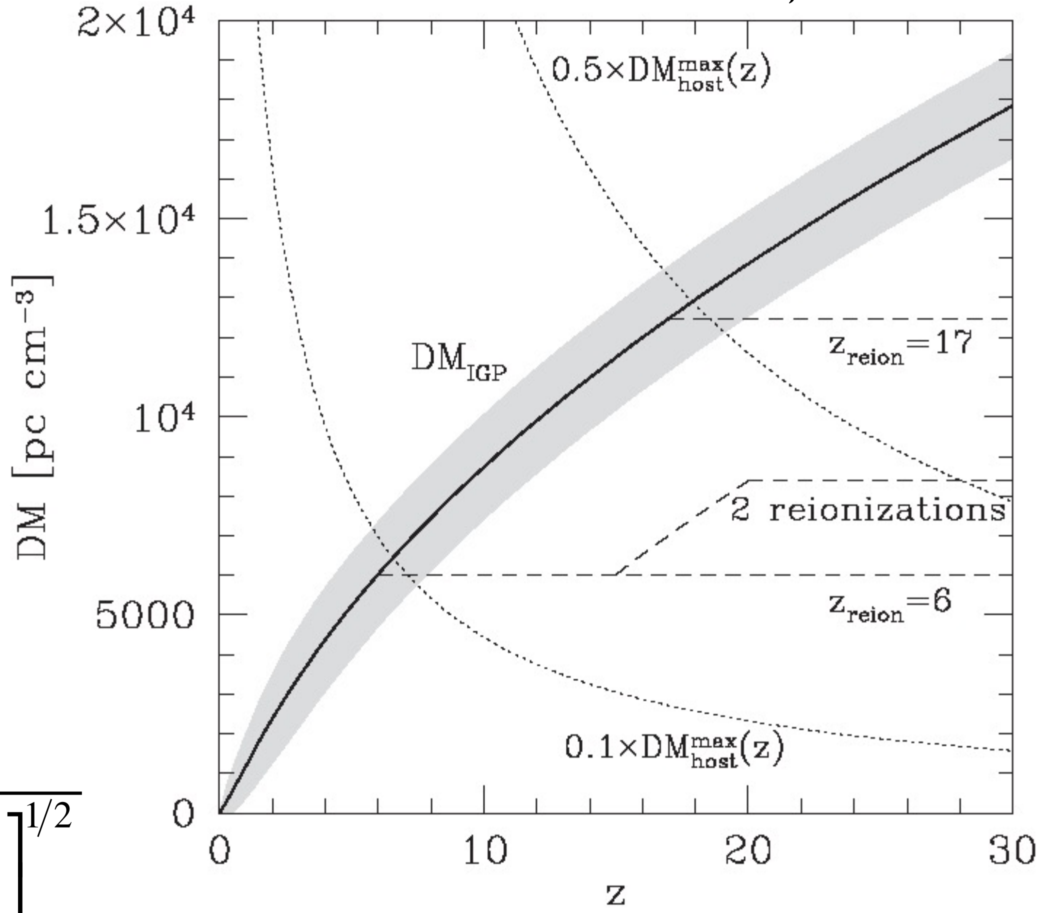

$$DM_{IGP} = \frac{3cH_0\Omega_b}{8\pi G m_p}\int_0^z \frac{(1+z)\,dz}{\left[\Omega_m(1+z)^3+\Omega_\Lambda\right]^{1/2}}$$

$$d_L = \frac{c(1+z)}{H_0}\int_0^z \frac{dz}{\left[\Omega_m(1+z)^3+\Omega_\Lambda\right]^{1/2}}$$

Fast radio bursts as cosmological tools

New frontier!!

$\mathrm{DM}_{\mathrm{cosmic}}$

$$\mathrm{DM}(\boldsymbol{\theta}; z_s) = \int_0^{z_s} \frac{c dz}{H(z)} n_e(\boldsymbol{r}; z)(1+z).$$

$$n_e(\boldsymbol{r}; z) = \bar{n}_e(z)\,[1 + \delta_e(\boldsymbol{r}; z)]$$

fluctuation

$$\bar{n}_{e,\mathrm{total}} = \left(X_p + \frac{1}{2} Y_p\right) \frac{\bar{\rho}_b}{m_p}$$

H He

$$\bar{n}_e(z) = f_e(z)\,\bar{n}_{e,\mathrm{total}}$$

free electron fraction

$$\mathrm{DM}(\boldsymbol{\theta}; z_s) = \overline{\mathrm{DM}}(z_s) + \delta\mathrm{DM}(\boldsymbol{\theta}; z_s)$$

Takahashi, KI, Mori & Funahashi 21

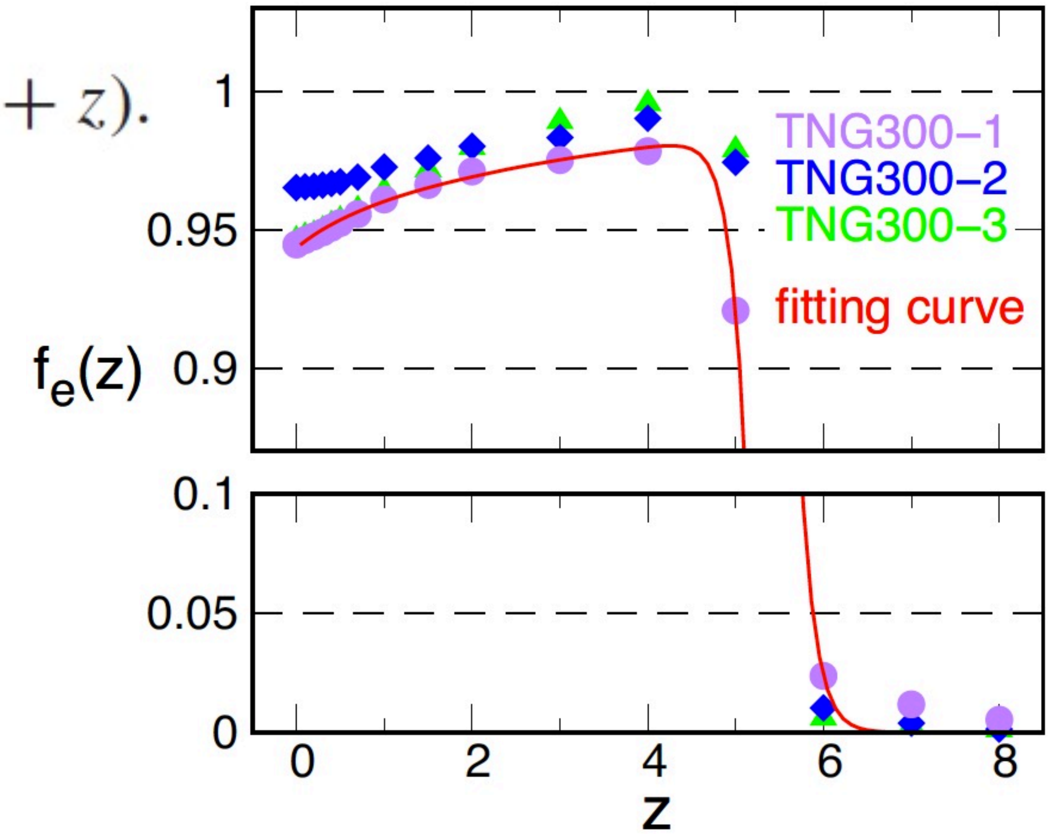

H reionized @z~6
He II reionized @z~3
e into * & BH @z<3

DM from IllustrisTNG

Nelson+ 19

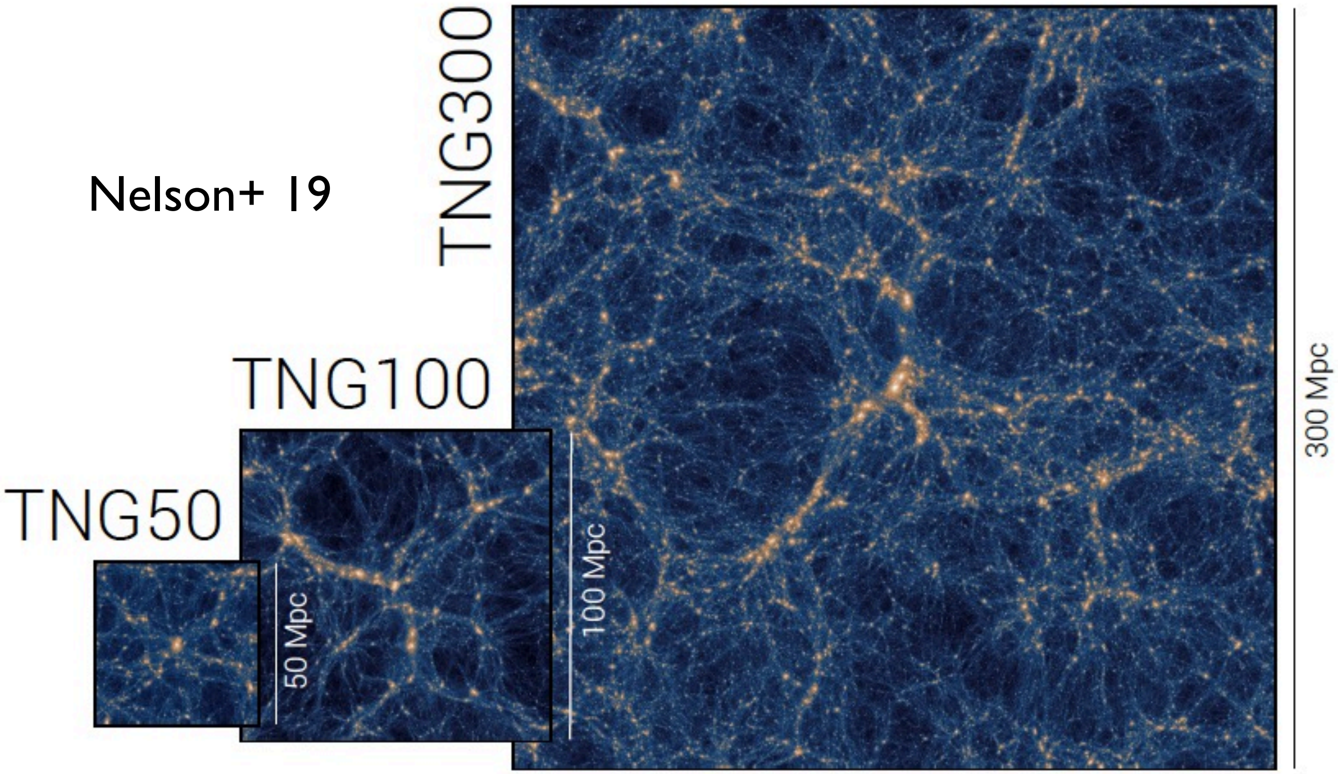

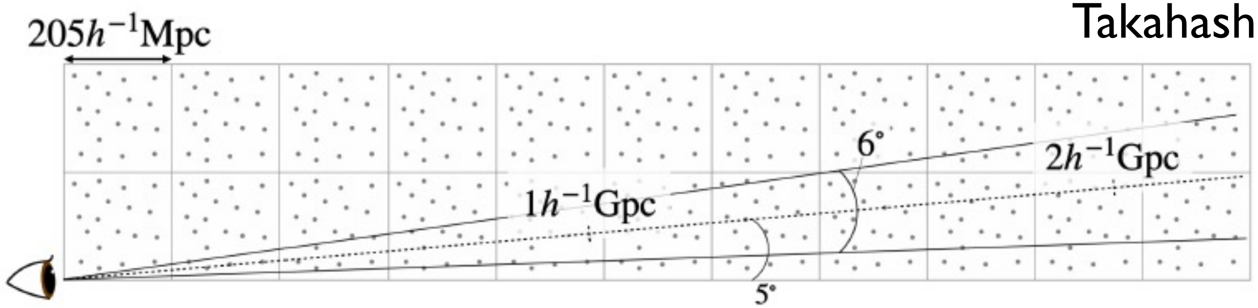

Takahashi+ 21

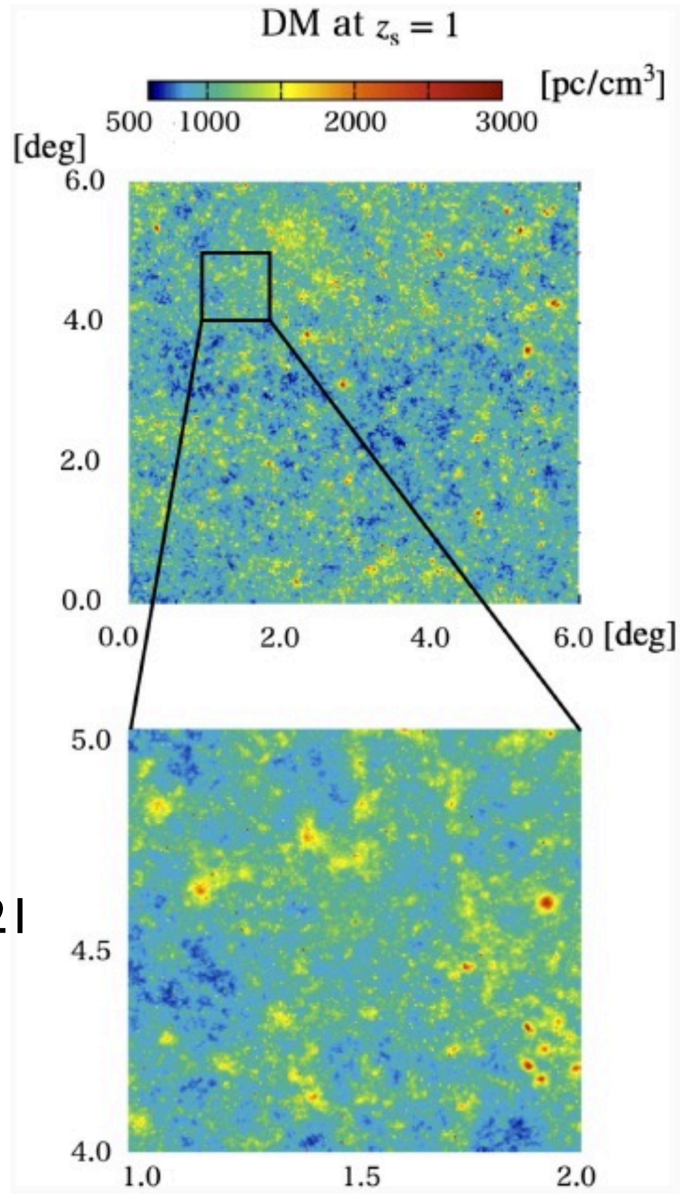

DM_{cosmic} & σ_{DM}

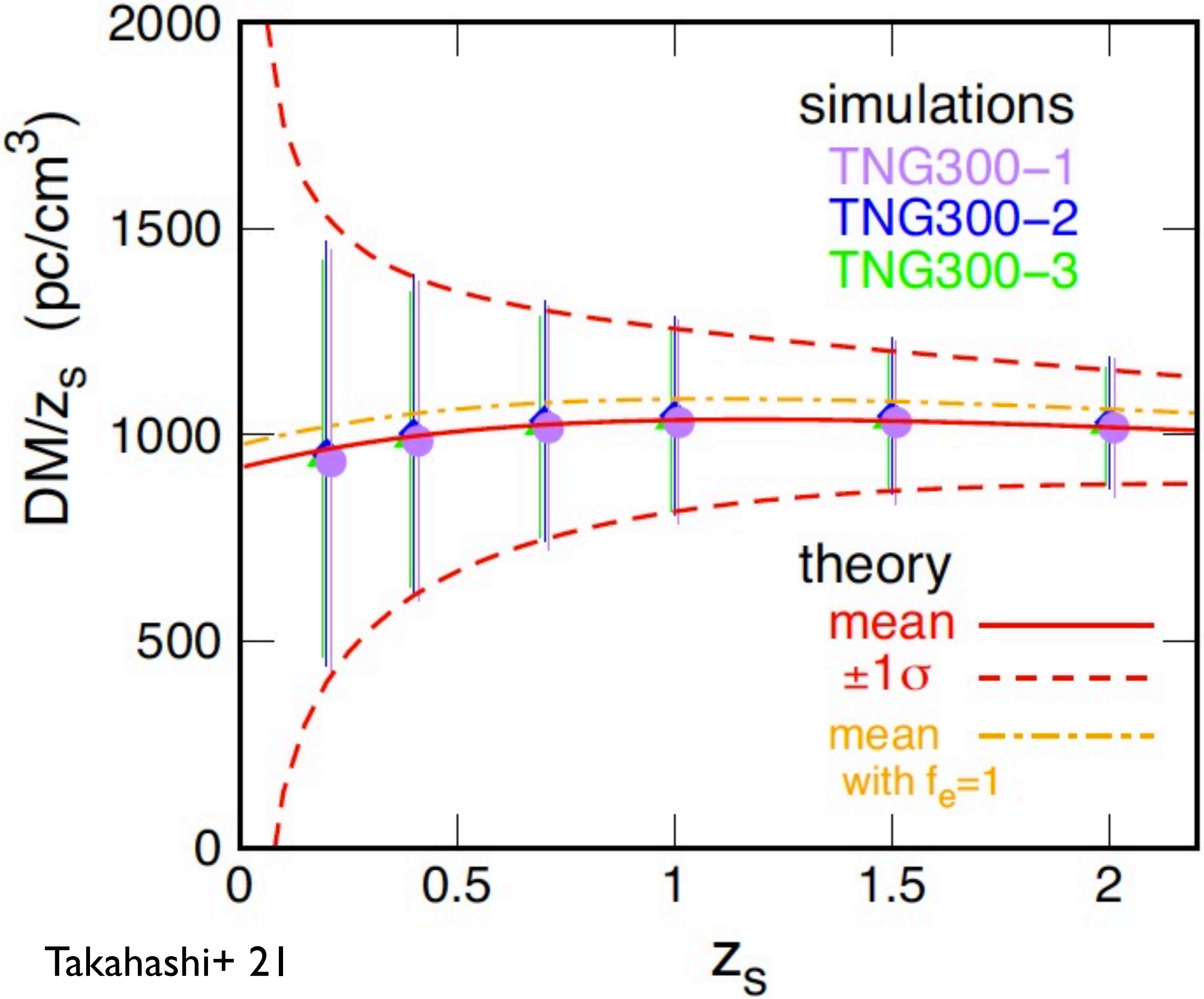

Takahashi+ 21

$DM \sim 1000z$

$\sigma_{DM} \sim 230z^{1/2}$

See Takahashi+ 21 for theoretical curves

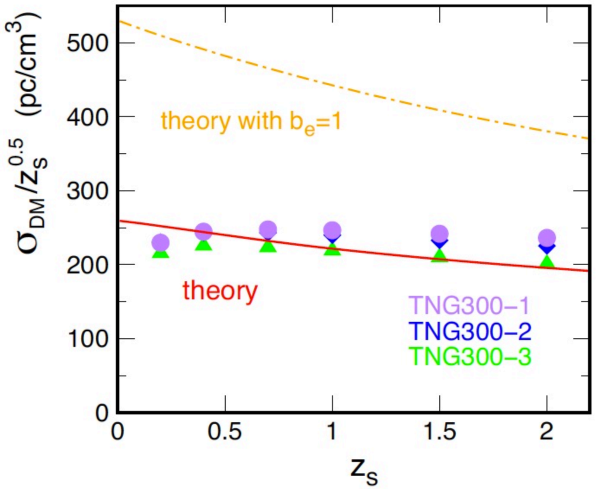

What Determines σ_{DM}?

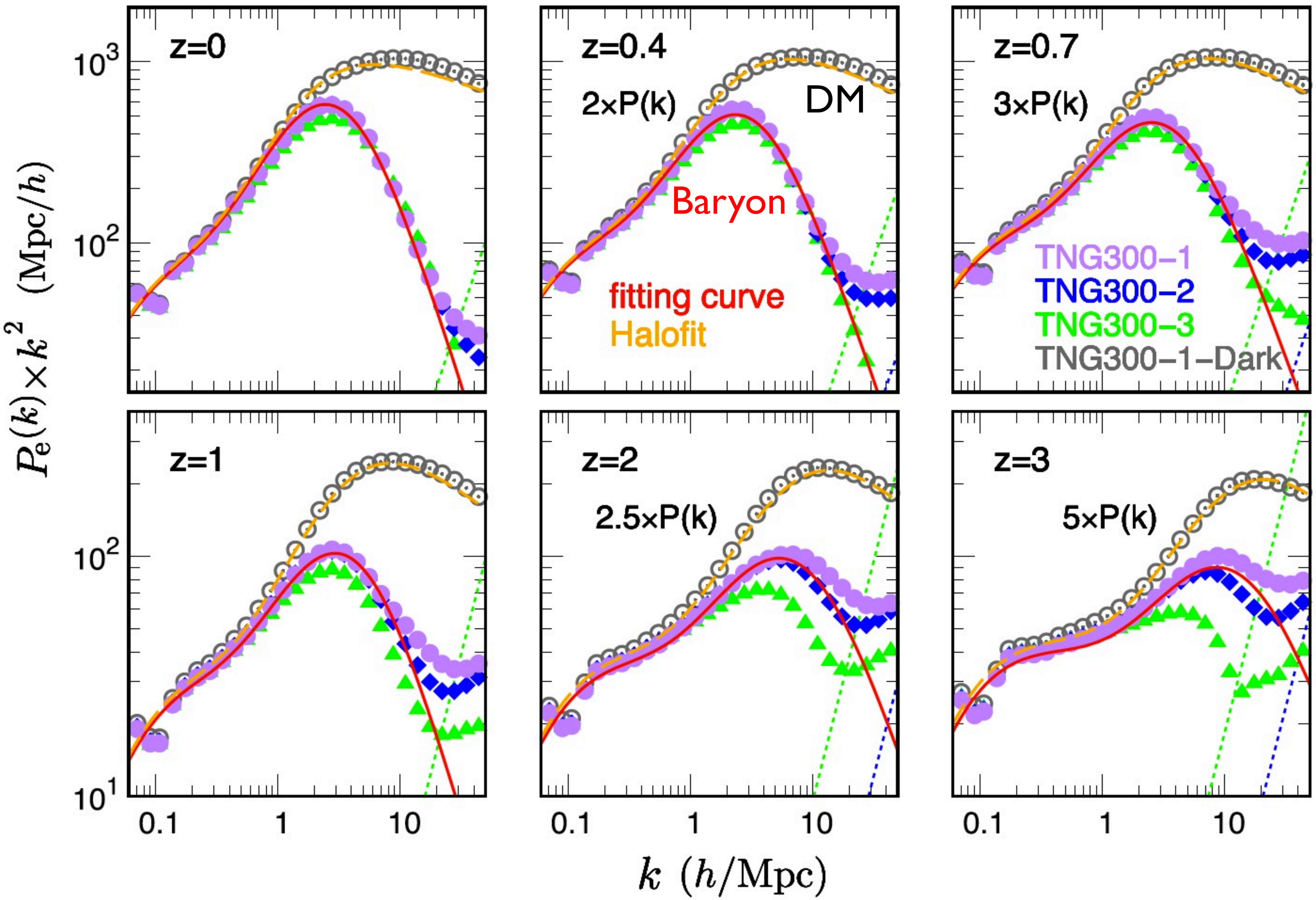

* & AGN feedbacks suppress <Mpc power

affect σ_{DM} by 2x

fitting curve = Halofit + correction

Order Estimate

$$\mathrm{DM} \sim \frac{3cH_0\Omega_b}{8\pi G m_p}\int_0^z \frac{(1+z)dz}{[\Omega_m(1+z)^3+\Omega_\Lambda]^{1/2}}$$

$$\sim \frac{3cH_0\Omega_b}{8\pi G m_p} z$$

$$\sim 1000\, z$$

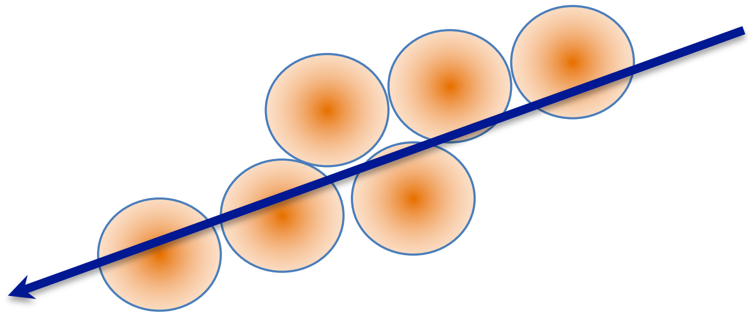

$$\sigma_{\mathrm{DM}} \sim \mathrm{DM}\frac{1}{\sqrt{N}}\frac{\delta\rho}{\rho}$$

$$\sim \mathrm{DM} \times \frac{1}{\sqrt{6z\,\mathrm{Gpc}/0.6\,\mathrm{Mpc}}} \times \frac{200}{2^3}$$

$$\sim 1000\, z \times \frac{1}{\sqrt{10000\, z}} \times 25$$

$$\sim 250\, z^{1/2}$$

DM Distributions

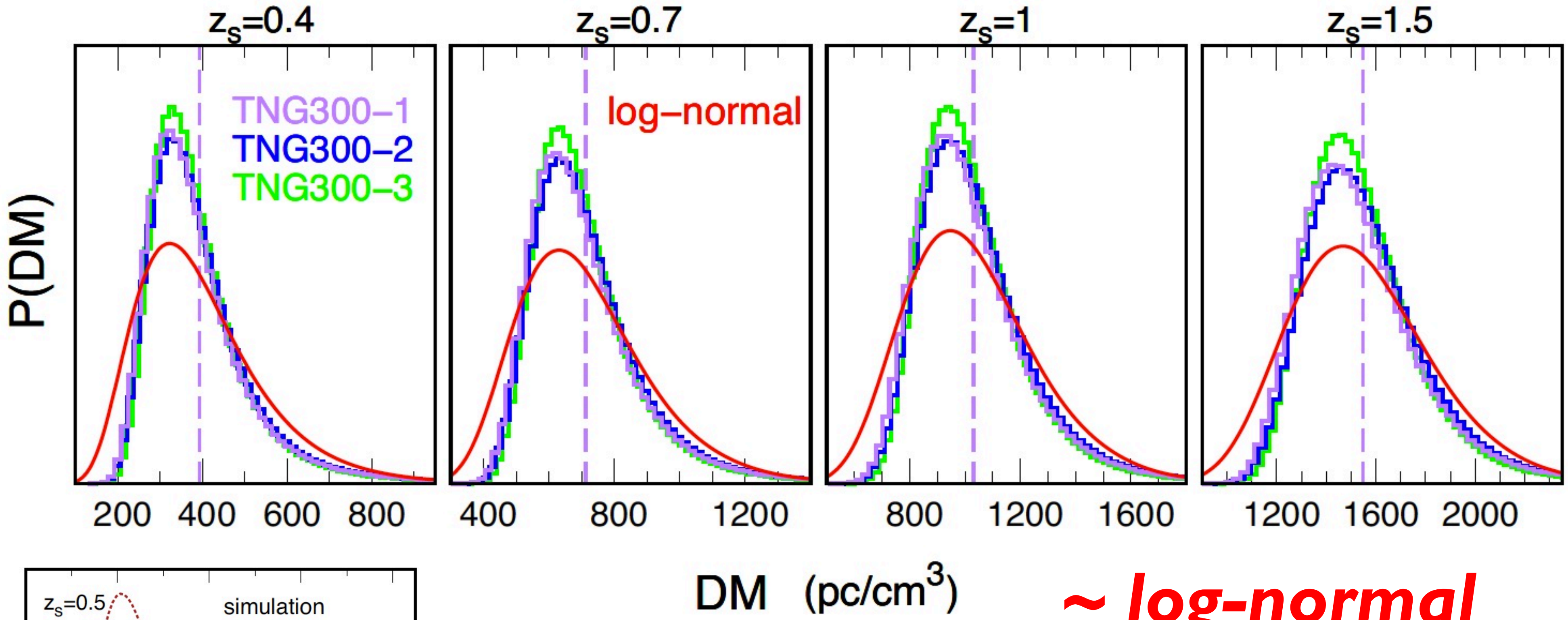

~ log-normal

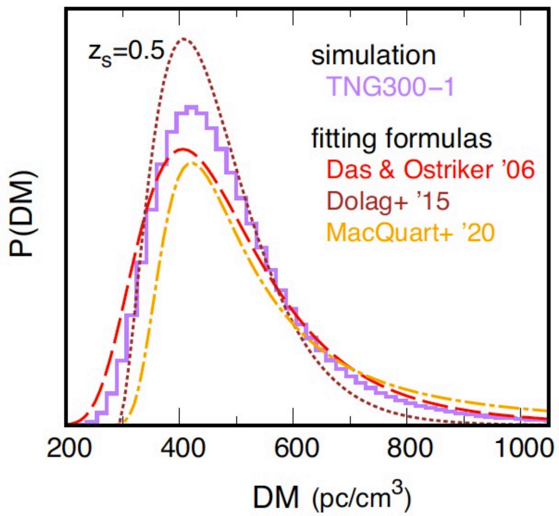

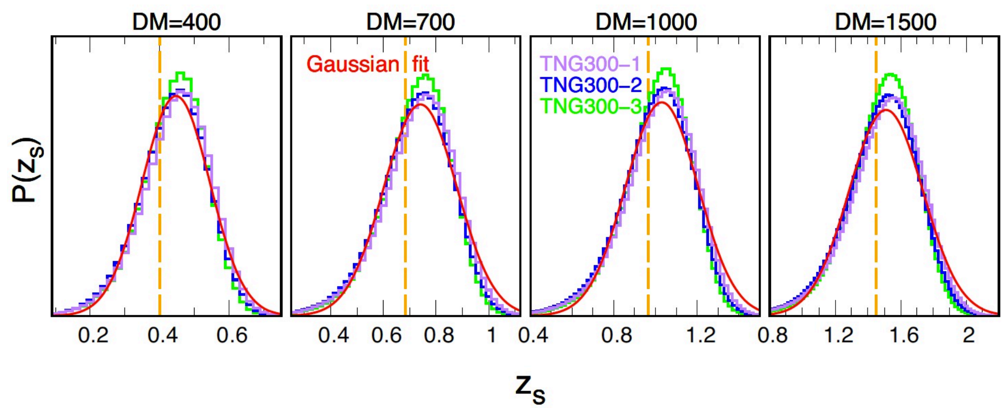

Takahashi+ 21

Cosmological Simulation

DM values from the NE2001 Model

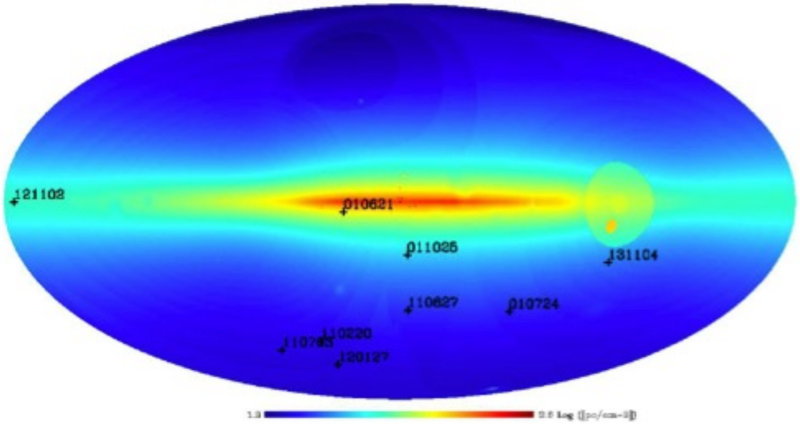

DM values from the simulated local universe out to 110 Mpc

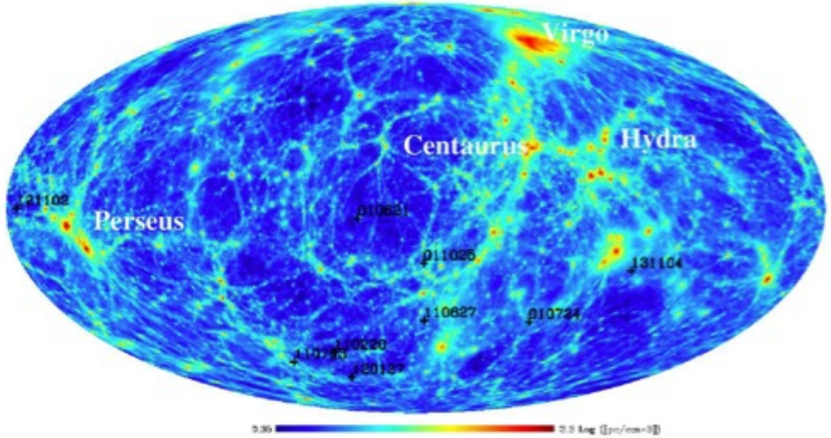

Dolag+14

DM values from a simulated galactic halo 5 kpc – 500 kpc

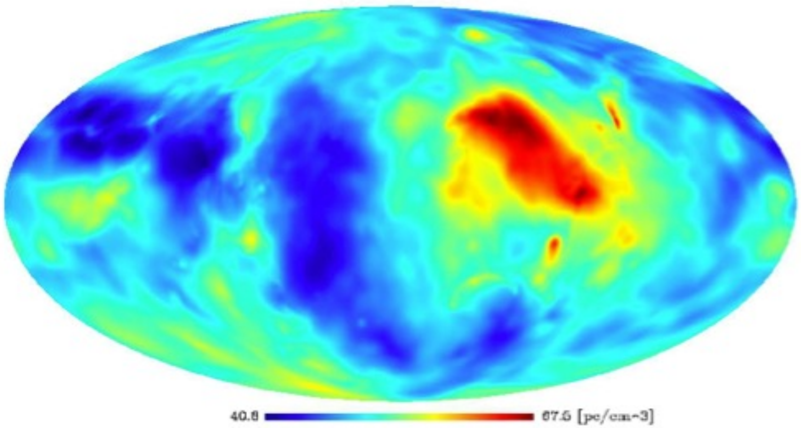

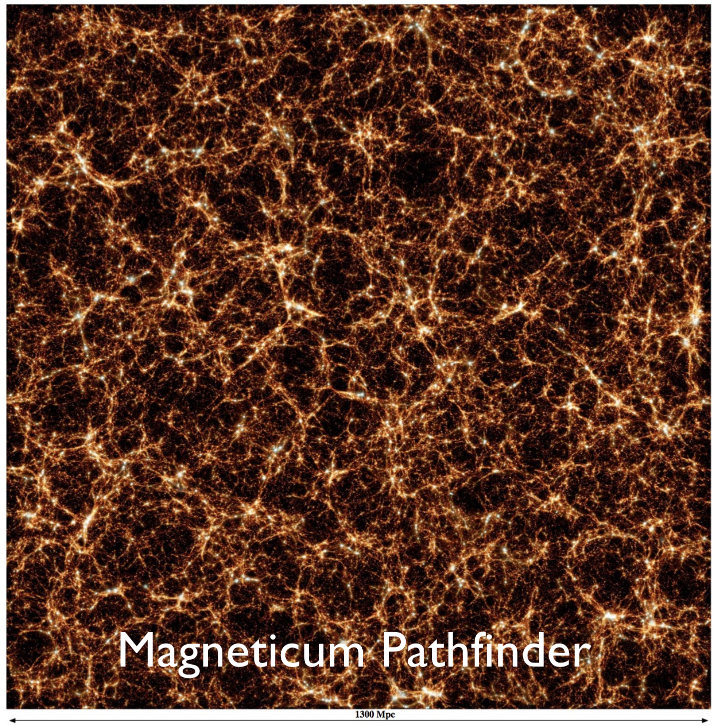

DM_{halo}~30pc/cc~DM_{Gal}

Distribution of DM_{cosmo}

DM Distribution

Dolag+14

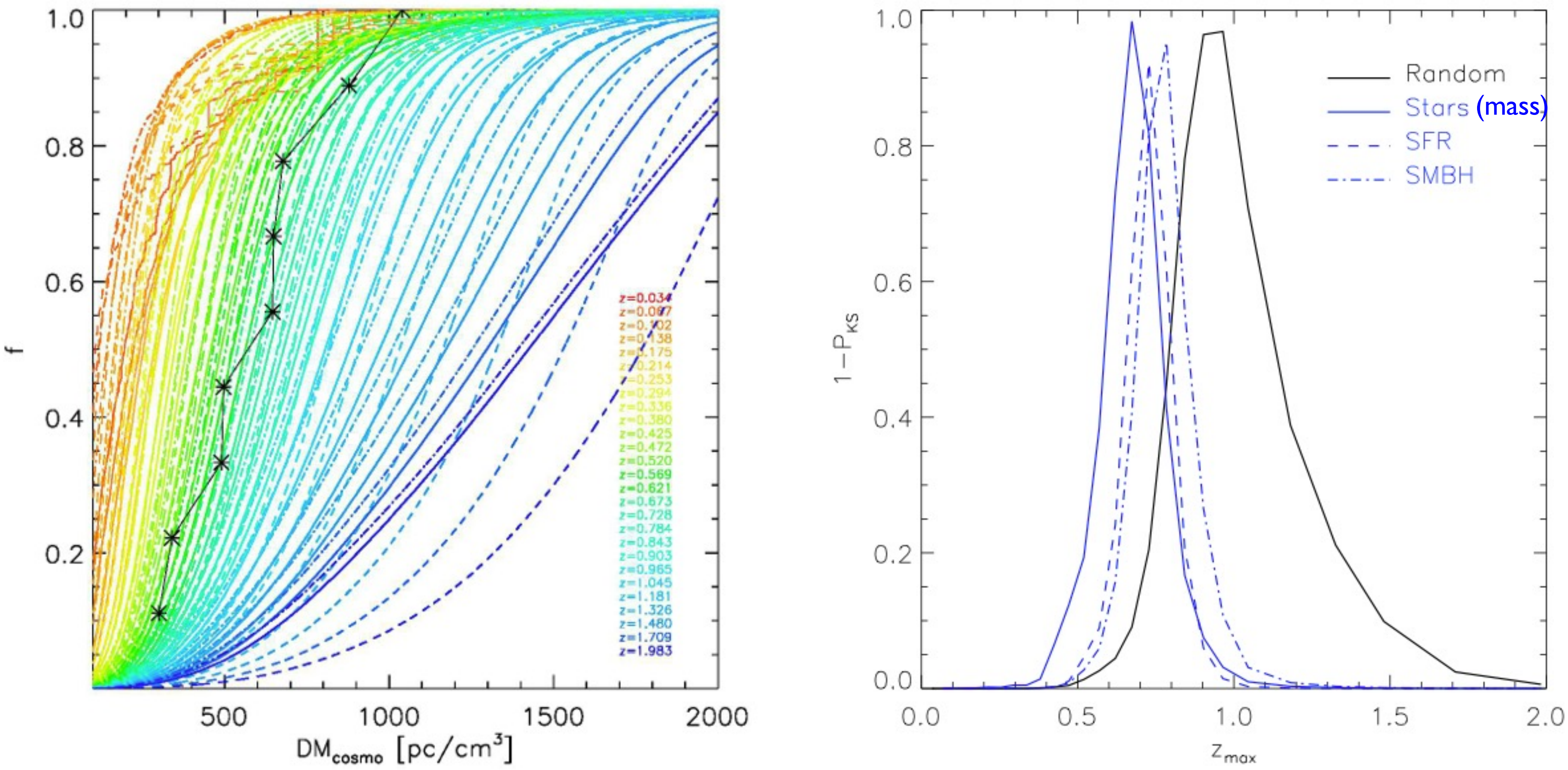

Distribution is consistent with extragalactic origin

see also Shirasaki+ 17, Pol+ 19, Jaroszynski+ 19 (Illustris)

Observed DM Distribution

CHIME/FRB 21

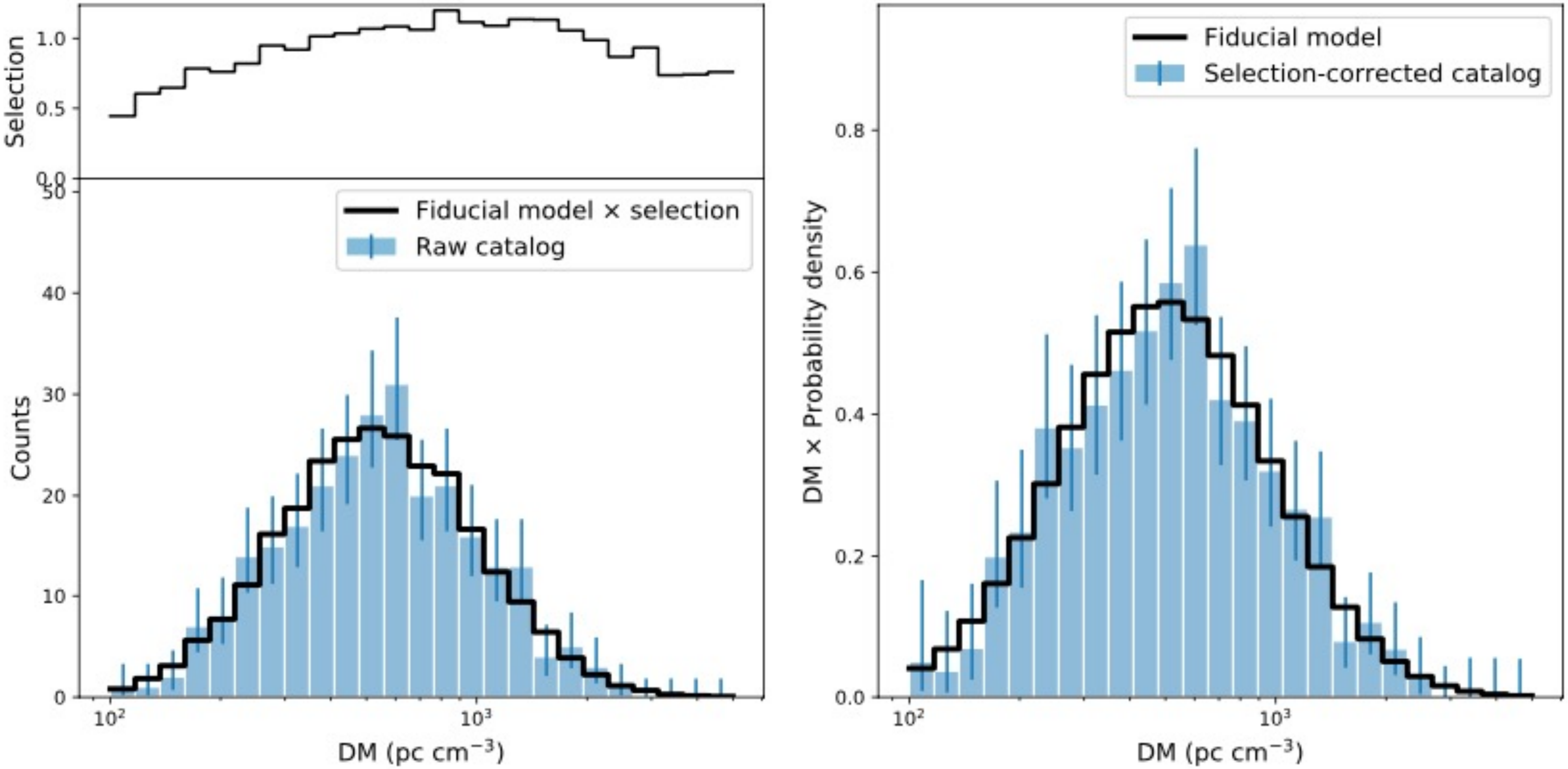

~ lognormal as expected

Macquart+ 20

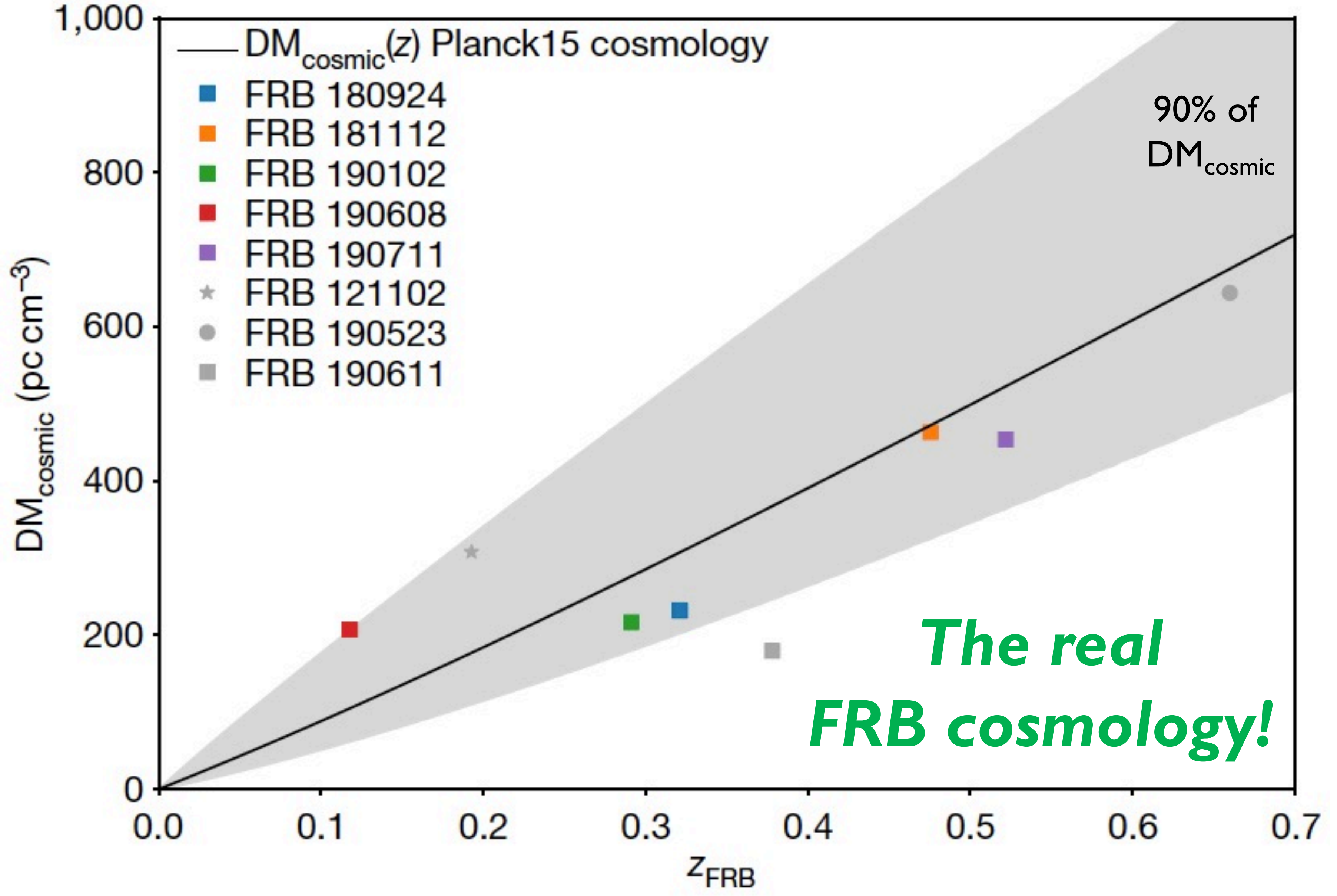
DMcosmic(z) Planck15 cosmology
FRB 180924
FRB 181112
FRB 190102
FRB 190608
FRB 190711
FRB 121102
FRB 190523
FRB 190611
90% of DMcosmic
DMcosmic (pc cm−3)
1,000
800
600
400
200
0
0.0
0.1
0.2
0.3
0.4
0.5
0.6
0.7
zFRB
The real FRB cosmology!

A Census of Baryons

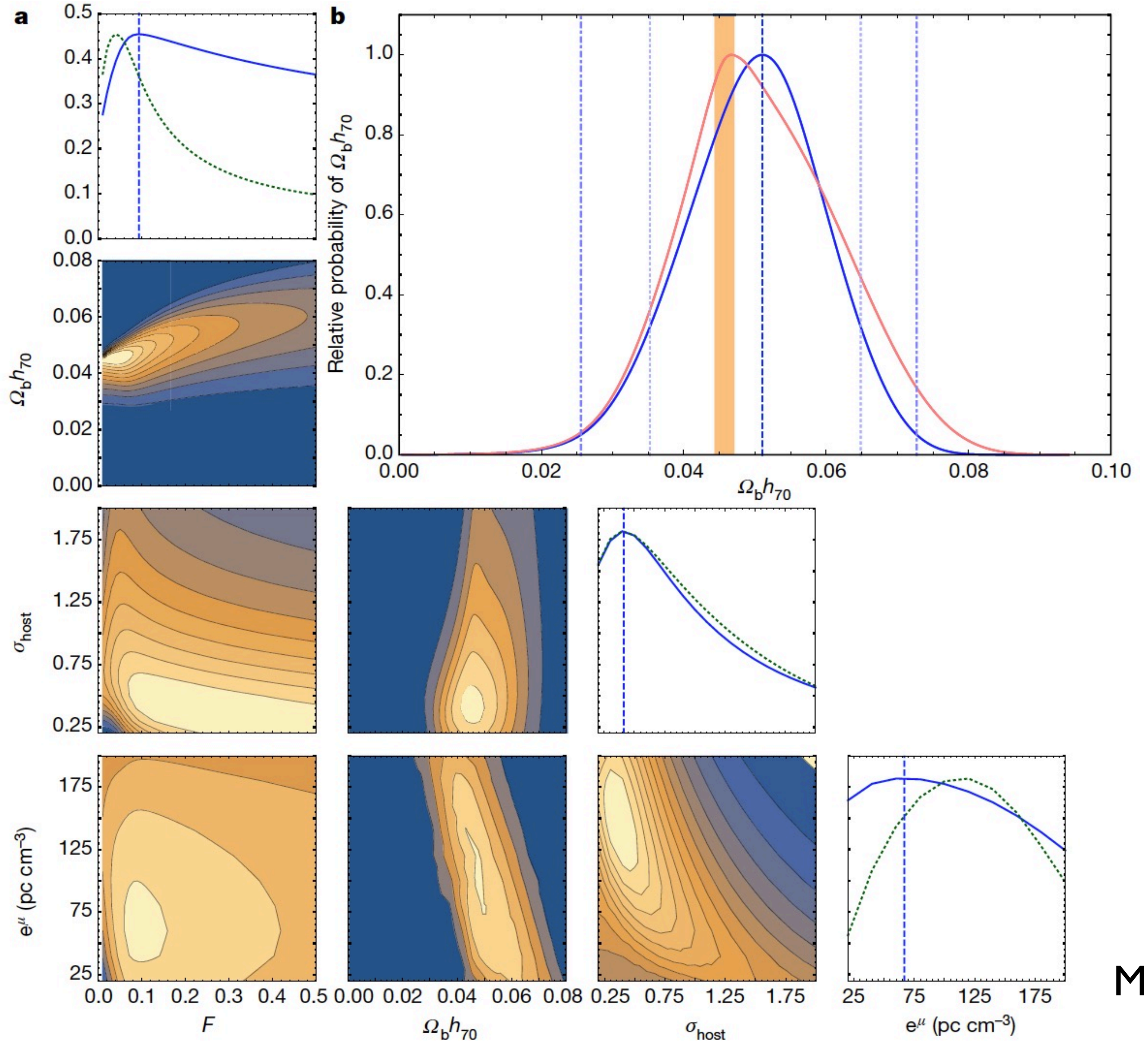

a:
DM_{host}: log-normal
median e^μ, log width σ_{host}
F: Baryon feedback
(0.1 strong, 0.4 weak)
Green dot: Ω_b=CMB+BBN
Contours: 10%

b:
Orange: CMB+BBN
Blue: F[0.09,0.32]
Red: F[0,0.5]
Dot, Dot-dashed: 68 & 95%

Macquart+ 20

Dark Energy & Ω_m

$$\mathrm{DM_{IGP}} = \frac{3cH_0\Omega_b}{8\pi G m_p}\int_0^z \frac{(1+z)\,dz}{\left[\Omega_m(1+z)^3+\Omega_\Lambda\right]^{1/2}}$$

$$d_L = \frac{c(1+z)}{H_0}\int_0^z \frac{dz}{\left[\Omega_m(1+z)^3+\Omega_\Lambda\right]^{1/2}}$$

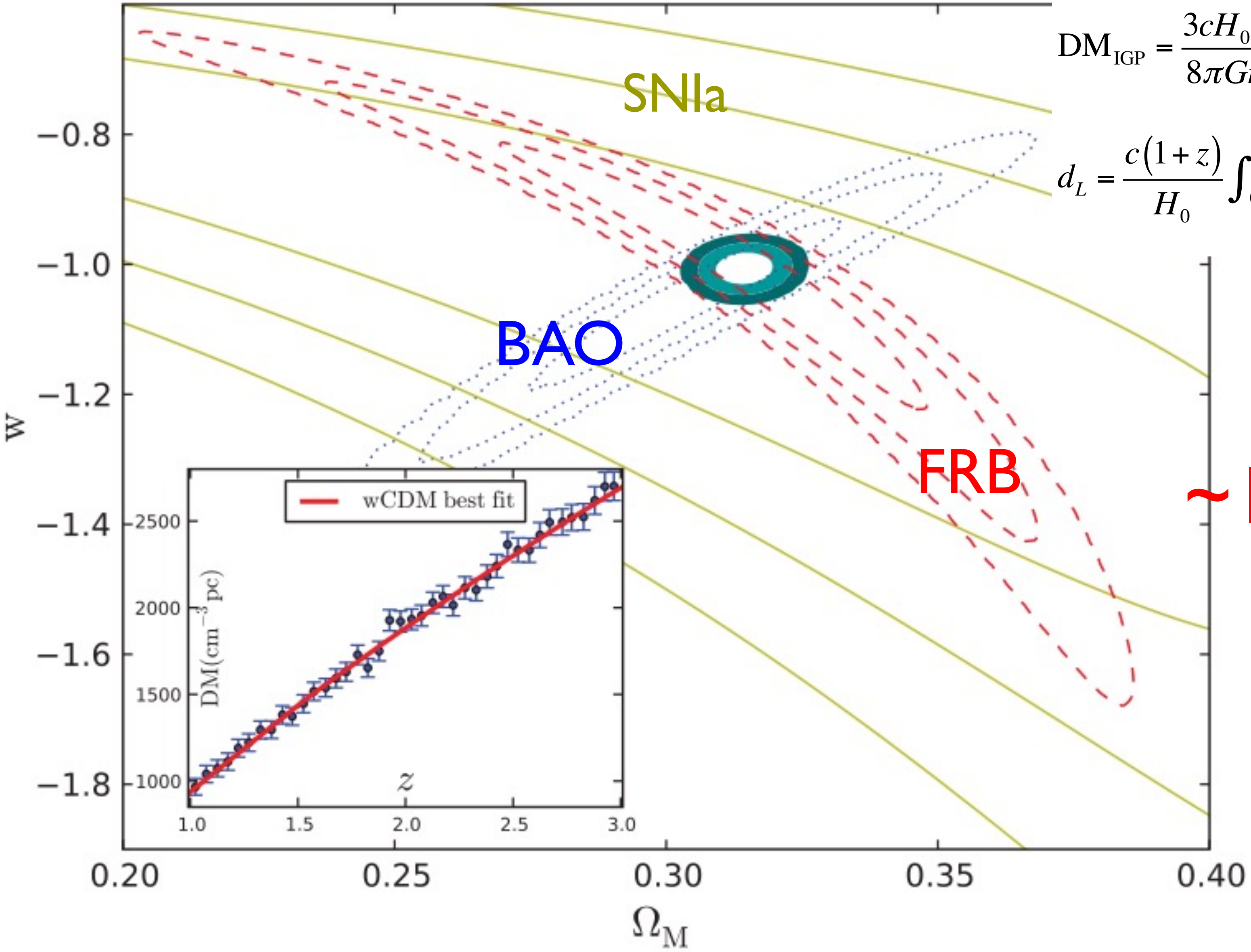

~1000 FRBs

Zhou+ 14
Gao+ 14
Zhao+ 20
Kashiyama+ 13

Hubble Constant

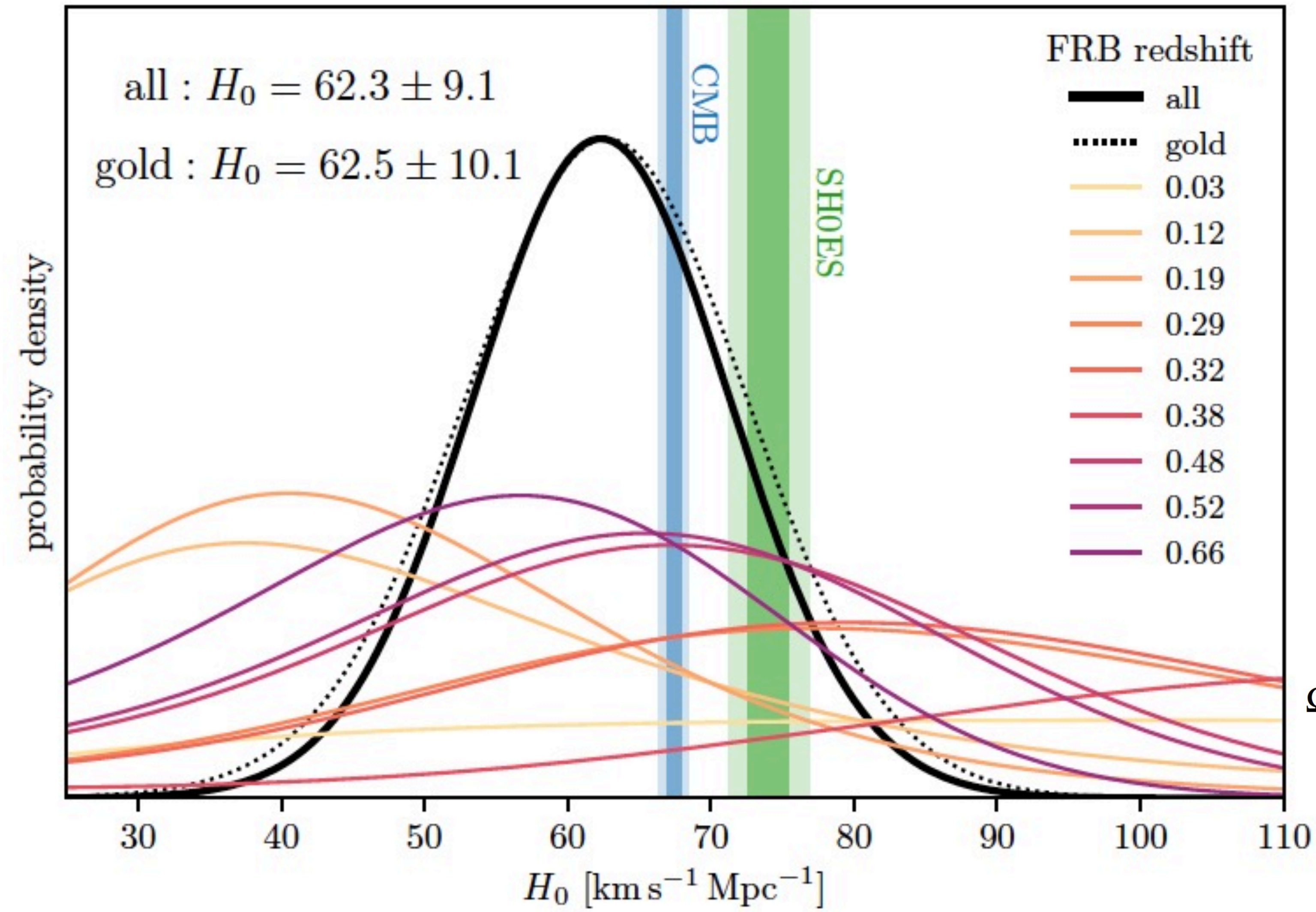

9 FRBs

H_0=62.3±9.1

Degeneracy btw Ω_b h is broken by the other obs. such as BBN

$$\Omega_b h^2 = (2.235 \pm 0.037) \times 10^{-2}$$

Hagstotz+ 21, Wu+ 21

He Reionization

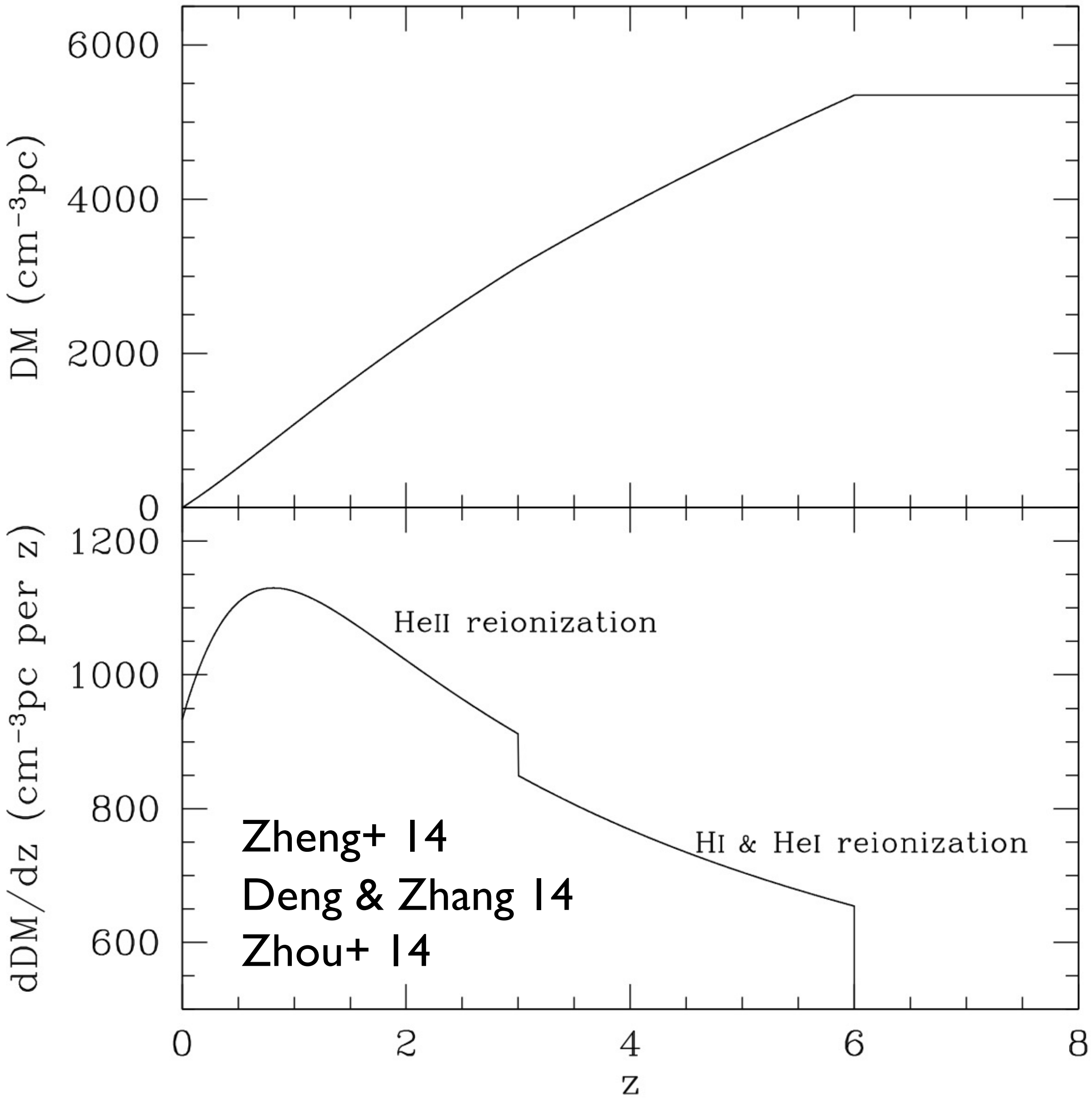

Zheng+ 14
Deng & Zhang 14
Zhou+ 14

H I: 13.6 eV
He I: 24.6 eV
He II:54.4 eV
HeII reionized @z<3

HeII reionization:
f_e=1-(3/4)Y~0.818
→ 1-(1/2)Y~0.879

500-10^4 FRBs are required

Caleb+ 19, Linder+ 20, Lau+ 21, Bhattacharya+ 21, Dai & Xia 21

Angular Power Spectrum

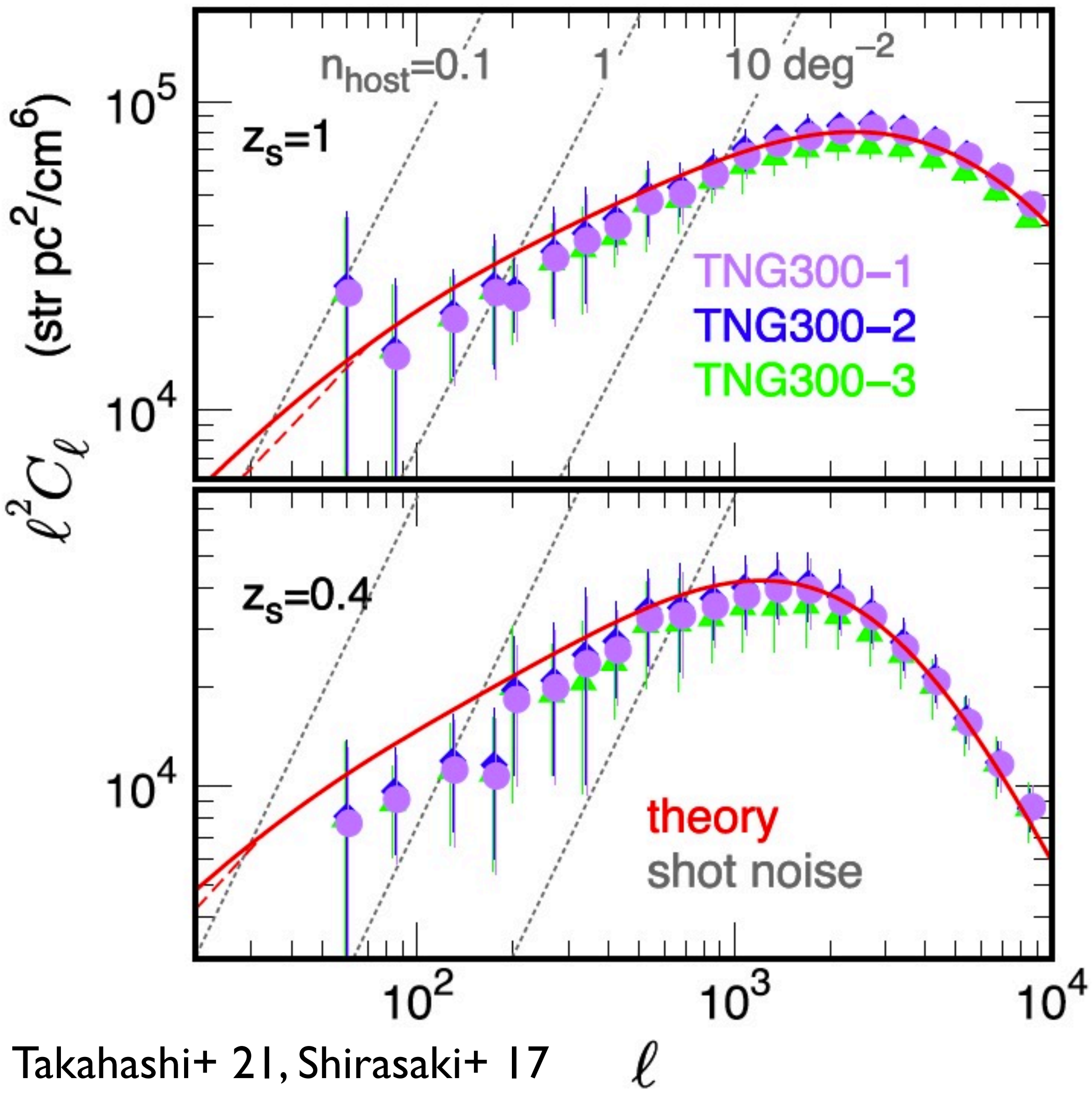

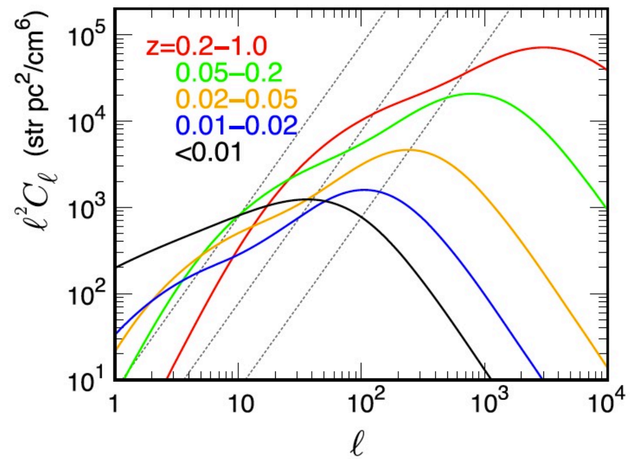

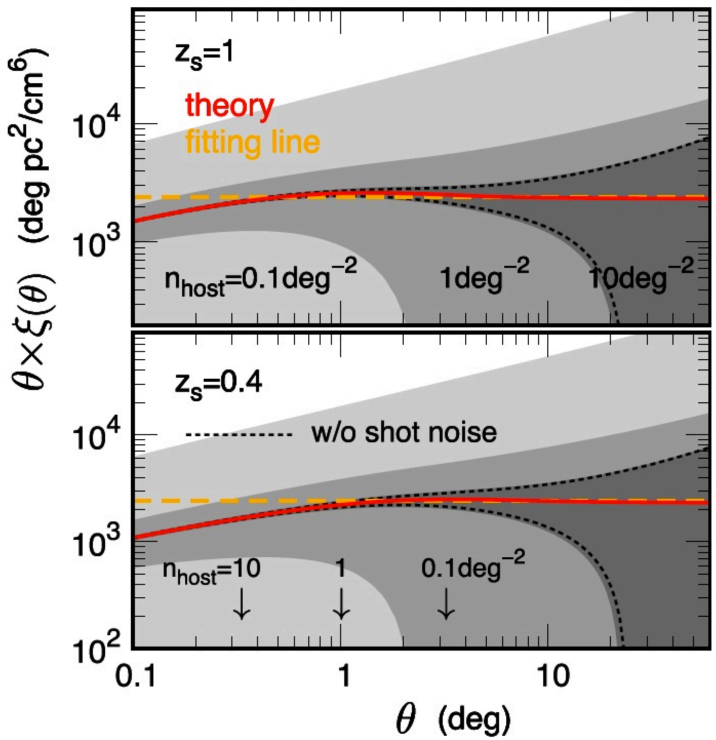

Takahashi+ 21, Shirasaki+ 17

Angular Correlation

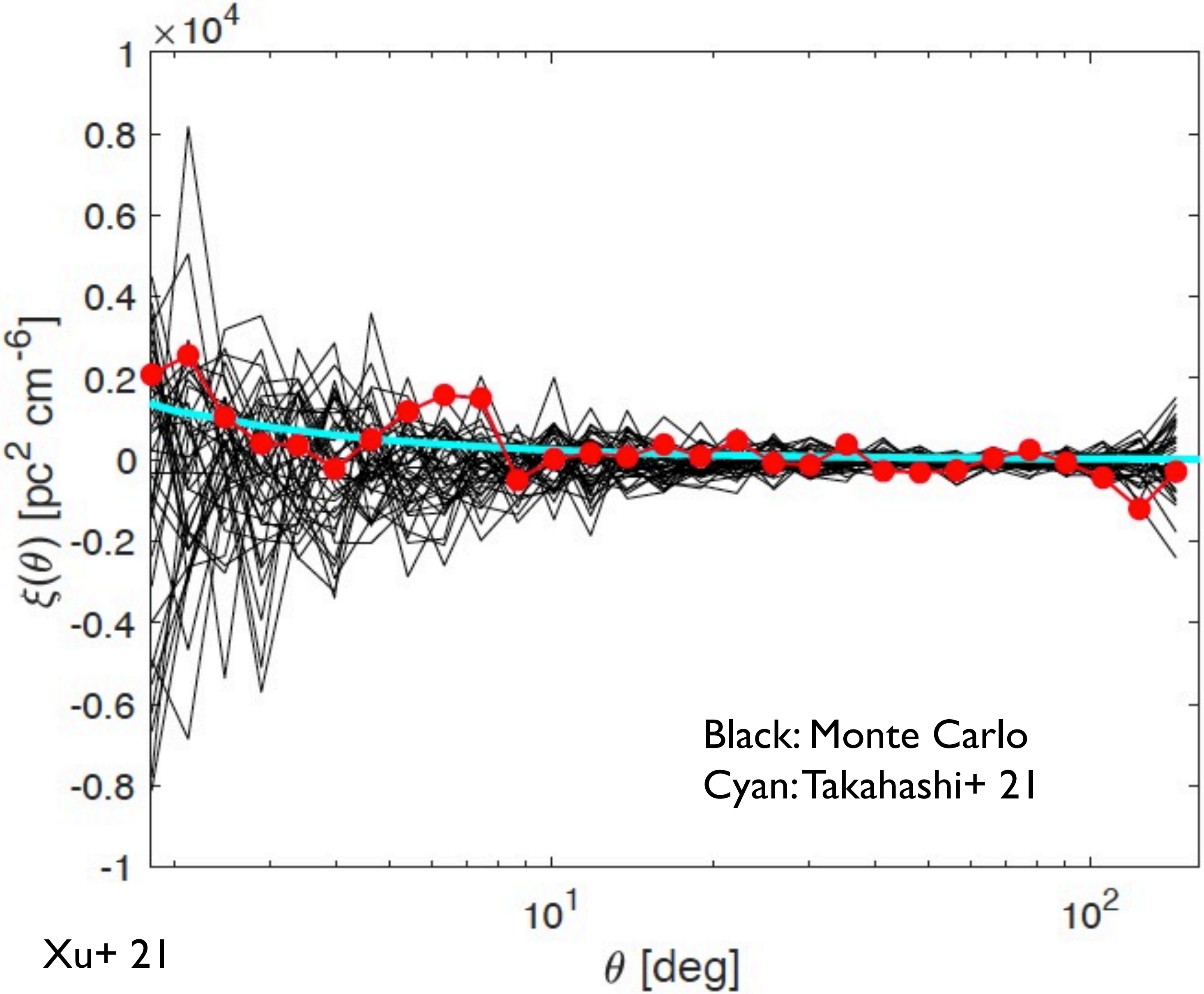

Xu+ 21

CHIME catalog
DM<500 pc/cm^3
210 FRBs

Still large statistical error

Cross Correlation

Shirasaki, Takahashi, Osato & KI 21

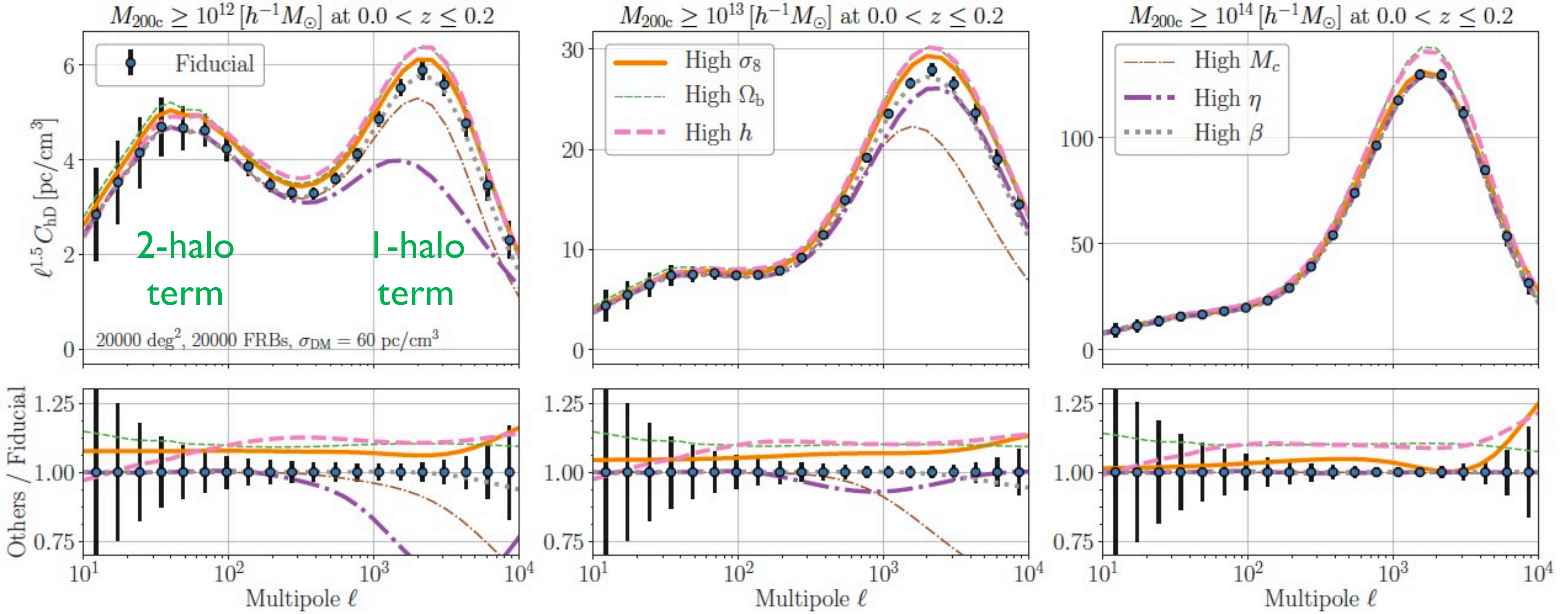

DM-Galaxy cross correlation breaks Ω_b, h & f_e degeneracy

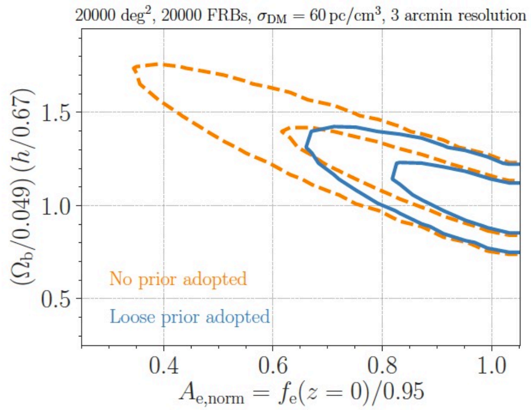

Gas-to-halo mass relation

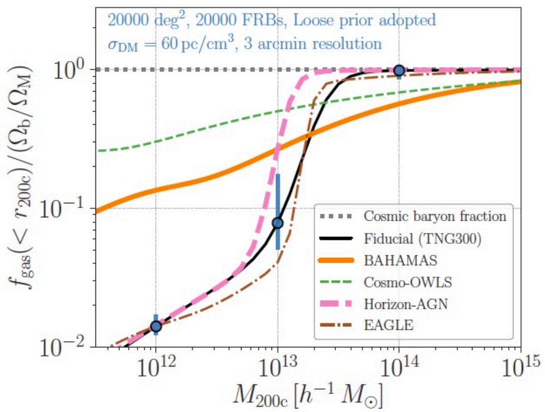

Table 3. Summary of the Fisher forecast of the cosmological and astrophysical parameters by the cross-correlation analysis with DM and dark matter haloes. We assume an effective survey area to be 20000 deg^2 used for the analysis. We consider three mass-limited samples with $M \geqslant 10^{12}$, 10^{13} and $10^{14}\,h^{-1}M_{\odot}$ at five separated redshift bins covering up to $z = 1$. For a hypothetical FRB catalogue, we examine three cases of $(\bar{n}_{\mathrm{FRB}}, \Delta\theta_{\mathrm{FRB}}) = (1\,\mathrm{deg}^{-2}, 3')$, $(0.1\,\mathrm{deg}^{-2}, 1')$ and $(10.0\,\mathrm{deg}^{-2}, 10')$, where $\bar{n}_{\mathrm{FRB}}$ is the average number density of FRBs and $\Delta\theta_{\mathrm{FRB}}$ is the localisation error for each FRB. In each table cell, the number without brackets show the 1σ constraint of single parameter when we marginalise other parameters, while the number in brackets is the marginalised error divided by the fiducial parameter in percentiles. We highlight the limit within a 5% level of precision in black bold, while the red bold font represents the limit better than a 1% level of precision. The details of the Fisher analysis is provided in Subsection 4.4.

Parameters	$\ell_{\max} = 3000$ w/o prior	$\ell_{\max} = 3000$ w/ prior	$\ell_{\max} = 10000$ w/o prior	$\ell_{\max} = 10000$ w/ prior
$\bar{n}_{\mathrm{FRB}} = 1\,\mathrm{deg}^{-2}$ and $\Delta\theta_{\mathrm{FRB}} = 3$ arcmin				
h	0.0646 (9.61%)	0.0354 (5.26%)	0.0590 (8.76%)	0.0342 (5.08%)
w_0	**0.0422** (4.22%)	**0.0389** (3.89%)	**0.0396** (3.96%)	**0.0371** (3.71%)
Ω_{M}	**0.0126** (4.00%)	**0.0109** (3.45%)	**0.0117** (3.71%)	**0.0102** (3.23%)
Ω_{b}	0.0094 (19.05%)	0.0057 (11.64%)	0.0085 (17.26%)	0.0055 (11.22%)
σ_8	**0.0118** (1.42%)	**0.0088** (1.06%)	**0.0112** (1.35%)	**0.0085** (1.03%)
n_s	**0.0223** (2.31%)	**0.0181** (1.88%)	**0.0191** (1.98%)	**0.0160** (1.65%)
$\log\eta$	**0.0129** (1.51%)	**0.0084** (0.98%)	**0.0120** (1.41%)	**0.0079** (0.93%)
$\log M_c$	**0.0227** (0.17%)	**0.0218** (0.16%)	**0.0212** (0.16%)	**0.0204** (0.15%)
$\log\beta$	0.2973 (48.60%)	0.2915 (47.65%)	0.2399 (39.21%)	0.2365 (38.66%)
$A_{\mathrm{e,norm}}$	0.2765 (27.65%)	0.1425 (14.25%)	0.2498 (24.98%)	0.1377 (13.77%)
α	**0.0277** (0.79%)	**0.0270** (0.77%)	**0.0270** (0.77%)	**0.0263** (0.75%)
$\bar{n}_{\mathrm{FRB}} = 0.1\,\mathrm{deg}^{-2}$ and $\Delta\theta_{\mathrm{FRB}} = 1$ arcmin				
h	0.1457 (21.67%)	0.0483 (7.19%)	0.1117 (16.60%)	0.0451 (6.71%)
w_0	0.1061 (10.61%)	0.0885 (8.85%)	0.0826 (8.26%)	0.0723 (7.23%)
Ω_{M}	0.0309 (9.80%)	0.0222 (7.04%)	0.0237 (7.53%)	0.0177 (5.61%)
Ω_{b}	0.0191 (38.85%)	0.0077 (15.70%)	0.0141 (28.72%)	0.0072 (14.69%)
σ_8	**0.0282** (3.39%)	**0.0171** (2.06%)	**0.0233** (2.80%)	**0.0145** (1.74%)
n_s	0.0529 (5.49%)	**0.0351** (3.64%)	**0.0304** (3.15%)	**0.0212** (2.20%)
$\log\eta$	**0.0297** (3.47%)	**0.0159** (1.87%)	**0.0227** (2.66%)	**0.0113** (1.32%)
$\log M_c$	**0.0535** (0.40%)	**0.0500** (0.37%)	**0.0365** (0.27%)	**0.0353** (0.26%)
$\log\beta$	0.6753 (110.39%)	0.6540 (106.92%)	0.3248 (53.09%)	0.3177 (51.94%)
$A_{\mathrm{e,norm}}$	0.5906 (59.06%)	0.1644 (16.44%)	0.4377 (43.77%)	0.1575 (15.75%)
α	**0.0681** (1.95%)	**0.0630** (1.80%)	**0.0591** (1.69%)	**0.0544** (1.55%)
$\bar{n}_{\mathrm{FRB}} = 10\,\mathrm{deg}^{-2}$ and $\Delta\theta_{\mathrm{FRB}} = 10$ arcmin				
h	0.0599 (8.90%)	**0.0335** (4.98%)	0.0598 (8.89%)	**0.0334** (4.97%)
w_0	**0.0427** (4.27%)	**0.0400** (4.00%)	**0.0424** (4.24%)	**0.0398** (3.98%)
Ω_{M}	**0.0130** (4.13%)	**0.0105** (3.33%)	**0.0129** (4.08%)	**0.0104** (3.30%)
Ω_{b}	0.0081 (16.54%)	0.0051 (10.46%)	0.0082 (16.60%)	0.0051 (10.43%)
σ_8	**0.0125** (1.51%)	**0.0088** (1.06%)	**0.0125** (1.50%)	**0.0088** (1.06%)
n_s	**0.0227** (2.35%)	**0.0189** (1.96%)	**0.0227** (2.35%)	**0.0189** (1.96%)
$\log\eta$	**0.0174** (2.04%)	**0.0119** (1.39%)	**0.0173** (2.03%)	**0.0118** (1.39%)
$\log M_c$	**0.0220** (0.16%)	**0.0208** (0.16%)	**0.0220** (0.16%)	**0.0208** (0.16%)
$\log\beta$	0.3397 (55.53%)	0.3356 (54.87%)	0.3400 (55.59%)	0.3359 (54.91%)
$A_{\mathrm{e,norm}}$	0.2549 (25.49%)	0.1365 (13.65%)	0.2558 (25.58%)	0.1366 (13.66%)
α	**0.0241** (0.69%)	**0.0237** (0.68%)	**0.0241** (0.69%)	**0.0237** (0.68%)

Circumgalactic Gas?

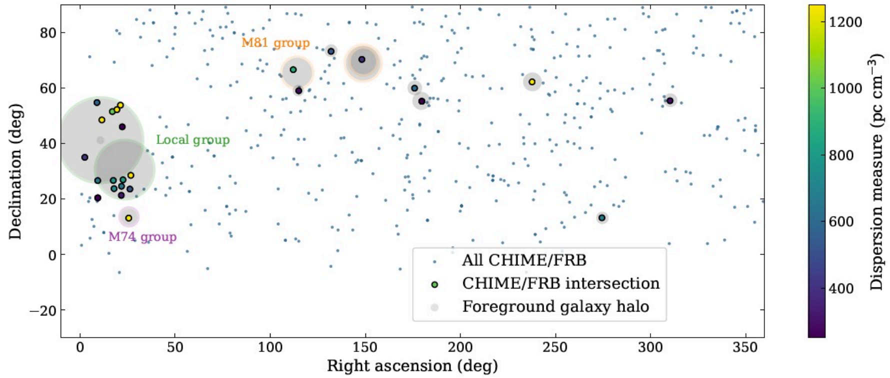

FRB intersecting nearby (<40Mpc) GW galaxy catalogue

DM_{excess}=200±100

larger than expected

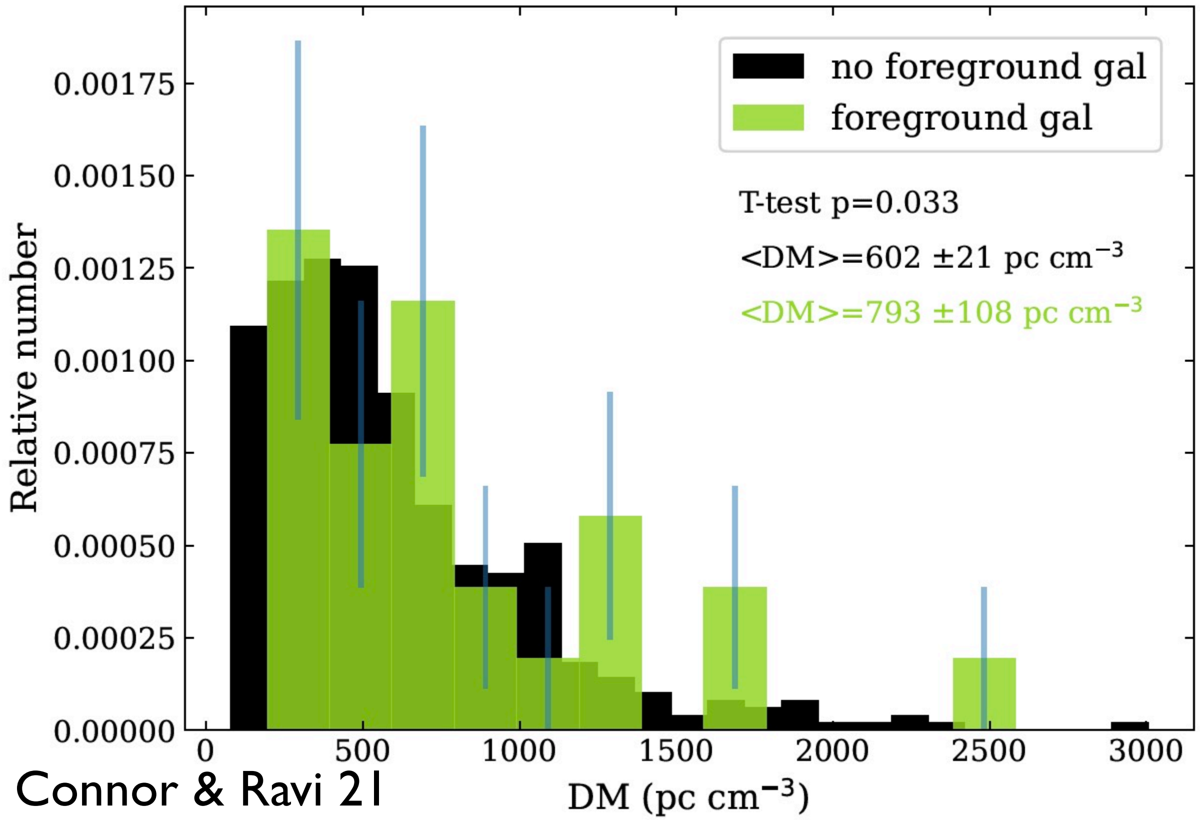

Connor & Ravi 21

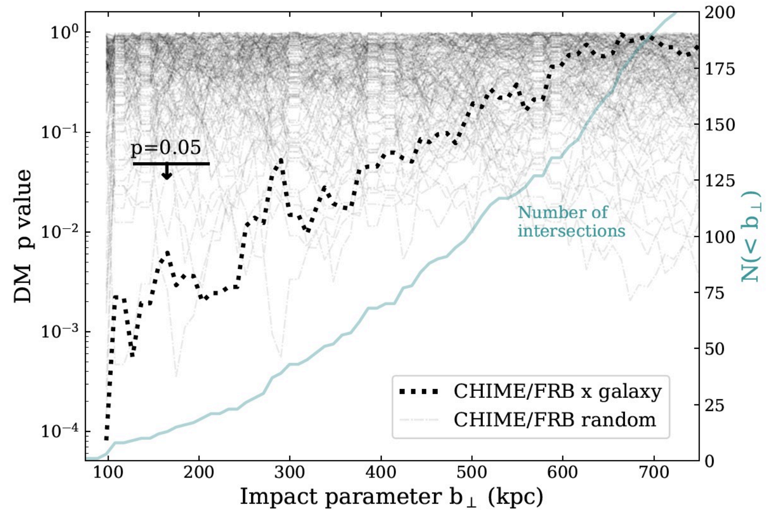

DM-Galaxy Correlation?

3 kinds of galaxy catalog

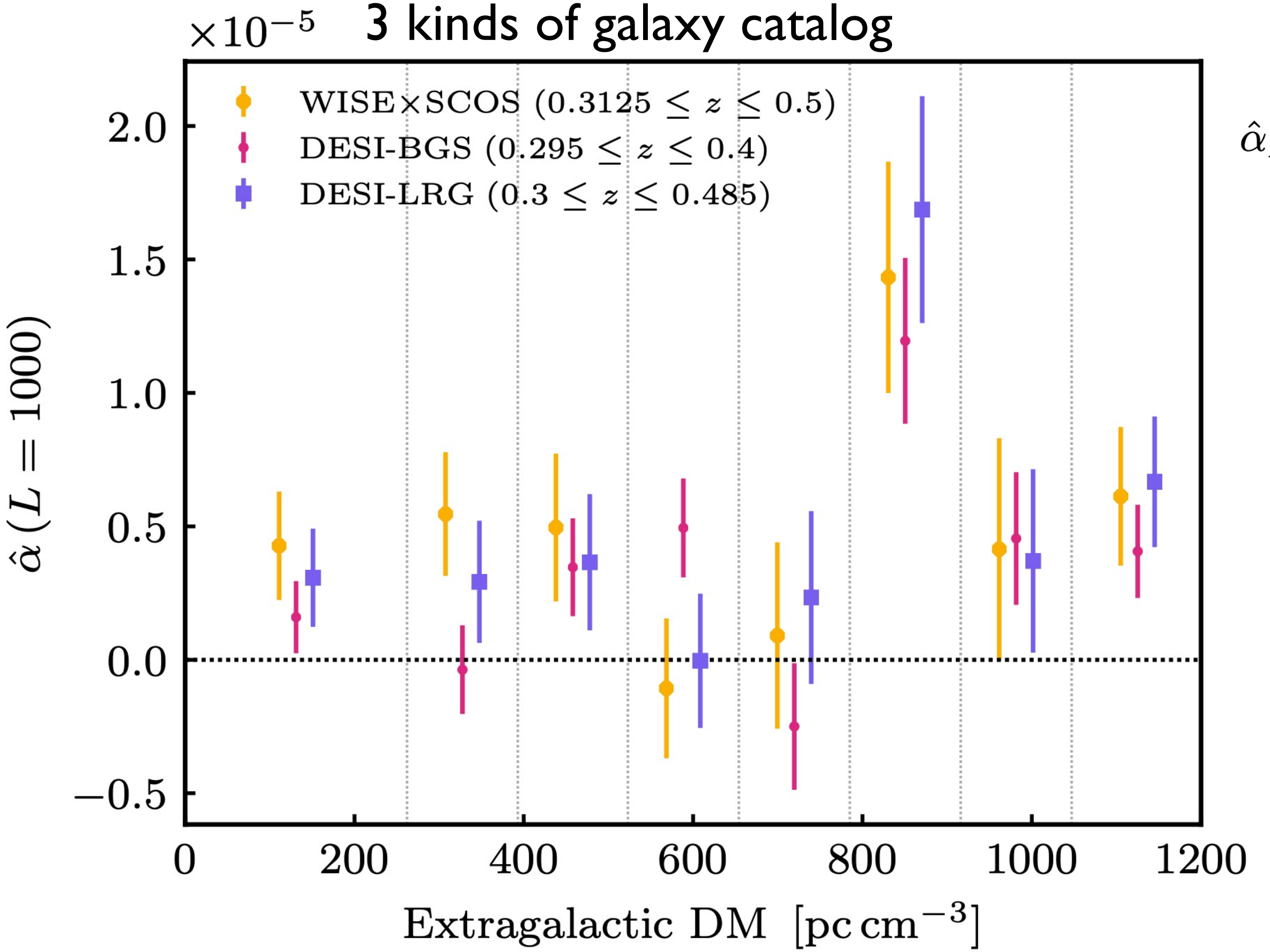

$$\hat{\alpha}_L = \frac{1}{\mathcal{N}_L} \sum_{\ell \geq \ell_{\min}} (2\ell+1) \frac{e^{-\ell^2/L^2}}{C_\ell^{gg}} \hat{C}_\ell^{fg}$$

$$\mathrm{SNR}_L = \frac{\hat{\alpha}_L}{\mathrm{Var}(\hat{\alpha}_L)^{1/2}}$$

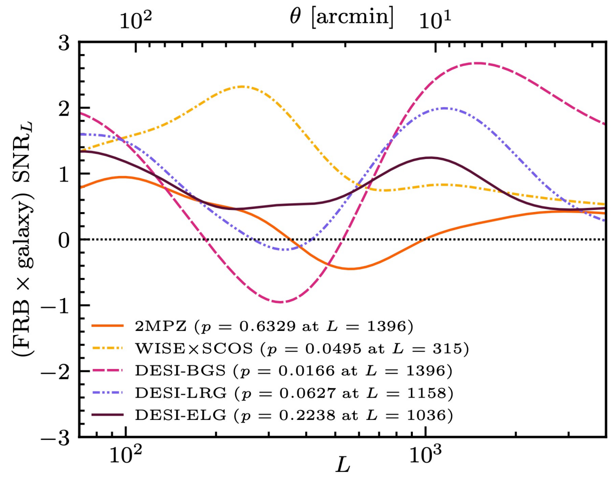

Rafiei-Ravandi+ 21

I do not understand this quantity…

DM × Sunyaev-Zel'dovich

WHIM of clusters @r>r$_{vir}$

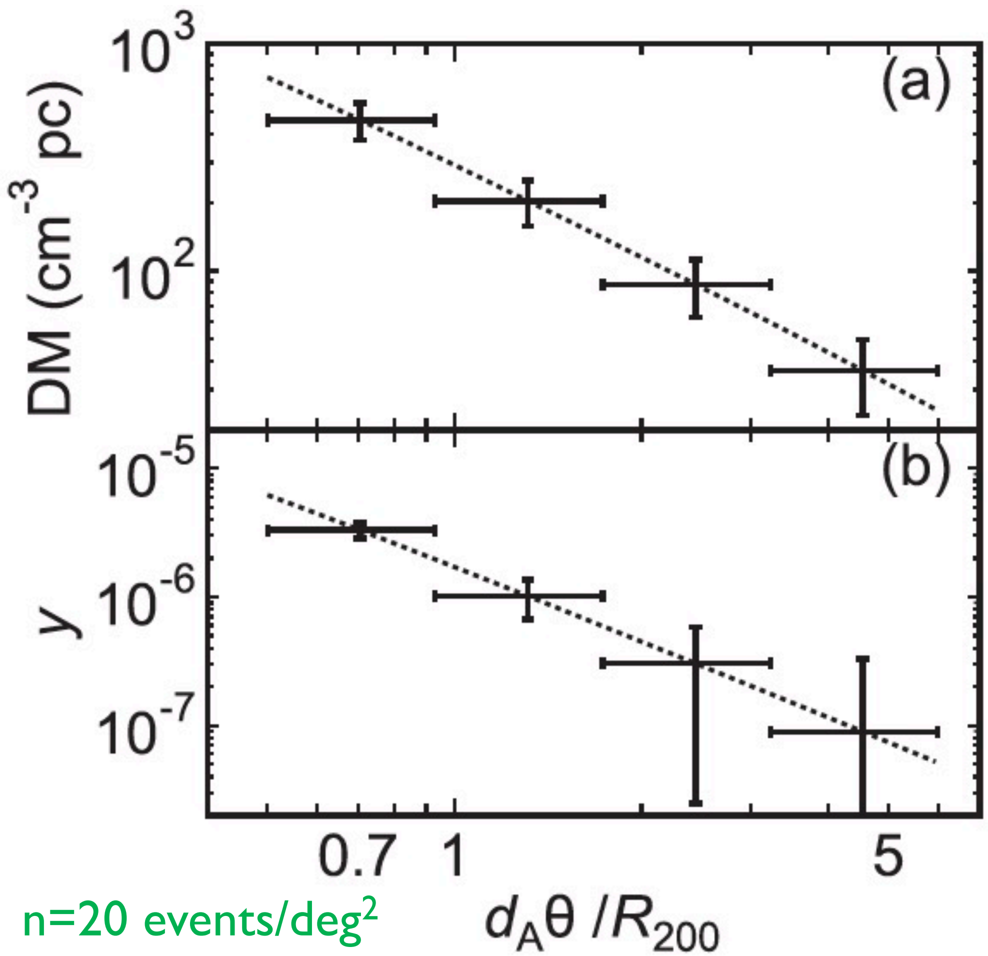

n=20 events/deg^2
for errors

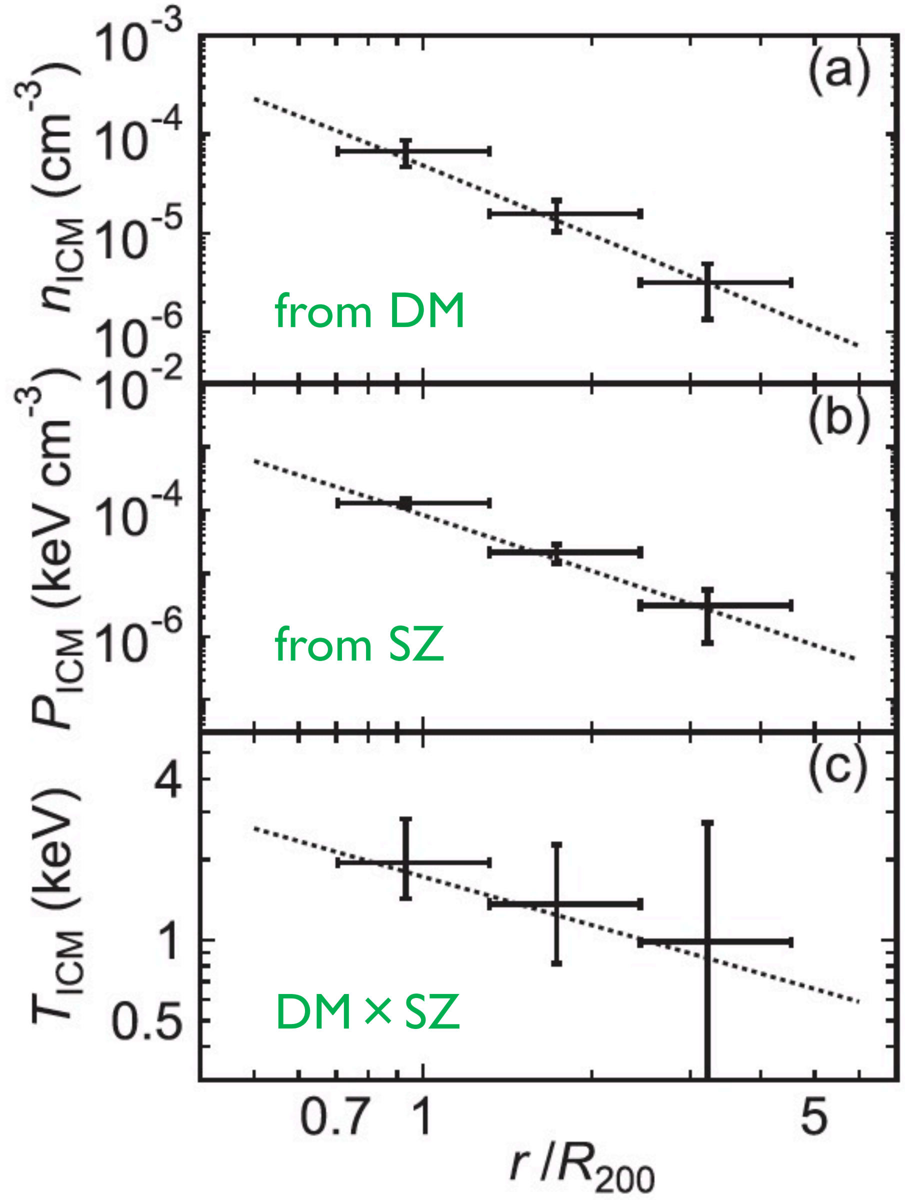

Fujita+ 17, Munoz & Loeb 18, Madhavacheril+ 19

Event Rate

$R \sim 3 \times 10^4$ Gpc^{-3} yr^{-1} $\sim R_{SN}/3$

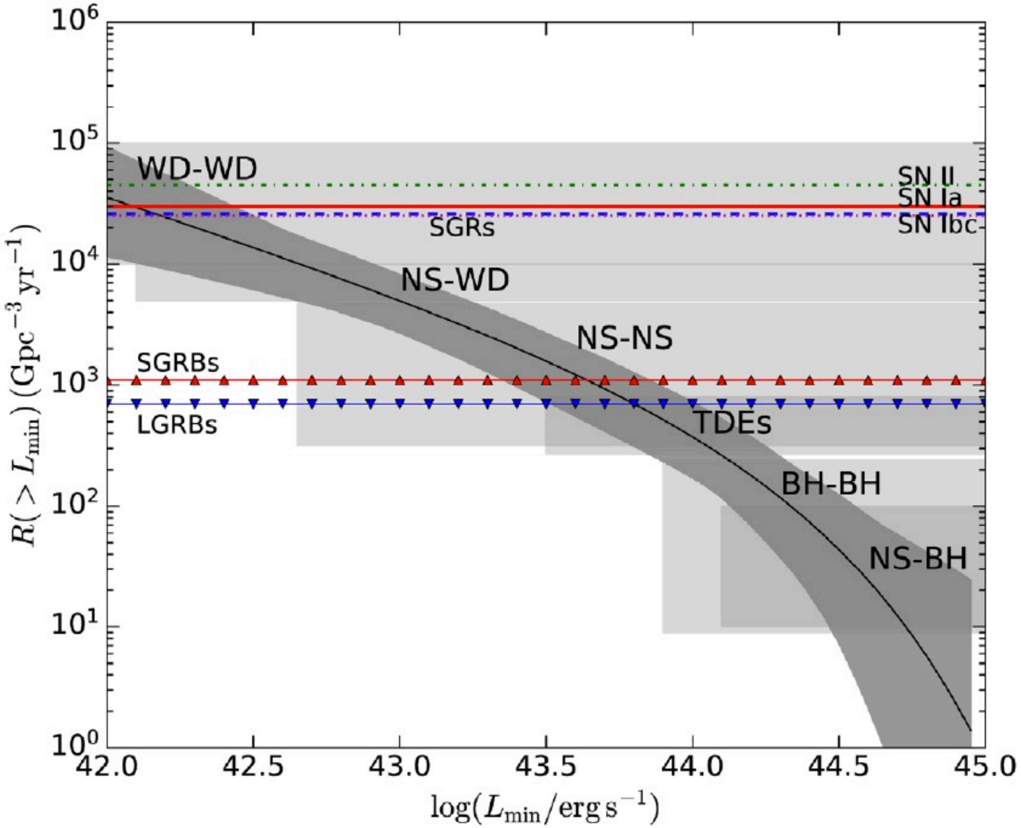

From 46 FRBs, Schechter function, No z-evolution

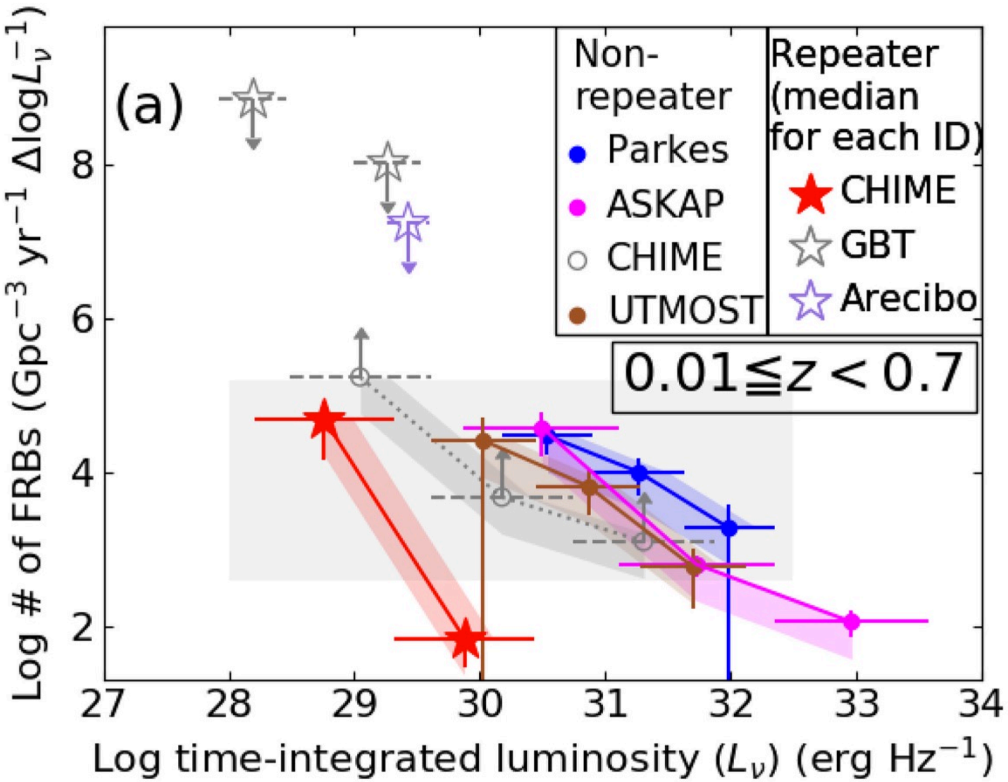

From 90 FRBs, No z-evolution

Luo+ 20, Lu & Piro 19

Hashimoto+ 20

Event Rate by CHIME

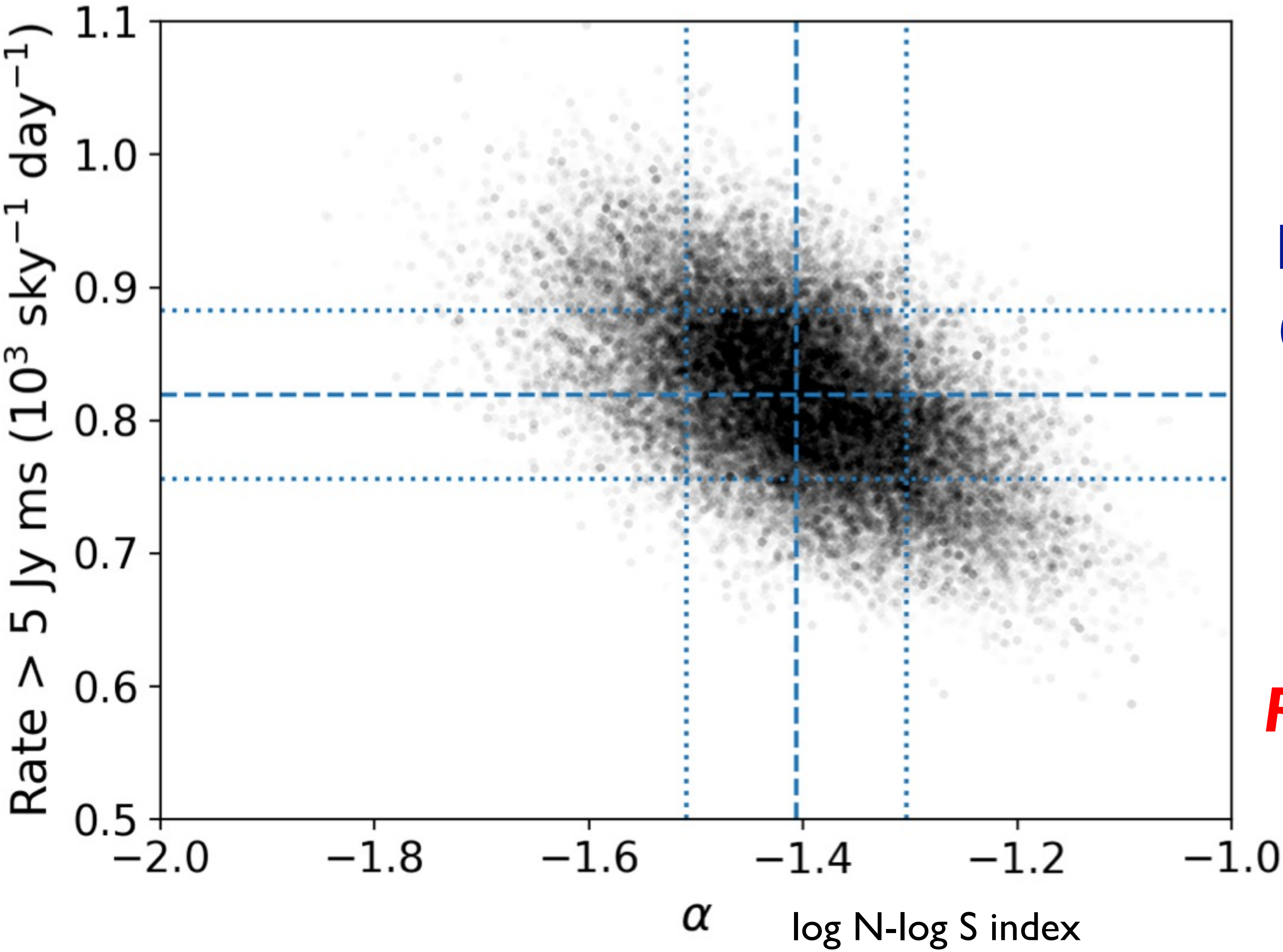

log N-log S index

535 FRBs
F > 5 Jy ms
@600MHz

α~-3/2
Euclidean

R~0.01 R_{SN}


500米口径球面射电望远镜
500米直径 2016年至今 中国贵州
FAST
©Li+ @FRB20

Event Rate by FAST

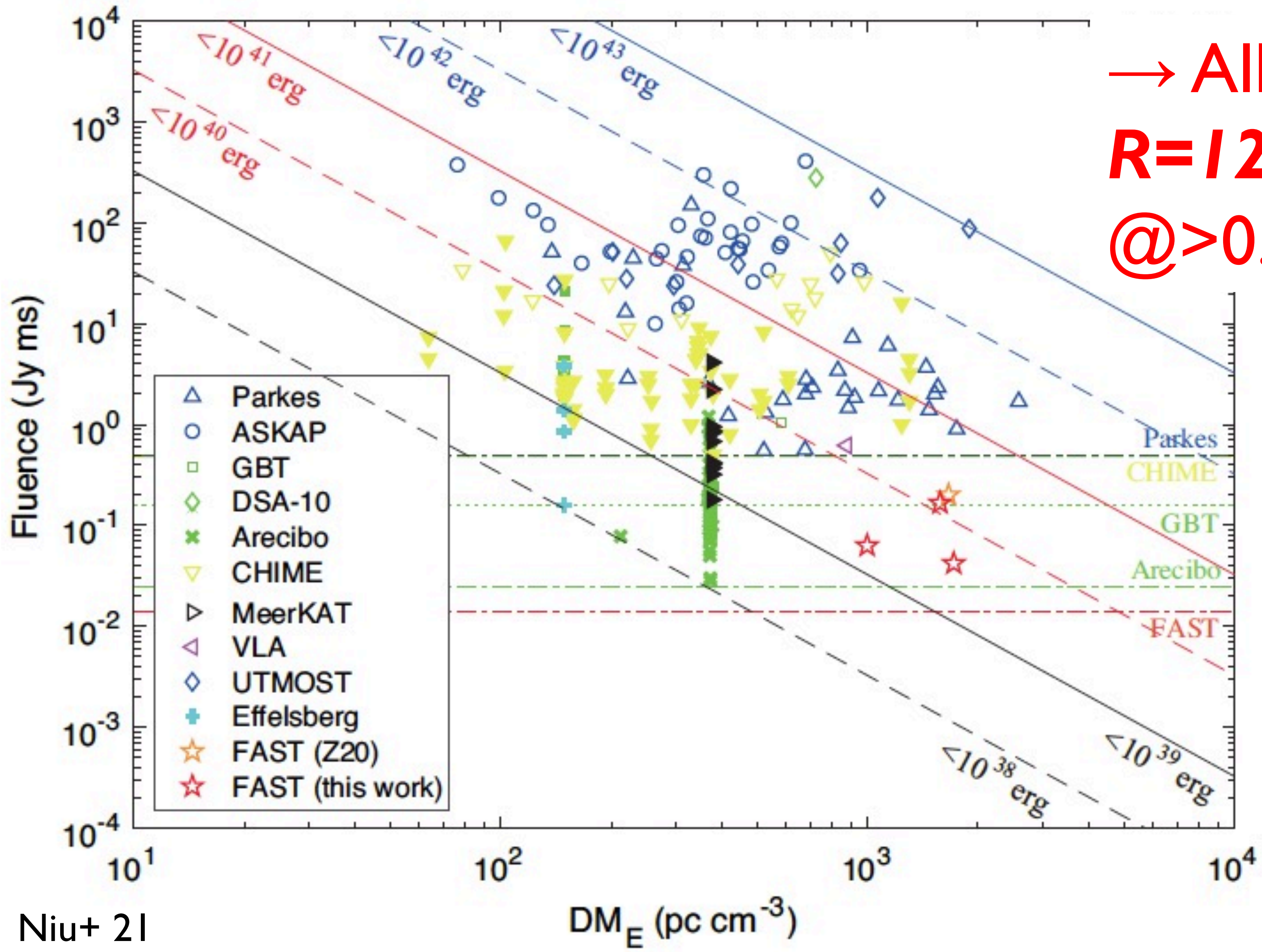

→ All sky

R=120,000/day

@>0.0146 Jy ms

From 4 FRBs

R~R$_{SN}$

~10/deg^2/day

Niu+ 21

Gravitational Lensing

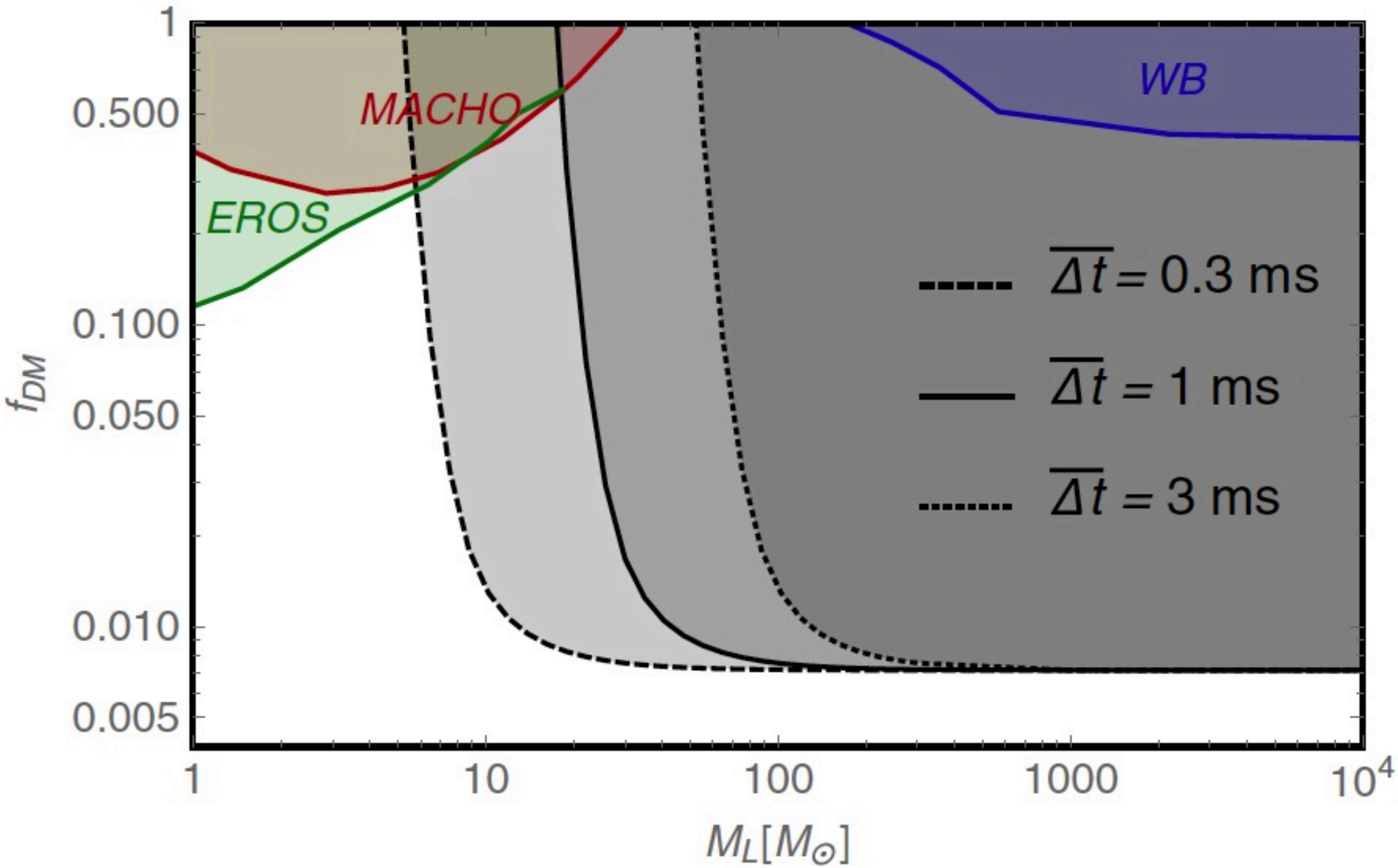

Munoz+ 16, see also Sammons+ 20 for the first trial

Λ Directly from Lensing

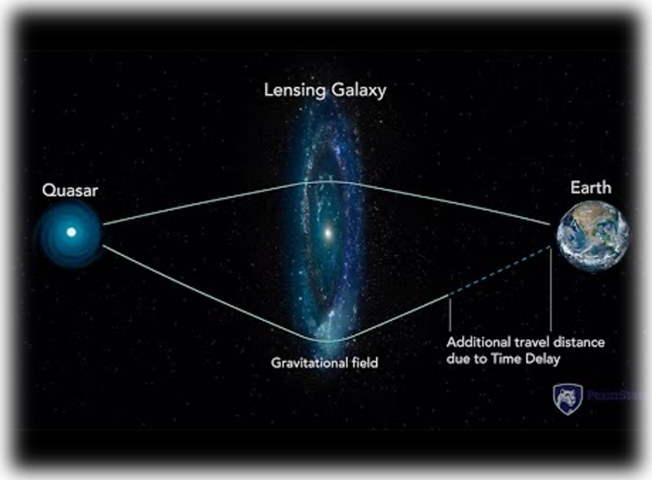

- D ~ Gpc ~ 3e27 cm
- r_s ~ 3e17 cm for a galaxy
- Einstein radius
  $r_E \sim (D\ r_s)^{1/2} \sim$ 3e22 cm
- $\theta \sim r_E/D \sim 10^{-5}$
- $\Delta T \sim \theta^2 D/c \sim 10^7$ s $(\propto H_0)$
- ***$\Delta t/\Delta T \sim 10^{-10}$ [~ 1yr/10^{10}yr]***
- Direct detection of cosmic acceleration

also can reach k < 0.076

Li+ 18, Zitrin & Eichler 18, Wucknitz+ 21

Rotation Measure

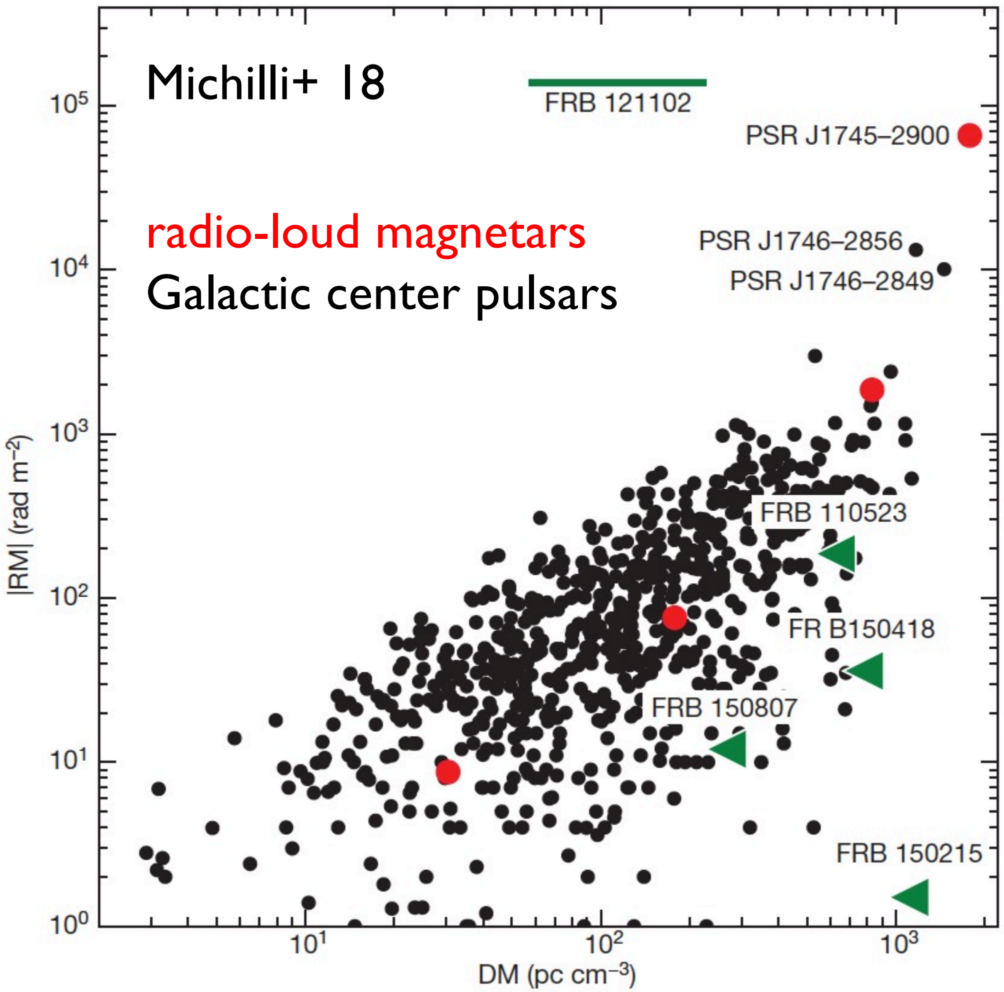

~100% linear polarization!

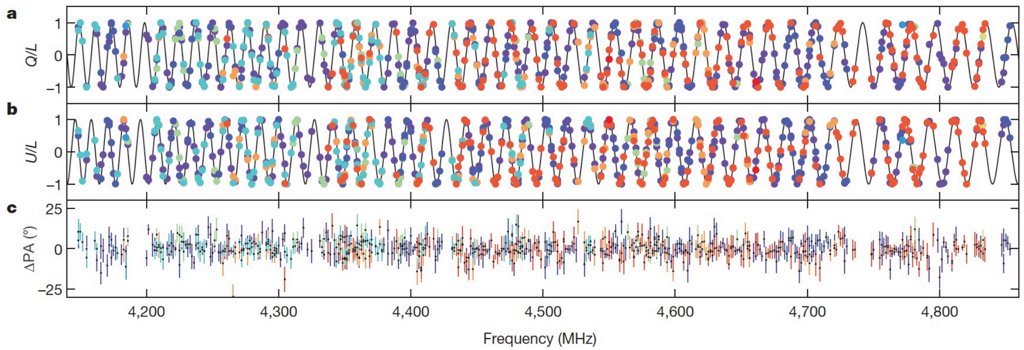

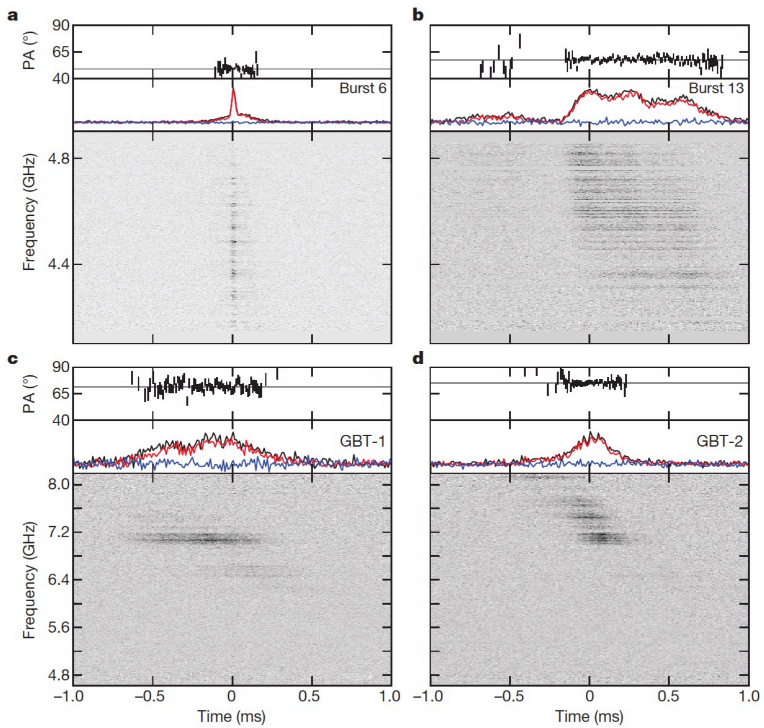

$$\mathrm{RM} = \frac{e^3}{2\pi m_e^2 c^4} \int_0^d n_e B_{||} dl,$$

1.46e5 to 1.33e5 in 7 months

$$\langle B_{||} \rangle = \frac{\mathrm{RM}}{0.81 \mathrm{DM}},$$

[μG]

Halo Magnetic Field

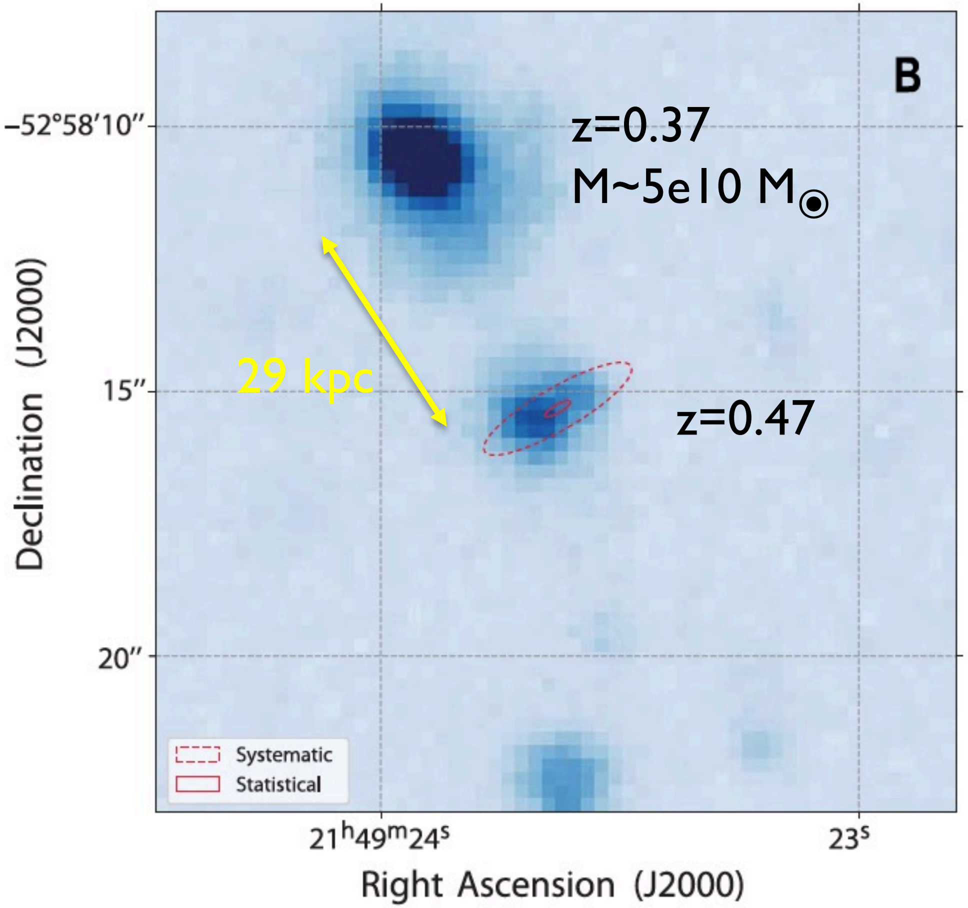

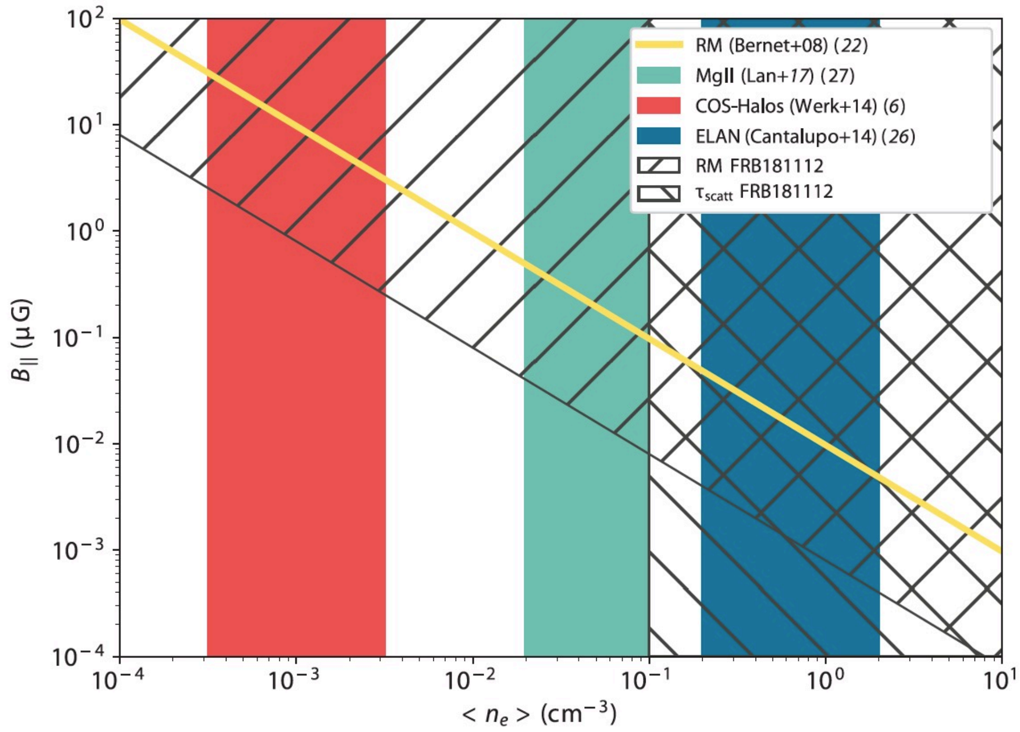

Prochaska+ 19
see also
Akahori+ 16
Ravi+ 16

RM=10.9±0.9 rad/m² < 11 rad/m²

$$B_{\parallel}^{\max} < 0.8\mu\mathrm{G}\left(\frac{n_e}{10^{-3}\ \mathrm{cm}^{-3}}\right)^{-1}\left(\frac{\Delta L}{30\mathrm{kpc}}\right)^{-1}$$

Pulse Scattering

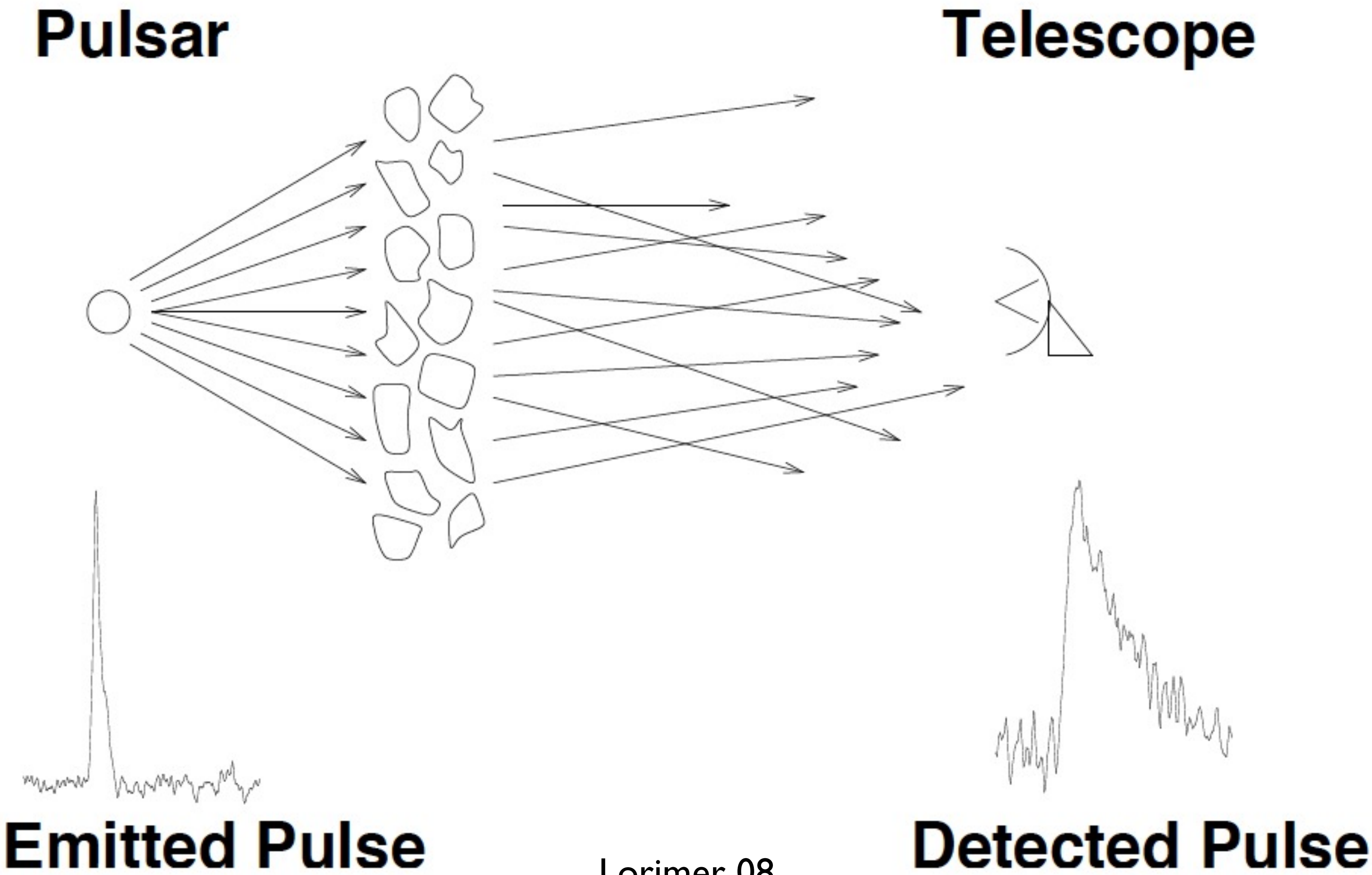

Lorimer 08

Below Galactic Scattering

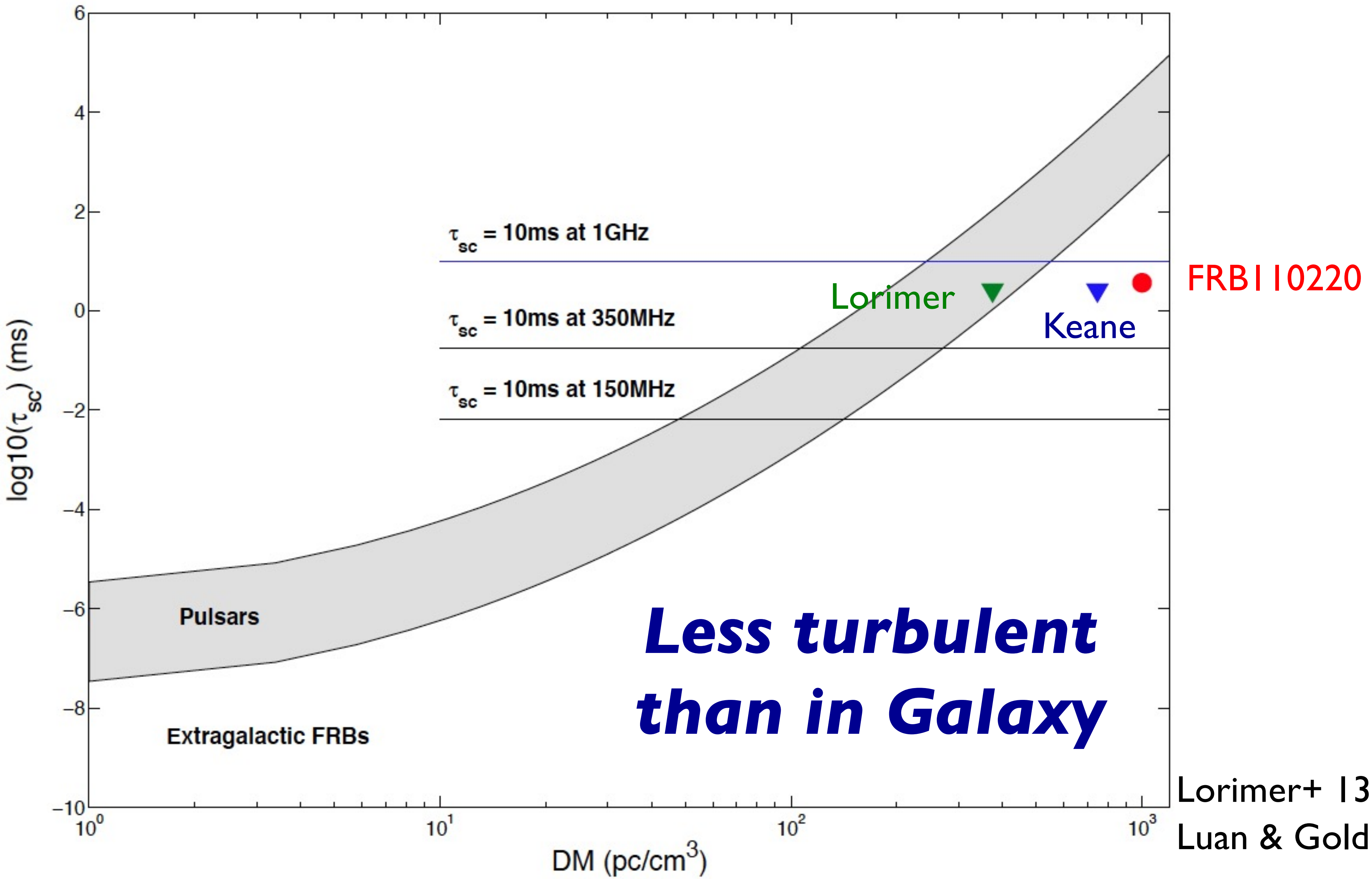

Lorimer+ 13
Luan & Goldreich 14

Scattering Time

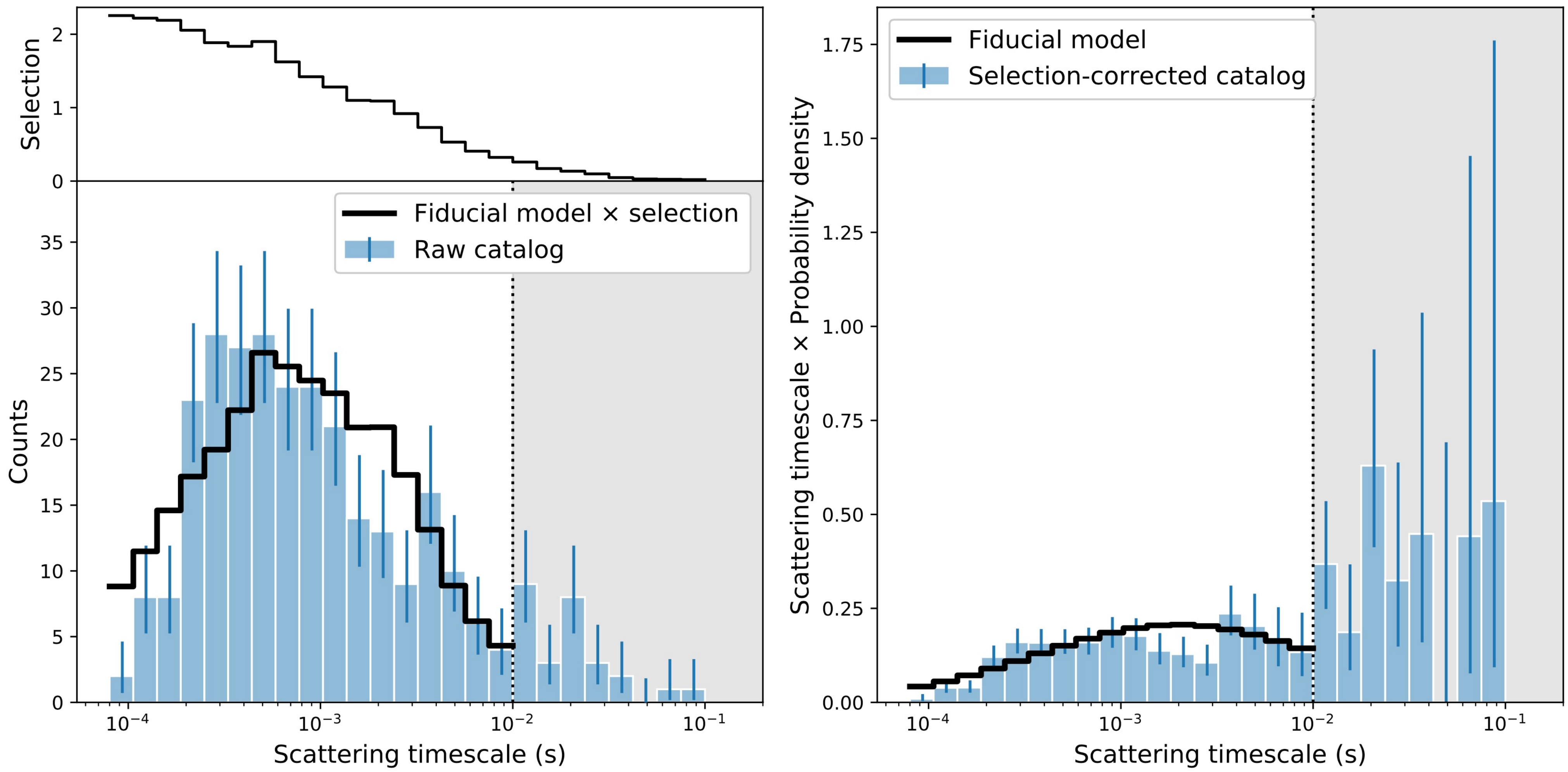

CHIME/FRB 21

Contents

- ***Introduction & History***
  - Dispersion measure
  - FRB repeaters & Host galaxies
  - Galactic FRB from a magnetar
- ***Host galaxies***
  - Diversity, Dwarf, Spiral, Globular cluster, …
- ***FRB cosmology***
  - DM, Cross-correlation, Lensing, RM, SM, …

Thank You

FRB from a Magnetar!

- Fast radio burst 200428
  - STARE2, CHIME
  - ~MJy, ~msec, E_{radio}~10^{35} erg
- Magnetar SGR 1935+2154 in our Galaxy
- With X-ray bursts
  - E_X~10^{40} erg, E_p~80 keV, E_X/E_{radio}~10^5
  - Other FRBs are >10^8 times fainter
- Cosmological FRBs are also magnetar bursts?

Non-Repeater & Repeater

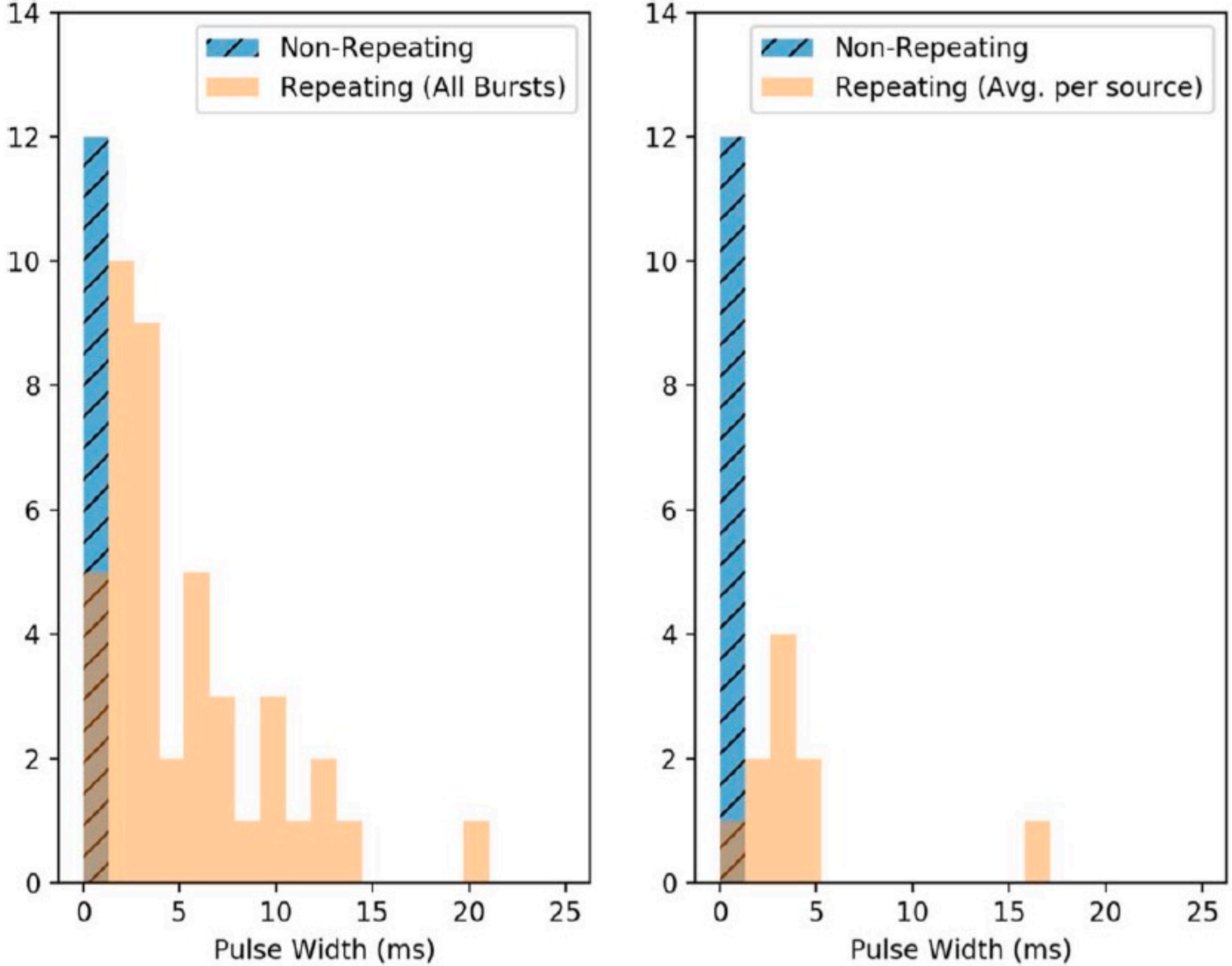

CHIME+ 19

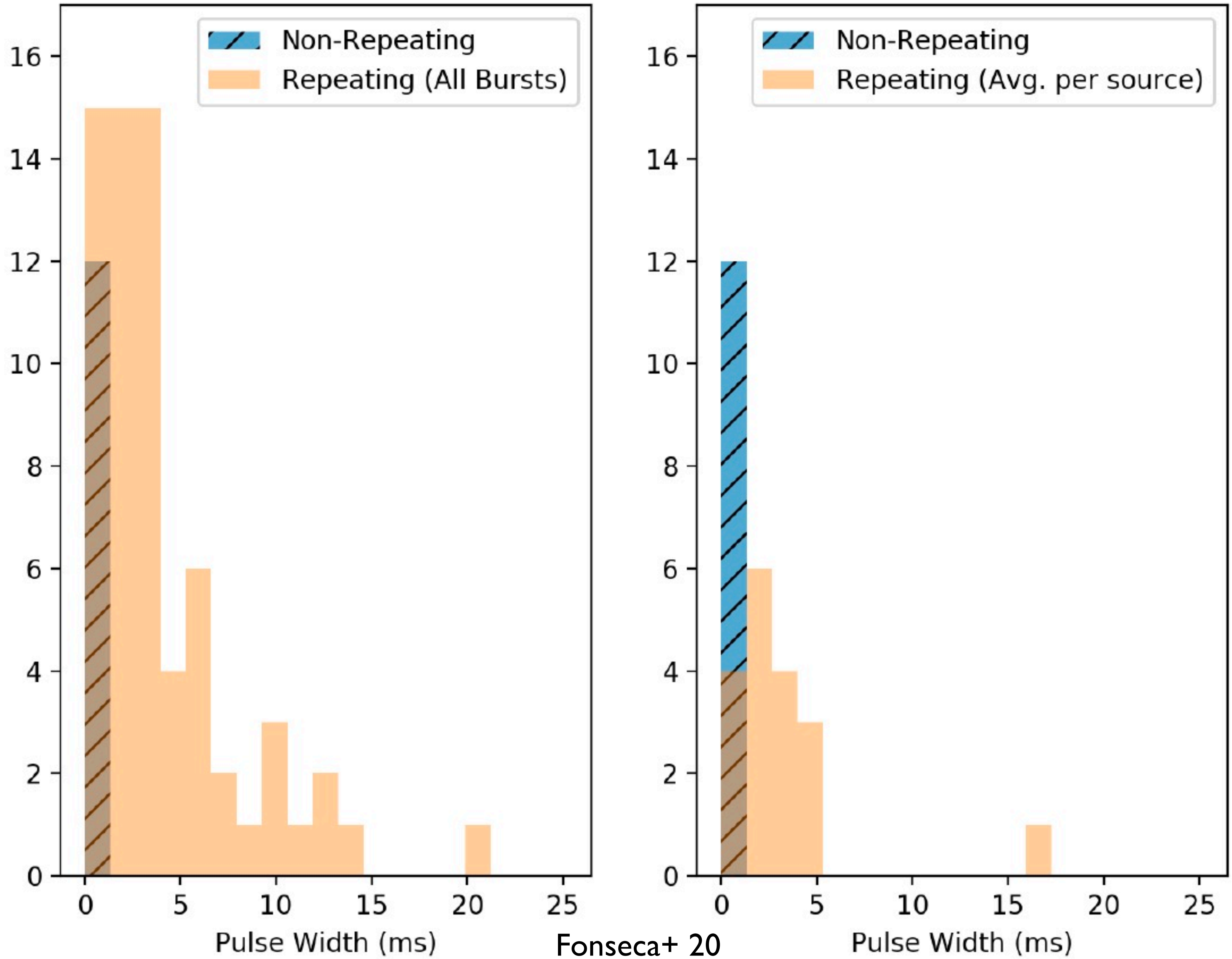
Non-Repeating
Repeating (All Bursts)
Pulse Width (ms)
Non-Repeating
Repeating (Avg. per source)
Pulse Width (ms)

Fonseca+ 20

FRB Morphology

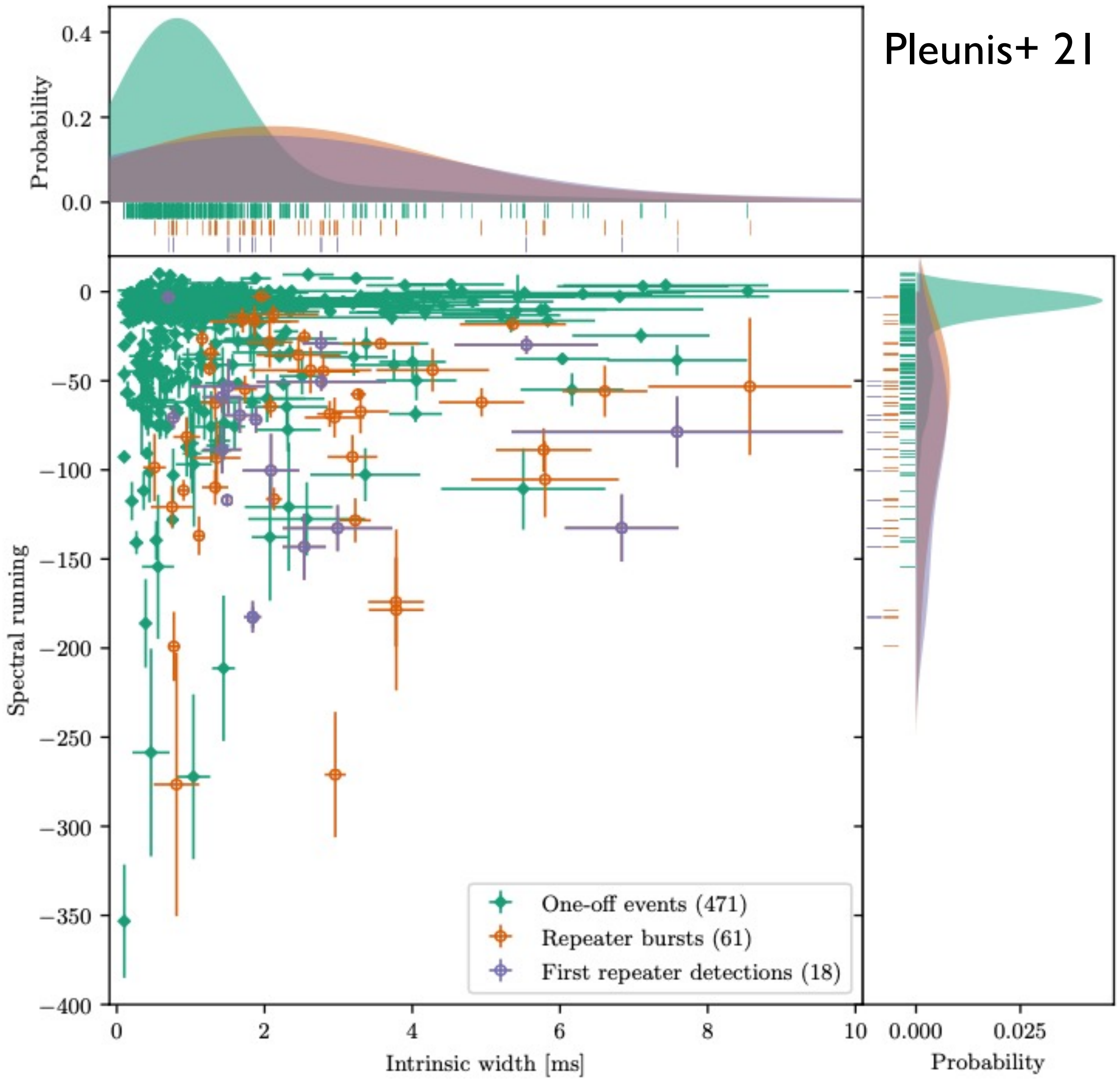

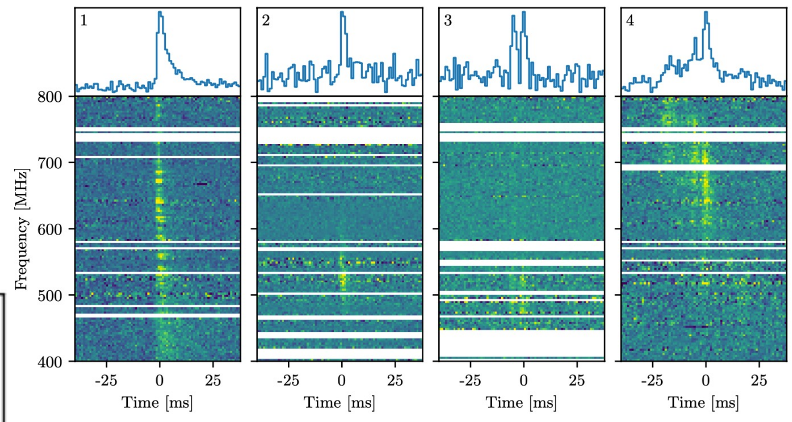

simple broadband
simple narrowband
temporally complex
downward drifting

Repeaters:
wider Δt
narrower $\delta\nu$?

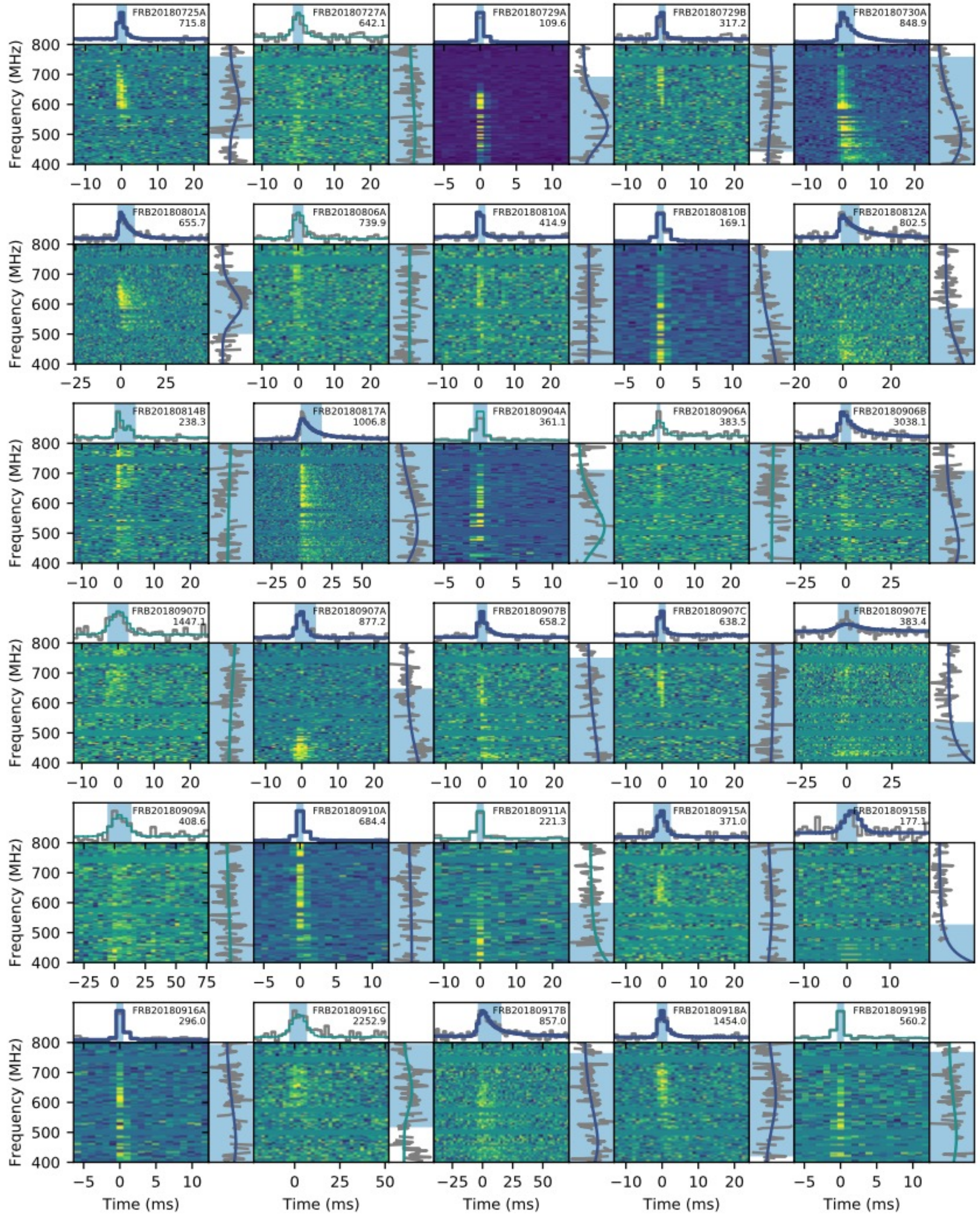

Figure 7. Dynamic spectra ("waterfall plots"), frequency-averaged time series and time-averaged spectra for all one-off FRBs in the Catalog, ordered by time. The TNS name and best-fit DM in units of $\mathrm{pc\,cm^{-3}}$ are in the top right corner of each panel. Model fits are overlaid on the time series and spectra, in green (thin lines) if scattering was not significant and in blue (thick lines) if scattering was significant. The blue shaded regions in the time series and spectra indicate the burst durations and emission bandwidths FWTM, respectively. Bursts indicated with an asterisk are published repeaters, for which only one burst was detected before the Catalog cut-off date. Panels for all catalog one-off bursts can be found at https://www.canfar.net/storage/list/AstroDataCitationDOI/CISTI.CANFAR/21.0007/data/additional_figures/waterfalls.

CHIME/FRB 21

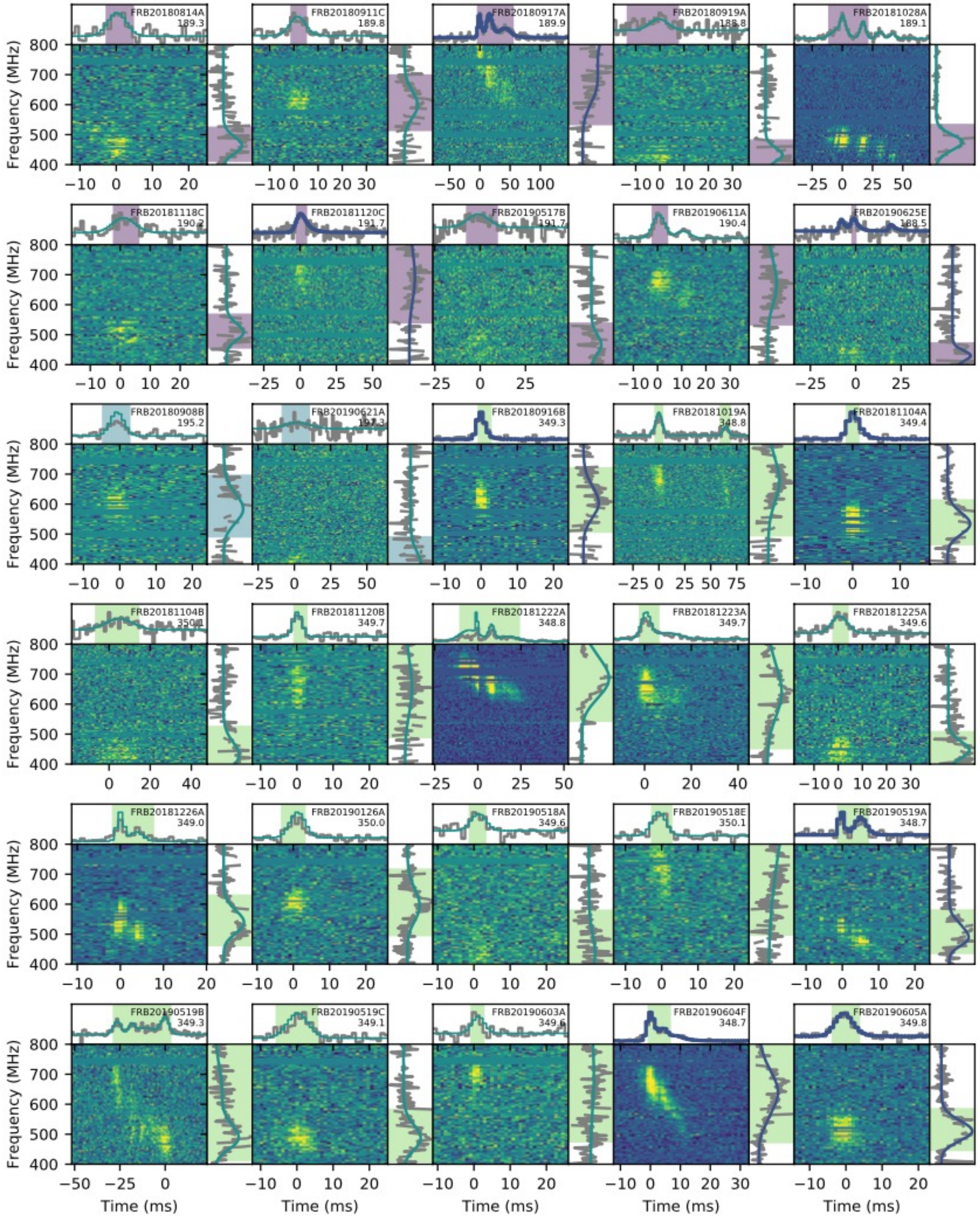

Figure 8. Same as Figure 7, but for all sources exhibiting more than one burst in this Catalog. Sources are ordered by their first detections, and bursts from any one source are ordered by time of detection. Differently colored shaded regions are used for different repeater sources. Panels for all catalog repeating bursts can be found at https://www.canfar.net/storage/list/AstroDataCitationDOI/CISTI.CANFAR/21.0007/data/additional_figures/waterfalls.

CHIME/FRB 21

FRB 20180916B

Tendulkar+ 21

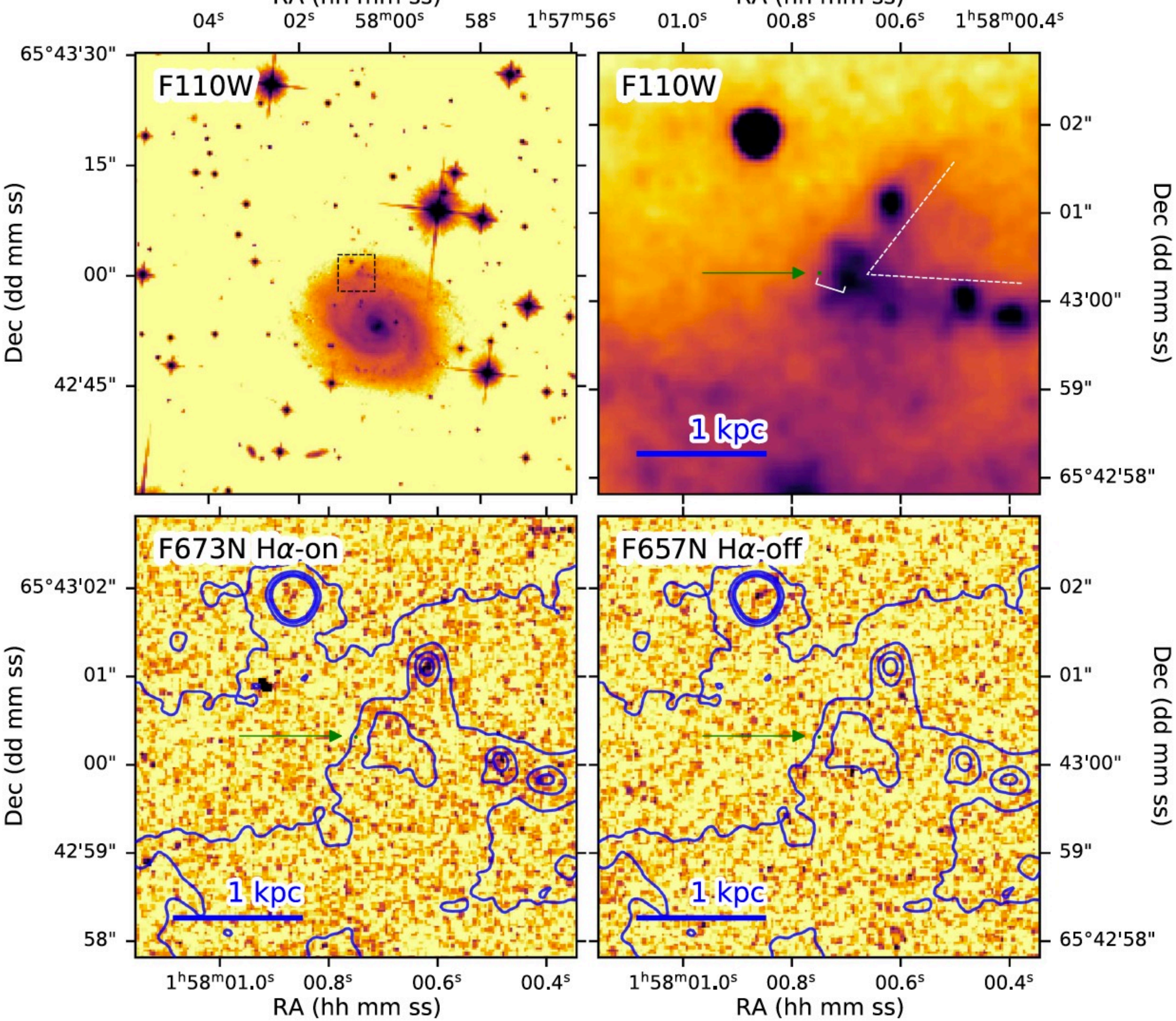

<1e-4 $M_\odot$/yr

~250pc away

from stellar clump

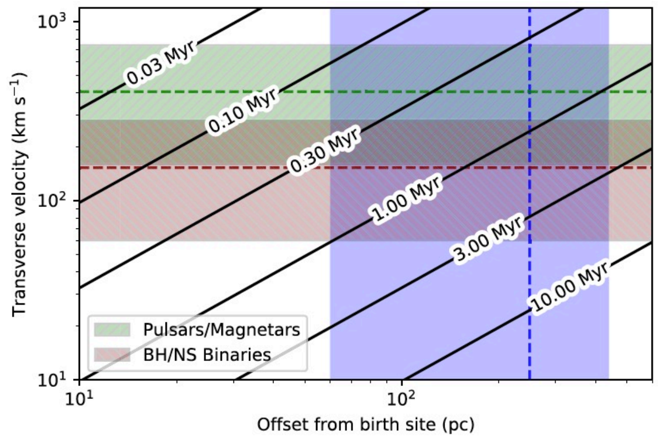

Not a magnetar?

but HMXB

& γ-ray binary?

Magnetar or Not?

Yes

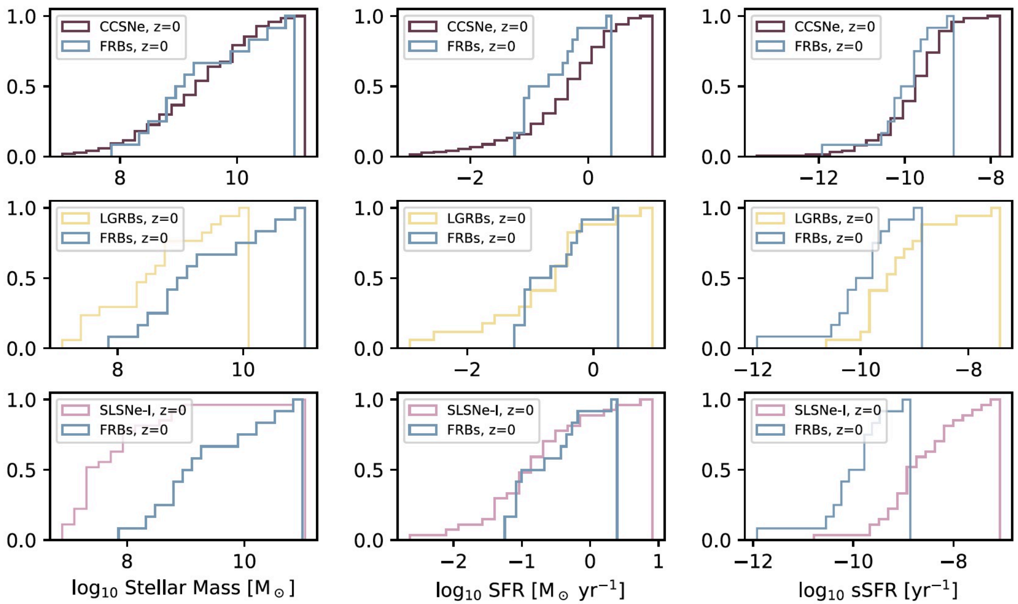

Bochenek+ 21

No

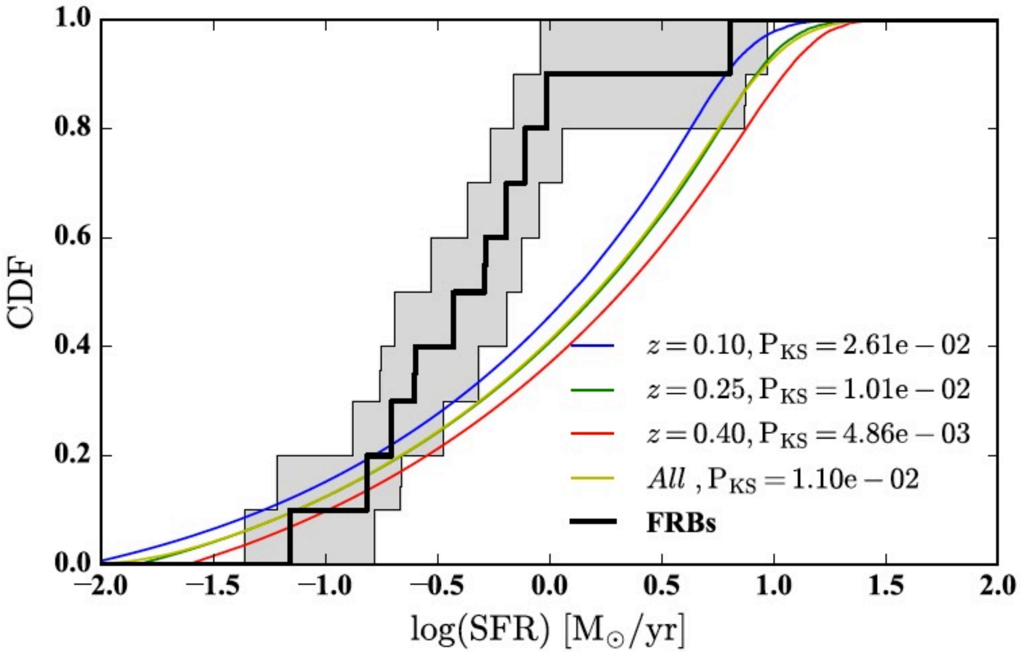

Safarzadeh+ 20

Conflicting with each other

Similar to Milky Way NS?

Face-on image of Milky Way

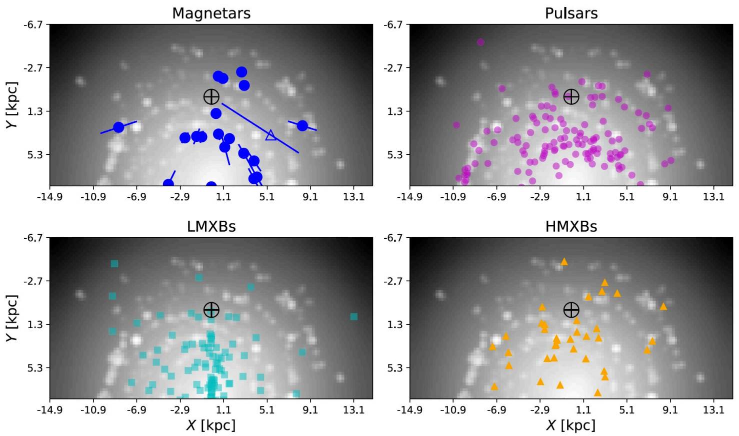

Table 6. For each extragalactic transient, the number of comparisons made to magnetar, pulsar, and XRB systems on the Milky Way is listed, along with the number and fraction of those tests which return at *p*-value >0.05. The results used to populate this table are listed in Tables 2 (offsets and host-normalized offsets in both bands), 3 (enclosed fluxes, *I*-band only), 4 (half-Galaxy F_{light}), and 5 (F_{light} in the local 4 kpc). Overall, FRBs are clearly distributed on their hosts in a similar manner to neutron stars on the Milky Way, and are a better match than the other transients tested.

Transient	$N_{AD-test} > 0.05$	$N_{AD-test}$	Fraction >0.05
LGRB	8	28	0.29
SLSN	4	20	0.20
CCSNe	6	28	0.21
FRB	24	32	0.75
SNe Ia	8	24	0.33
SGRB	2	28	0.07

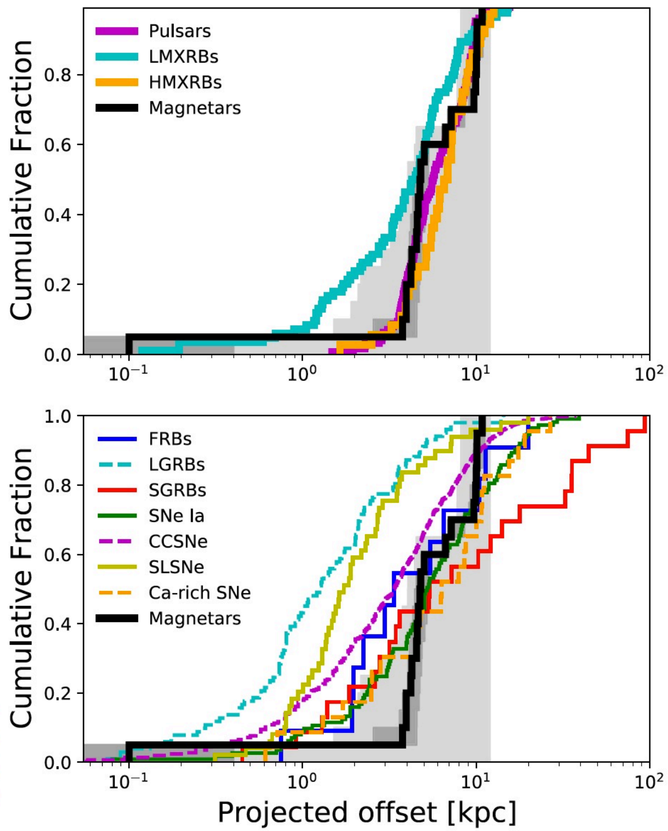

Chrimes+ 21

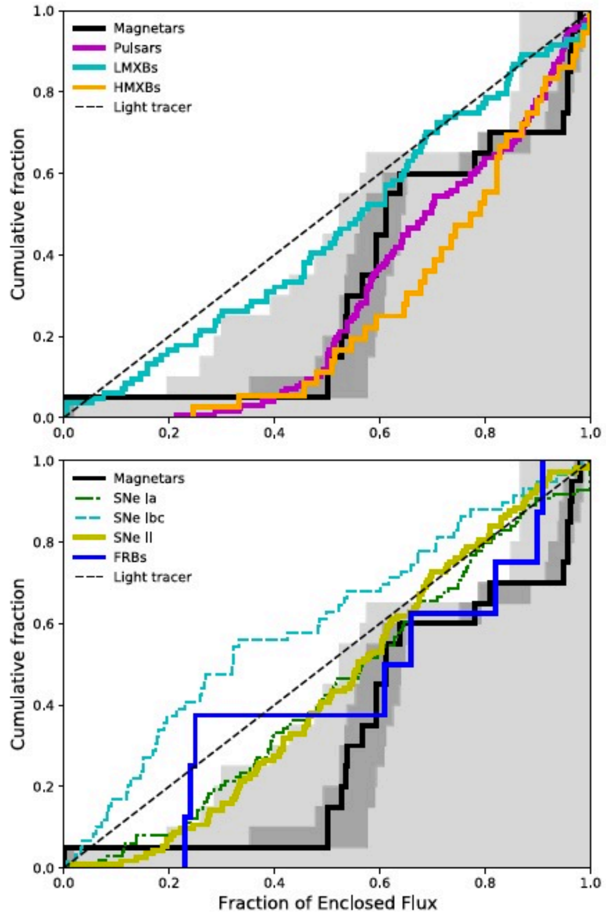

FRB distribution
~ Galactic NSs in MW

Highest Redshift by FAST

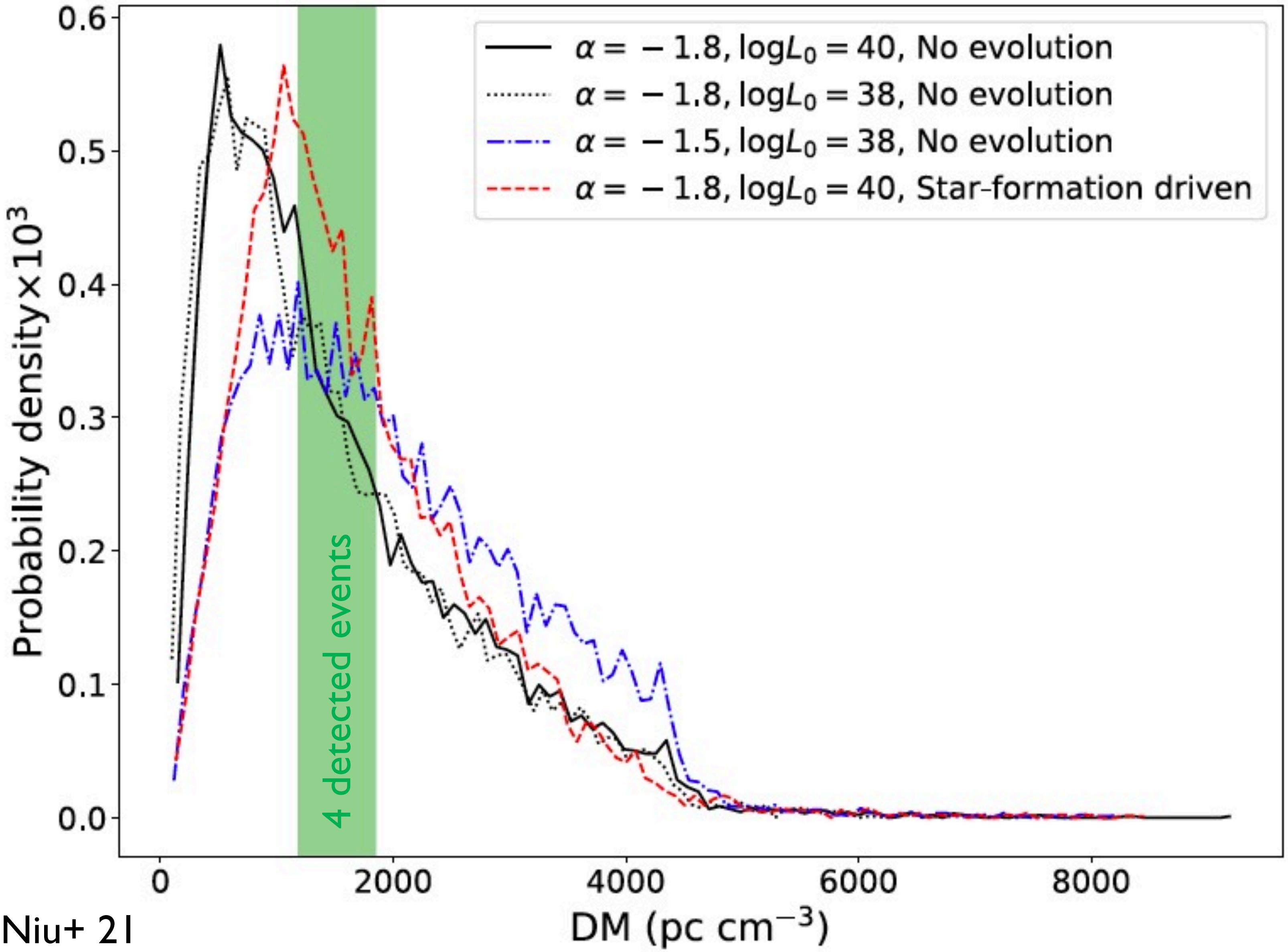

Niu+ 21

Please plot log!

At least up to DM~4000

z~4

Event Rate

CHIME/FRB 21

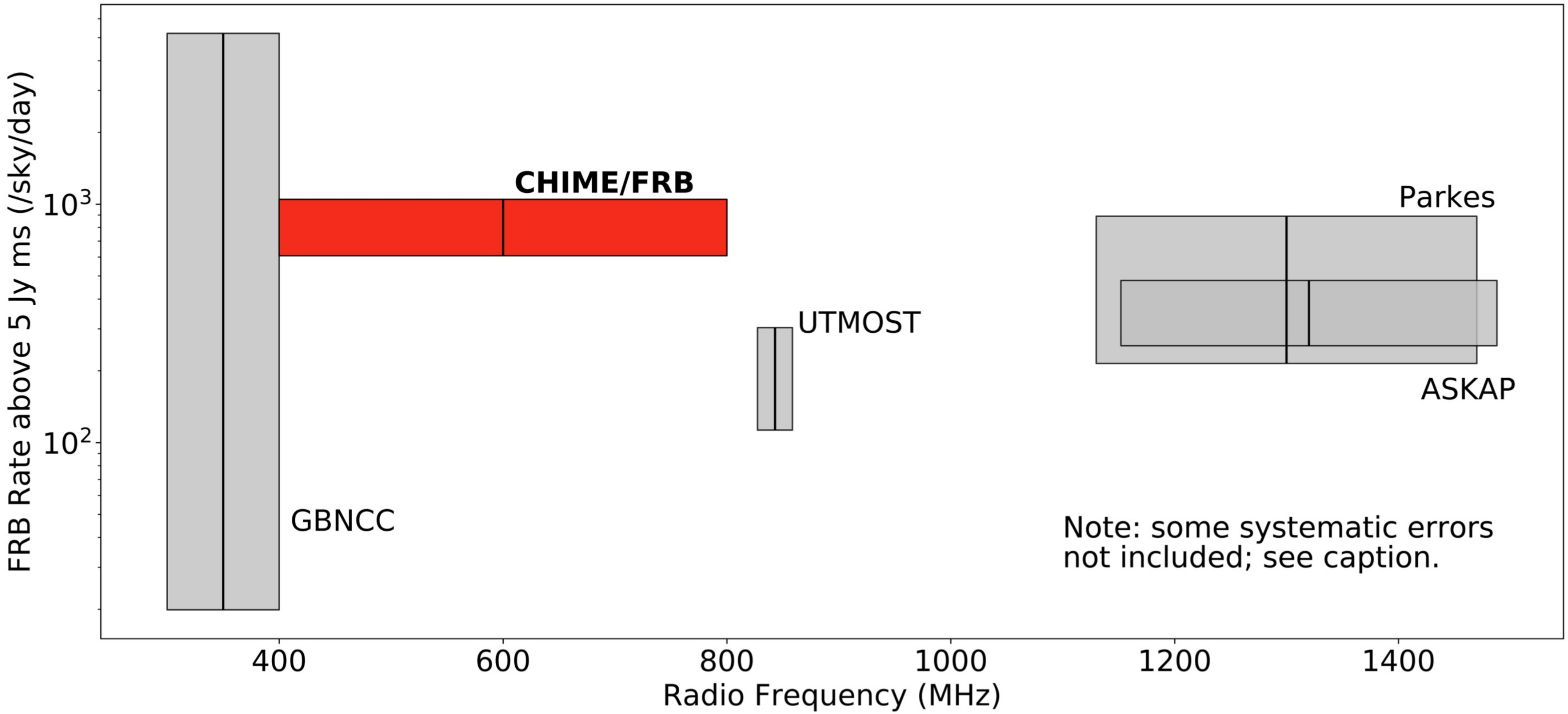

RM Evolution

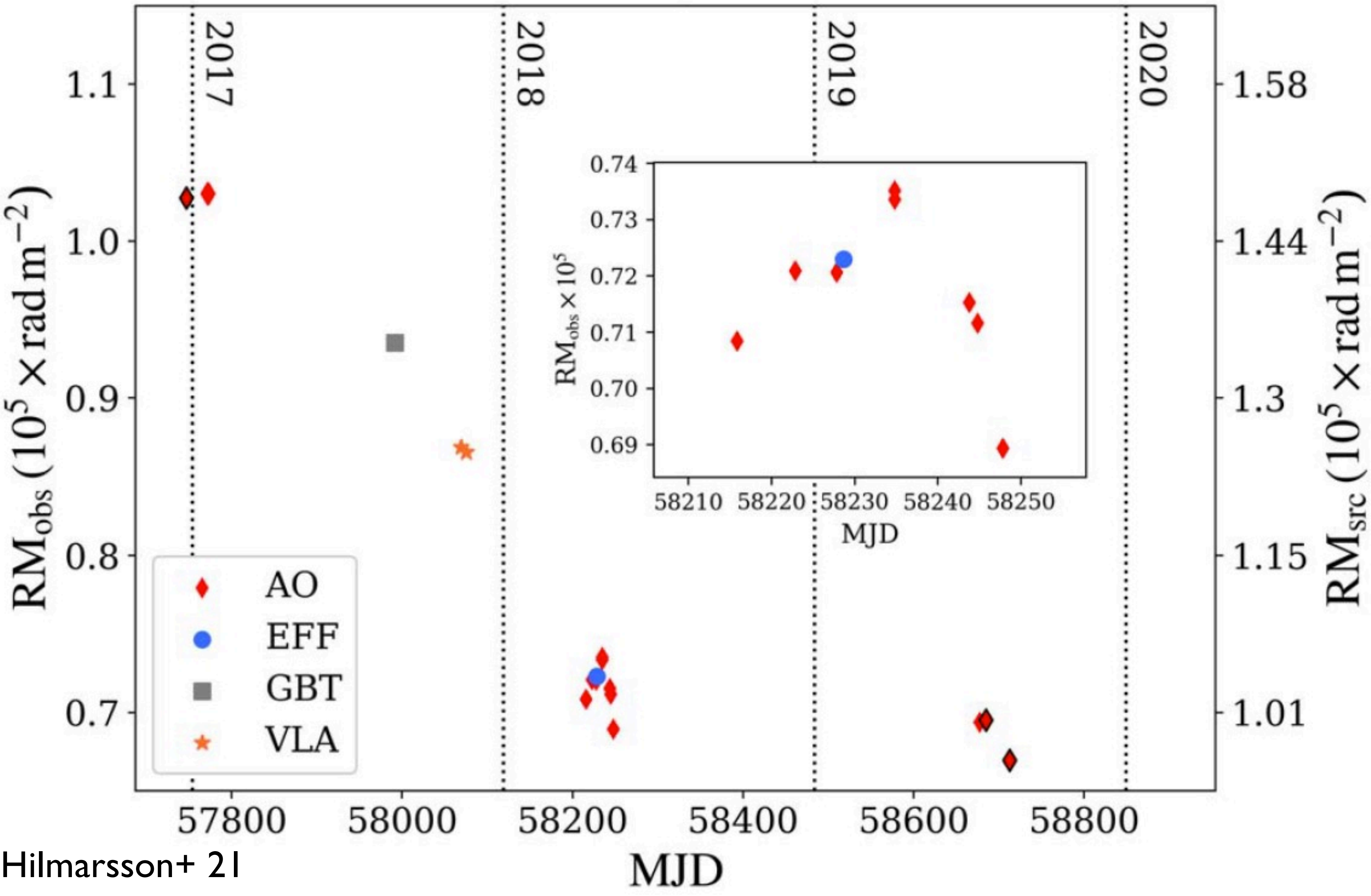

Hilmarsson+ 21

Scattering

$$\tau_{\rm host} \propto \begin{cases} (1+z)^{-3} & \text{for diffractive scales less than the inner scale of the turbulence,} \\ (1+z)^{-17/5} & \text{otherwise.} \end{cases}$$

$$\tau_{\rm IGM} \sim \begin{cases} z^2 & z \leq 1 \\ (1+z)^{0.2-0.5} & z \geq 1. \end{cases}$$

Bhandari & Flynn 21

Table 1. Total number of FRBs that are required for cosmological applications.

Cosmological Applications of FRBs	No. of FRBs	References
Distribution of baryons between the CGM and IGM	10^1–10^2	Ravi [160]
Radial density profile of the CGM	10^2–10^3	McQuinn [102]
Detection of He II reionisation	10^2–10^3	Kit Lau et al. [207]
FRBs as cosmic rulers	10^3	Macquart et al. [107]
Origin and distribution of extragalactic magnetic fields	10^3–10^4	Vazza et al. [133]
Cosmological constraints ($\Omega_b h^2$, H_0 and w)	10^3–10^4	Zhao et al. [188], Walters et al. [187]

Bhandari & Flynn 21

Polarization

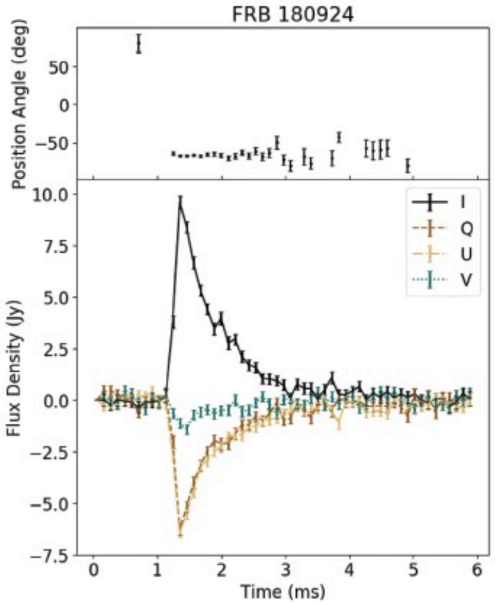

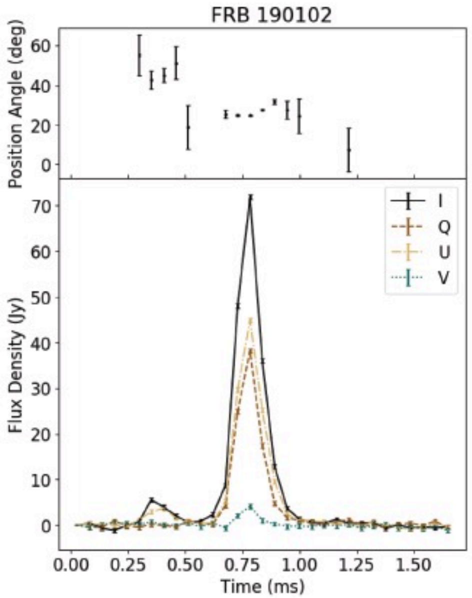

Table 5. The polarization fractions along with their uncertainties derived for each FRB over the time range t_{int}.

FRB	$\frac{P_{was}}{I_{was}} \pm \sigma_{P_{was}/I_{was}}$	$L_{was}/I_{was} \pm \sigma_{L_{was}/I_{was}}$	$V_{was}/I_{was} \pm \sigma_{V_{was}/I_{was}}$	t_{int} (ms)
FRB 180924	91.3 ± 2.0	90.2 ± 2.0	− 13.3 ± 1.4	1.08 – 3.24
FRB 190102				
Subpulse 1	70 ± 8	69 ± 8	9 ± 7	0.216 – 0.54
Subpulse 2	82.3 ± 0.7	82.2 ± 0.7	4.8 ± 0.5	0.54 – 1.026
FRB 190608	92 ± 3	91 ± 3	− 9 ± 2	1.944 – 12.744
FRB 190611				
Subpulse 1	94 ± 3	93 ± 3	15 ± 2	1.296 – 1.944
Subpulse 2	91 ± 3	70 ± 3	57 ± 3	2.268 – 3.024
FRB 190711				
Sub-burst 1	101 ± 2	101 ± 2	− 1 ± 2	0.216 – 4.536
Sub-burst 2	93.9 ± 2.0	93.7 ± 2.0	0.9 ± 1.5	4.536 – 8.856
Sub-burst 3	98 ± 4	98 ± 4	1 ± 3	8.856 – 11.448

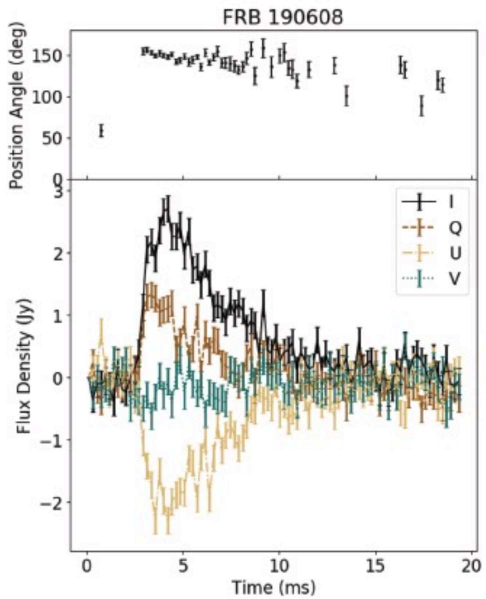

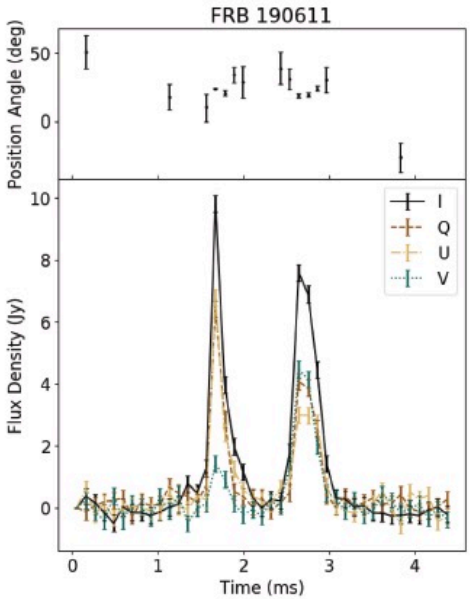

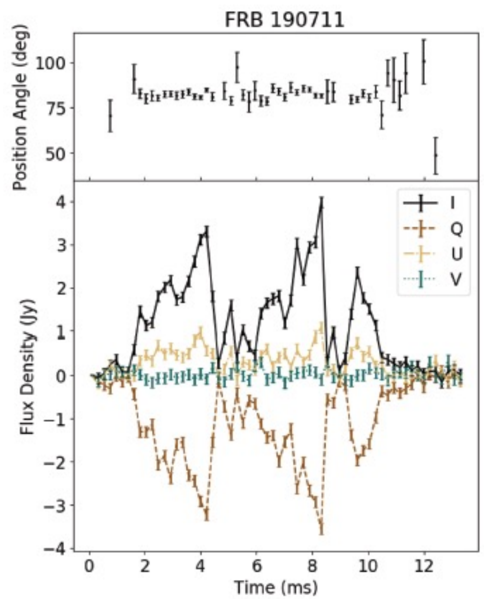

Day+ 20

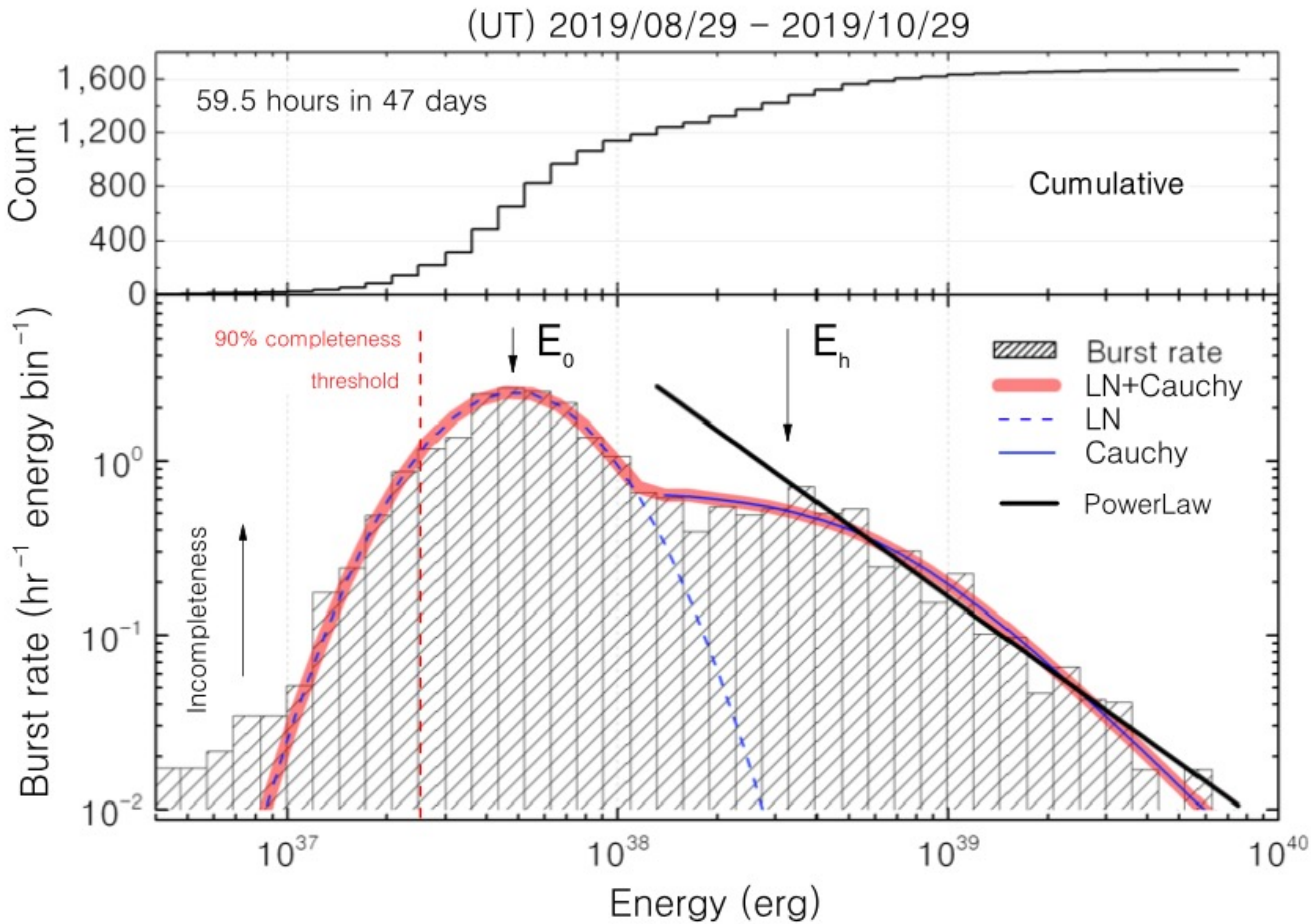

(UT) 2019/08/29 – 2019/10/29
Count
1,600
1,200
800
400
0
59.5 hours in 47 days
Cumulative
Burst rate (hr⁻¹ energy bin⁻¹)
10^0
10^{-1}
10^{-2}
90% completeness
threshold
E_0
E_h
Incompleteness
Burst rate
LN+Cauchy
LN
Cauchy
PowerLaw
10^{37}
10^{38}
10^{39}
10^{40}
Energy (erg)

Li+ 21

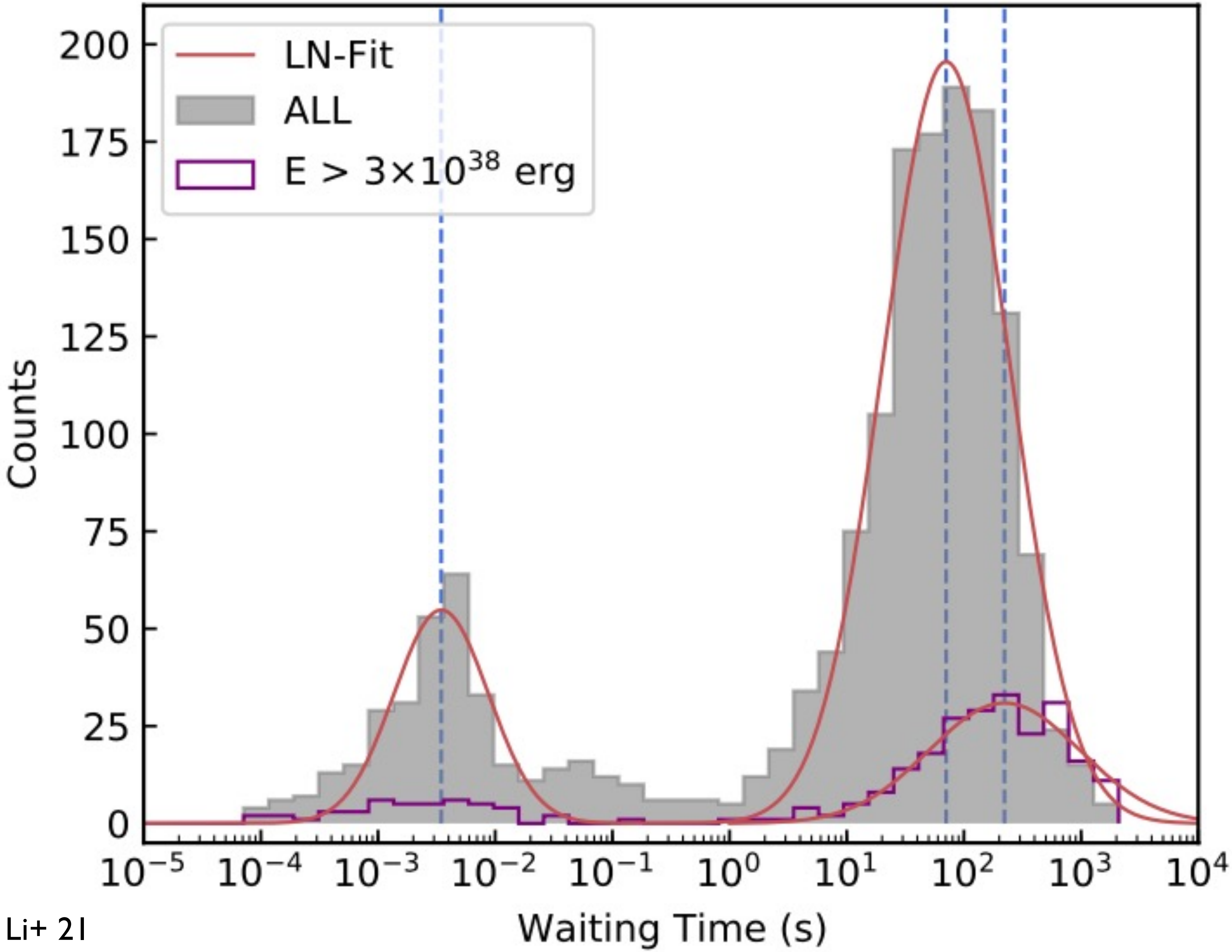
LN-Fit
ALL
E > 3×10^38 erg
Counts
Waiting Time (s)
200
175
150
125
100
75
50
25
0
10^-5
10^-4
10^-3
10^-2
10^-1
10^0
10^1
10^2
10^3
10^4

Li+ 21

Future Prospects

GOAL:

Localize Every CHIME-Detected FRB (few thousand) to < 50 mas

4

Single-Dish Localization

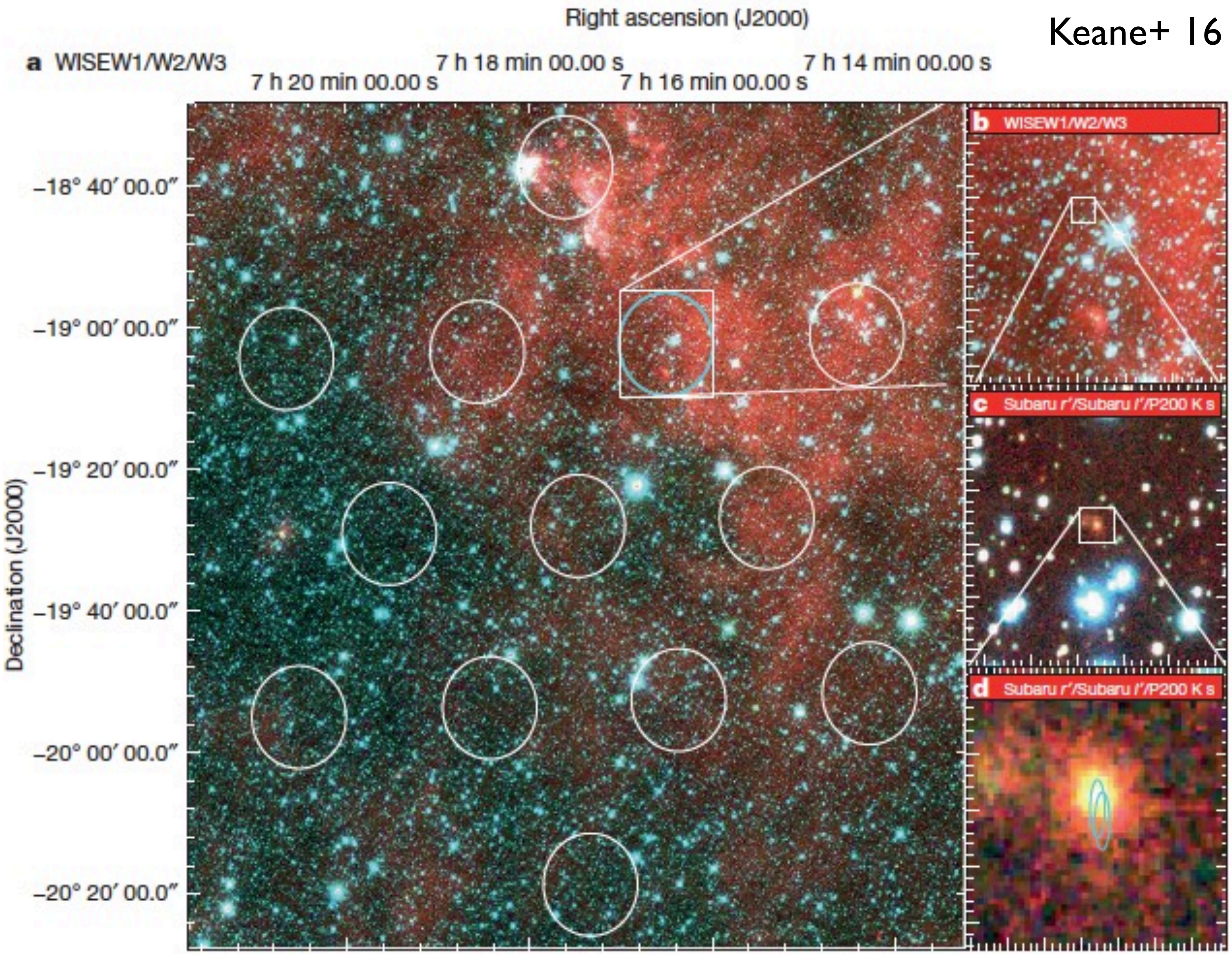

Keane+ 16

Parkes radio telescope
64 m dish size

Bad localization

FRB 150418

→ variability

→ the source?

But it is AGN

Uncertainty Principle?

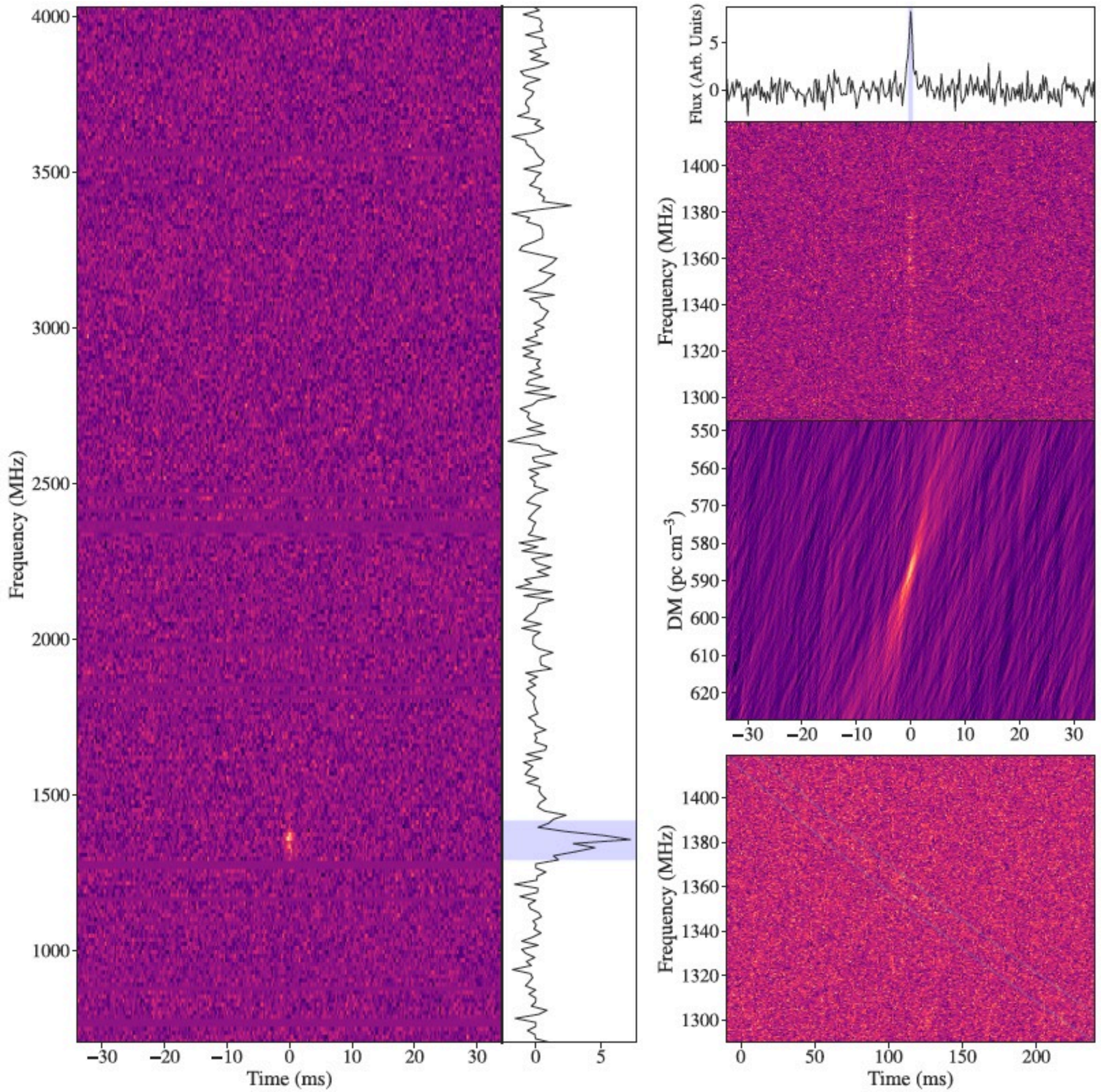

Kumar+ 21

$\Delta\nu \sim 65$ MHz

$\Delta\tau \sim 1$ ms

$\Delta\nu\, \Delta\tau \sim 65000$

$\Delta\tau$ may be $\sim \mu$s

* Crab nanoshot

$\Delta\nu \sim 500$ MHz

$\Delta\tau \sim 2$ ns

$\Delta\nu\, \Delta\tau \sim 1$

Hankins+ 03

Lorimer Burst 010724

Lorimer+ 07

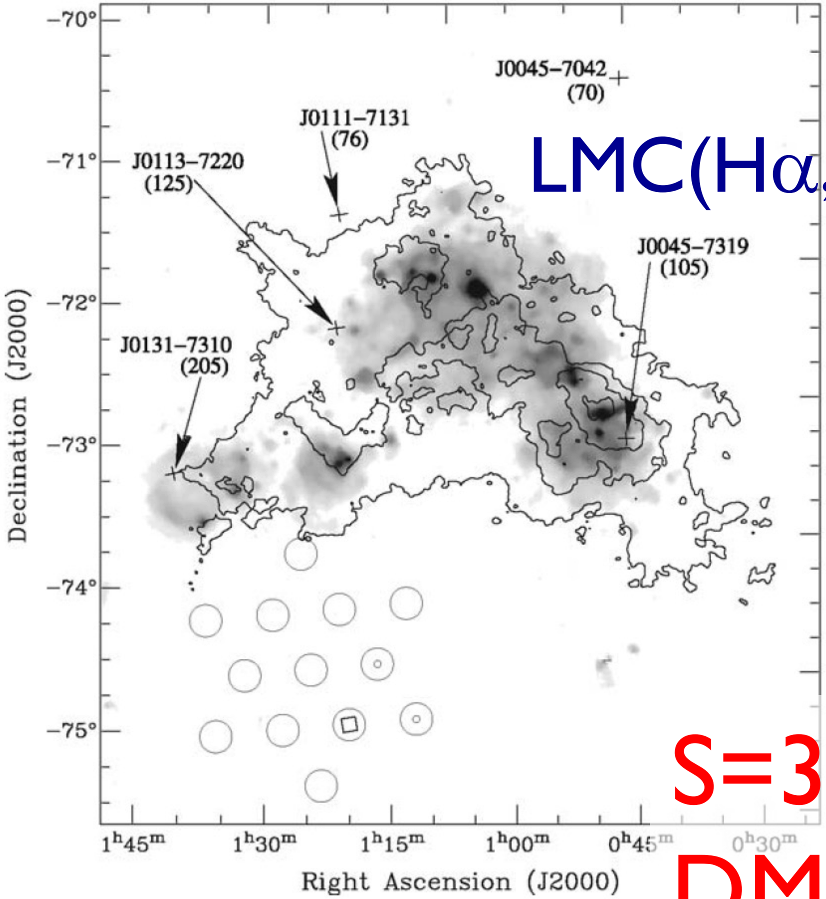

LMC(Hα, HI)

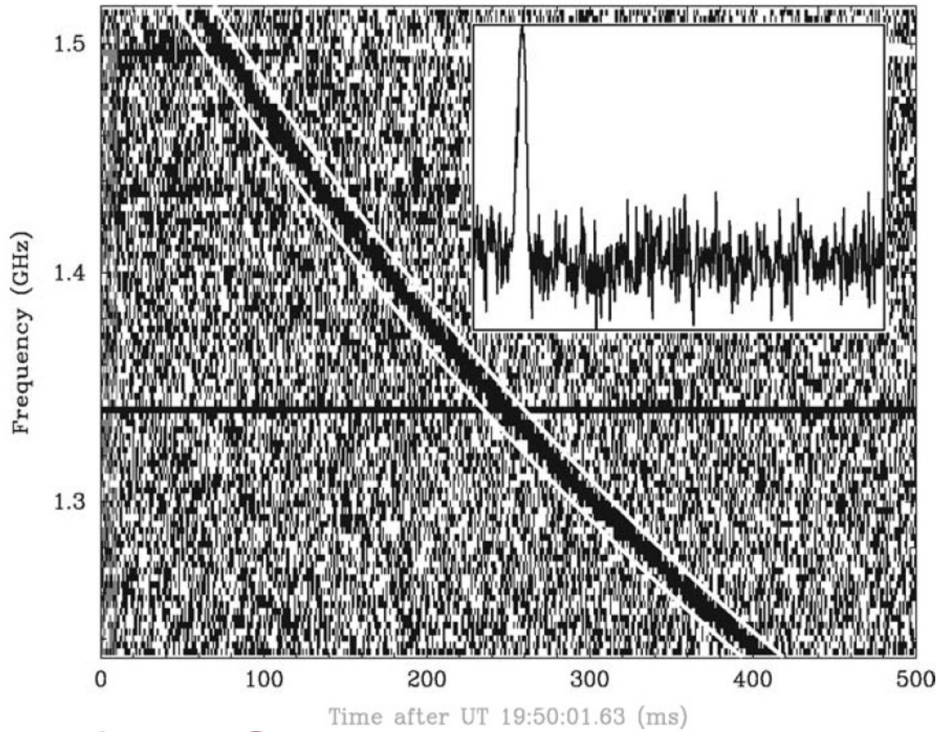

Fig. 1. Multiwavelength image of the field surrounding the burst. The gray scale and contours respectively show Hα and H I emission associated with the SMC (32, 33). Crosses mark the positions of the five known radio pulsars in the SMC and are annotated with their names and DMs in parentheses in units of cm^{-3} pc. The open circles show the positions of each of the 13 beams in the survey pointing with a diameter equal to the half-power width. The strongest detection saturated the single-bit digitizers in the data acquisition system, indicating that its S/N >> 23. Its location is marked with a square at right ascension 01^h 18^m 06^s and declination −75° 12′ 19″ (J2000 coordinates). The other two detections (with S/Ns of 14 and 21) are marked with smaller circles. The saturation makes the true position difficult to localize accurately. The positional uncertainty is nominally ±7′ on the basis of the half-power width of the multibeam system. However, the true position is probably slightly (a few arcmin) northwest of this position, given the nondetection of the burst in the other beams.

Fig. 2. Frequency evolution and integrated pulse shape of the radio burst. The survey data, collected on 24 August 2001, are shown here as a two-dimensional "waterfall plot" of intensity as a function of radio frequency versus time. The dispersion is clearly seen as a quadratic sweep across the frequency band, with broadening toward lower frequencies. From a measurement of the pulse delay across the receiver band, we used standard pulsar timing techniques and determined the DM to be 375 ± 1 cm^{-3} pc. The two white lines separated by 15 ms that bound the pulse show the expected behavior for the cold-plasma dispersion law assuming a DM of 375 cm^{-3} pc. The horizontal line at ~1.34 GHz is an artifact in the data caused by a malfunctioning frequency channel. This plot is for one of the offset beams in which the digitizers were not saturated. By splitting the data into four frequency subbands, we have measured both the half-power pulse width and flux density spectrum over the observing bandwidth. Accounting for pulse broadening due to known instrumental effects, we determine a frequency scaling relationship for the observed width $W = 4.6$ ms $(f/1.4 \text{ GHz})^{-4.8 \pm 0.4}$, where f is the observing frequency. A power-law fit to the mean flux densities obtained in each subband yields a spectral index of −4 ± 1. The inset shows the total-power signal after a dispersive delay correction assuming a DM of 375 cm^{-3} pc and a reference frequency of 1.5165 GHz. The time axis on the inner figure also spans the range 0 to 500 ms.

S=30±10Jy, δt<5ms

DM=375 cm^{-3} pc ⇒ z~0.1-0.3

$W \propto f^{-4.8\pm0.4}$, $S \propto f^{-4}$

b=-41.8deg

Terrestrial?

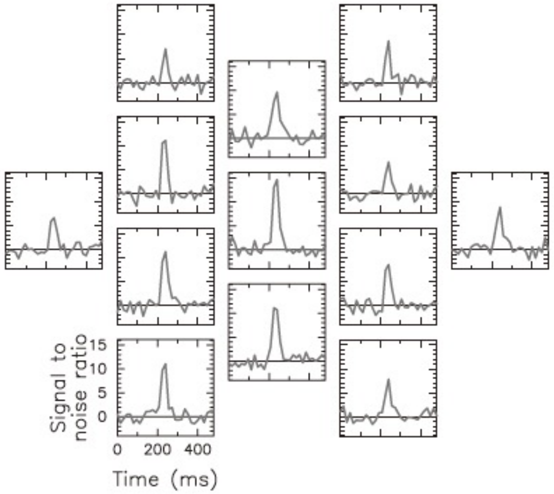

(a) Peryton 08 in 13 beams

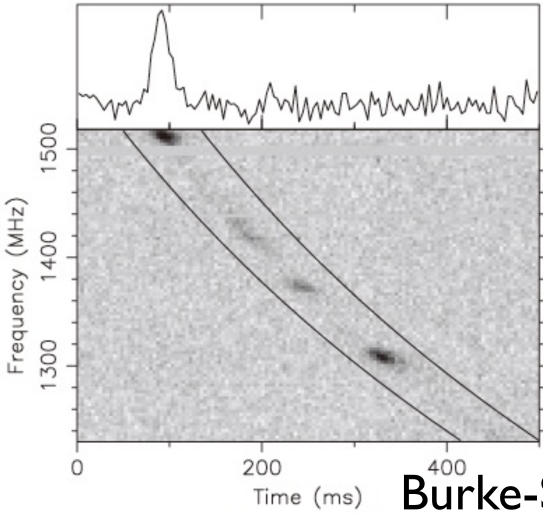

(b) Peryton 08

16 "Perytons" in all
13 telescope receivers

Burke-Spolaor+ 11; Kocz+ 12; Saint-Hilaire+ 12

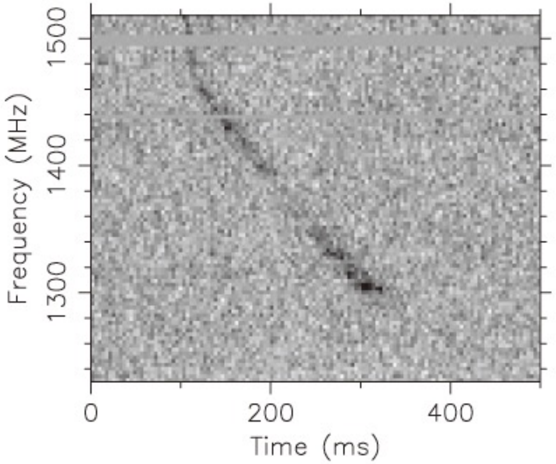

(c) Peryton 06

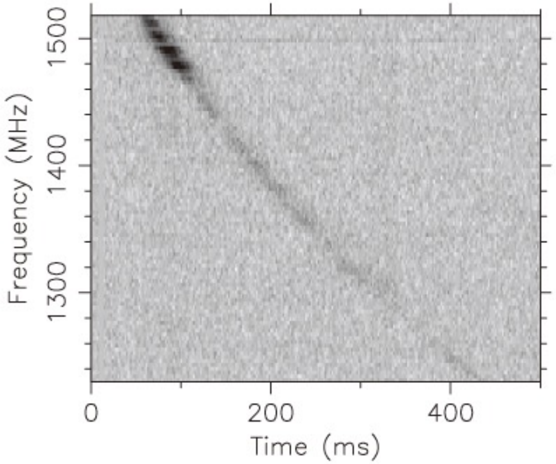

(d) Peryton 15

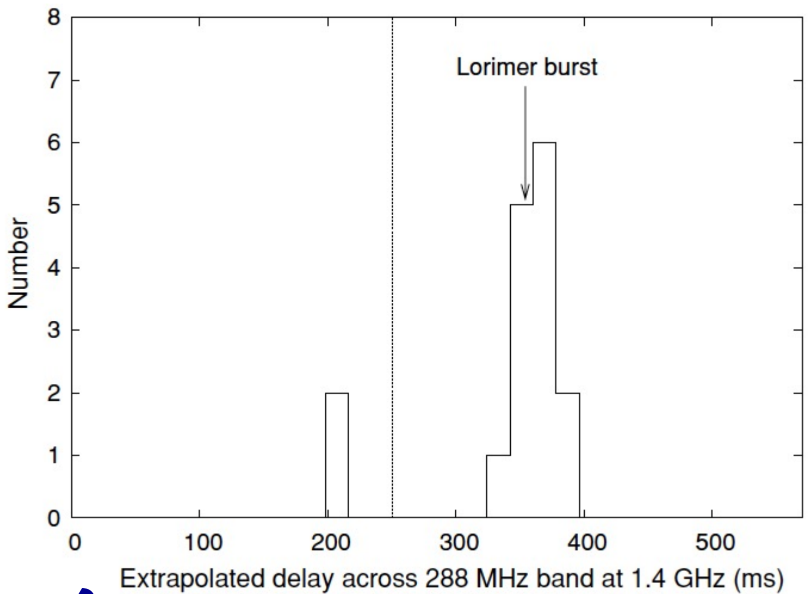

Dispersion Measure

Lightening, Aircraft, Microwave oven, …?

DM from Afterglow

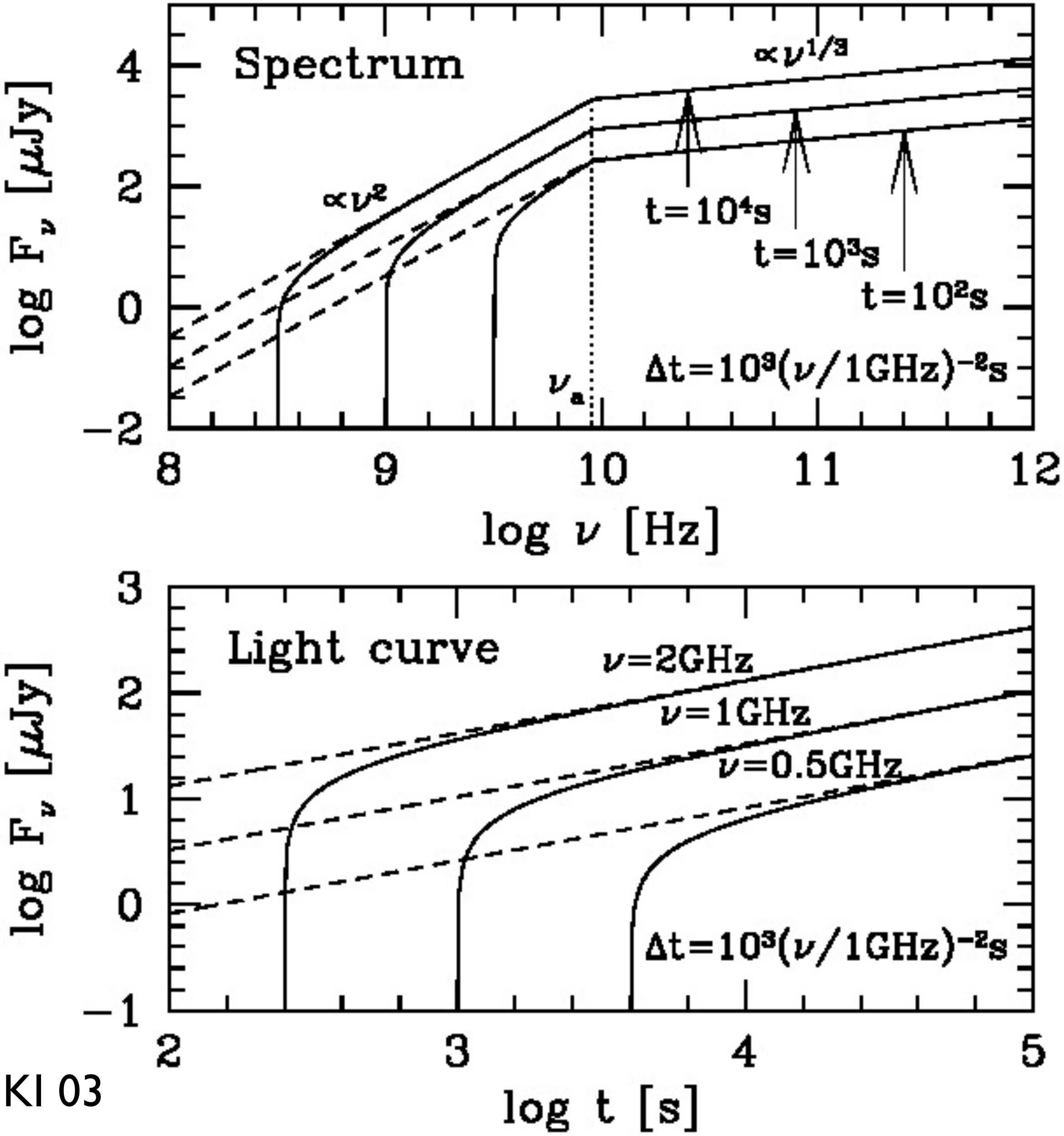

KI 03

Distortion at t~Δt

⇒ DM

$\Delta t \propto \nu^{-2}$

Unfortunately radio afterglows are not so bright

Table 1: **Properties of burst from SGR 1935+2154.**

Parameter	Component 1	Component 2
Dispersion measure (pc cm^{-3})	332.7206(9)	
Scattering timescale (ms)[a]	0.759(8)	
Arrival time (UTC, topocentric)[b]	14:34:24.40858(2)	14:34:24.43755(2)
Arrival time (UTC, geocentric)[b,c]	14:34:24.42848(2)	14:34:24.45745(2)
Scattering-corrected width (ms)	0.585(14)	0.335(7)
Spectral index[a,d]	−5.75(11)	3.61(8)
Spectral running[d]	1.0(3)	−19.9(3)
Fluence (kJy ms)	480	220
Peak flux density (kJy)	110	150

Values in parentheses denote statistical uncertainties corresponding to the 68.3% confidence interval in the last digit(s).

[a] Quantities are referenced to 600 MHz.

[b] Listed arrival times were corrected for the frequency-dependent time delay from interstellar dispersion using the listed dispersion measure, and are referenced to infinite frequency.

[c] Arrival times at the geocenter were obtained after correcting the listed topocentric times for the geometric delay, assuming an ICRS source position of (R. A., Dec.) = ($19^h34^m55.606^s$, $21°53'47.4''$)[13], and an observatory position of $(\text{Long., Lat.,Height})_{\text{CHIME}}$ = (119°36′26″ W, 49°19′16″ N, 545 m.).

[d] Quantity defined in Methods.

CHIME+ 2005.10324

Table 1: **Data on ST 200428A.** Standard errors in the final significant figures (68% confidence) given in parentheses.
[a] The correction to the infinite-frequency ($\nu = \infty$) arrival time is done using the DM quoted in this table, and assuming a dispersion constant of $\frac{1}{2.41} \times 10^4\,\mathrm{s\,MHz^2\,pc^{-1}\,cm^3}$ [14].
[b] The full-width half-maximum (FWHM) of the Gaussian used to model the intrinsic burst structure (Methods).
[c] This assumes a distance to SGR 1935+2154 of 9.5 kpc.

Property	**Measurement**
OVRO arrival time at $\nu = 1529.267578$ MHz (UTC)	28 April 2020 14:34:25.02657(2)
OVRO arrival time at $\nu = \infty$[a] (UTC)	28 April 2020 14:34:24.43627(3)
Earth centre arrival time at $\nu = \infty$[a] (UTC)	28 April 2020 14:34:24.45548(3)
Fluence (MJy ms)	1.5(3)
Dispersion measure ($\mathrm{pc\,cm^{-3}}$)	332.702(8)
Intrinsic burst FWHM[b] (ms)	0.61(9)
Isotropic-equivalent energy release[c] (erg)	$2.2(4) \times 10^{35}$

scattering ~0.4(1) ms@1GHz

T_b~1.4e32 K

No evidence for a local DM

Bochenek+ 2005.10828

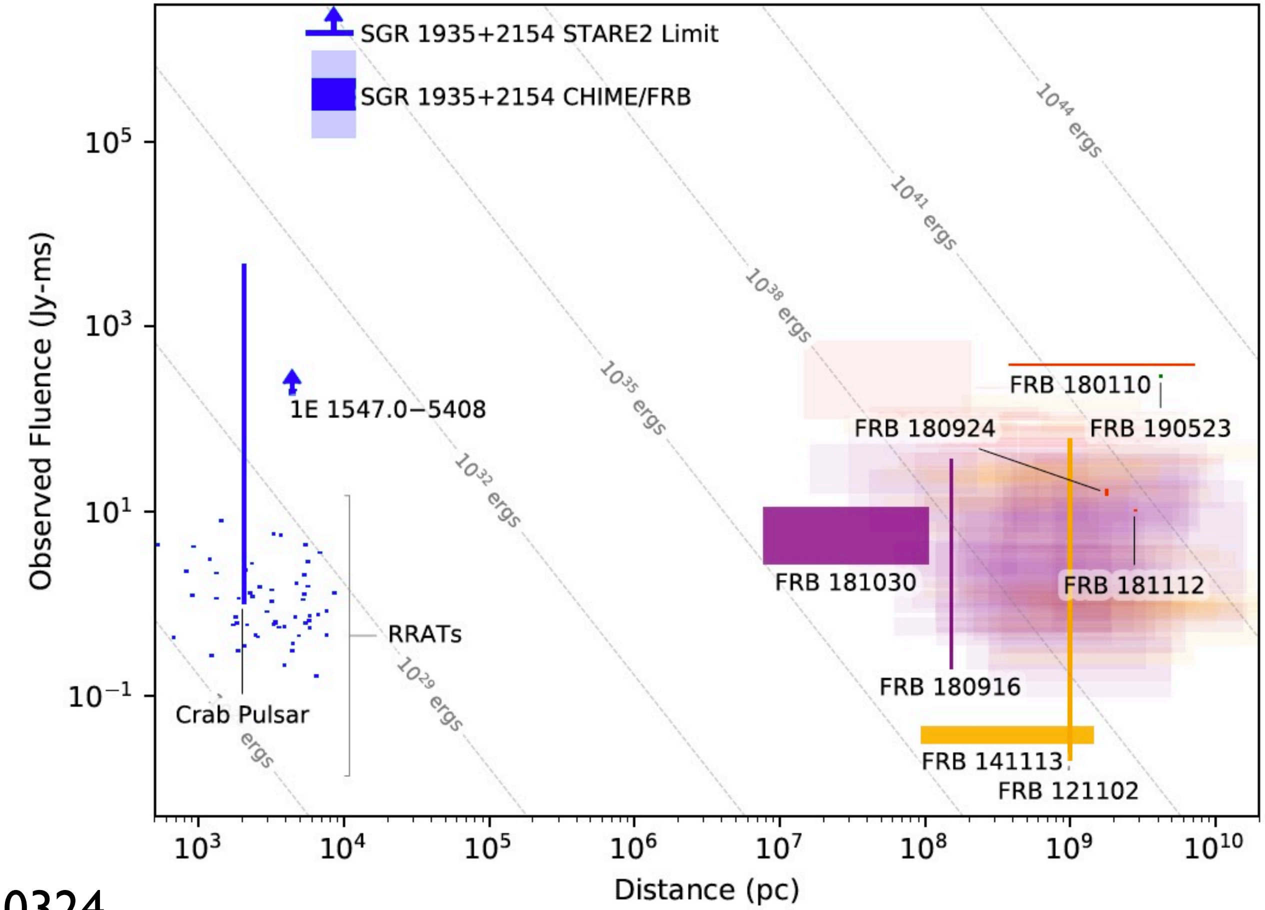

CHIME+ 2005.10324

Figure 2: **Comparison of short radio burst energetics.** The observed burst fluences at radio frequencies from 300 MHz to 1.5 GHz for Galactic neutron stars and extragalactic FRBs are plotted with their estimated distances. The fluence ranges include the uncertainties in fluence measurements as well as ranges of individual bursts for repeating FRBs and pulsars. FRBs colours indicate their detection telescope: CHIME/FRB (purple), ASKAP (red), DSA-10 (green, FRB 190523), Arecibo and Parkes (orange). Galactic sources are plotted in blue. For SGR 1935+2154 the blue rectangle indicates the nominal range of 400–800-MHz fluences measured for the two bursts while the light blue region incorporates the possible systematic uncertainty in the CHIME/FRB fluence as described in the text. The STARE2 lower limit on the fluence at 1.4 GHz is also shown. Gray diagonal lines indicate loci of equal isotropic burst energy with an assumed fiducial bandwidth of 500 MHz. FRB distances are estimated from their extragalactic dispersion measure contribution including the simulated variance [36]. Pulsar distances are estimated based on the NE2001 Galactic electron distribution model [14]. Objects with accurately measured distances (parallax or host galaxy redshift) are indicated with vertical lines.

Konus-*WIND*

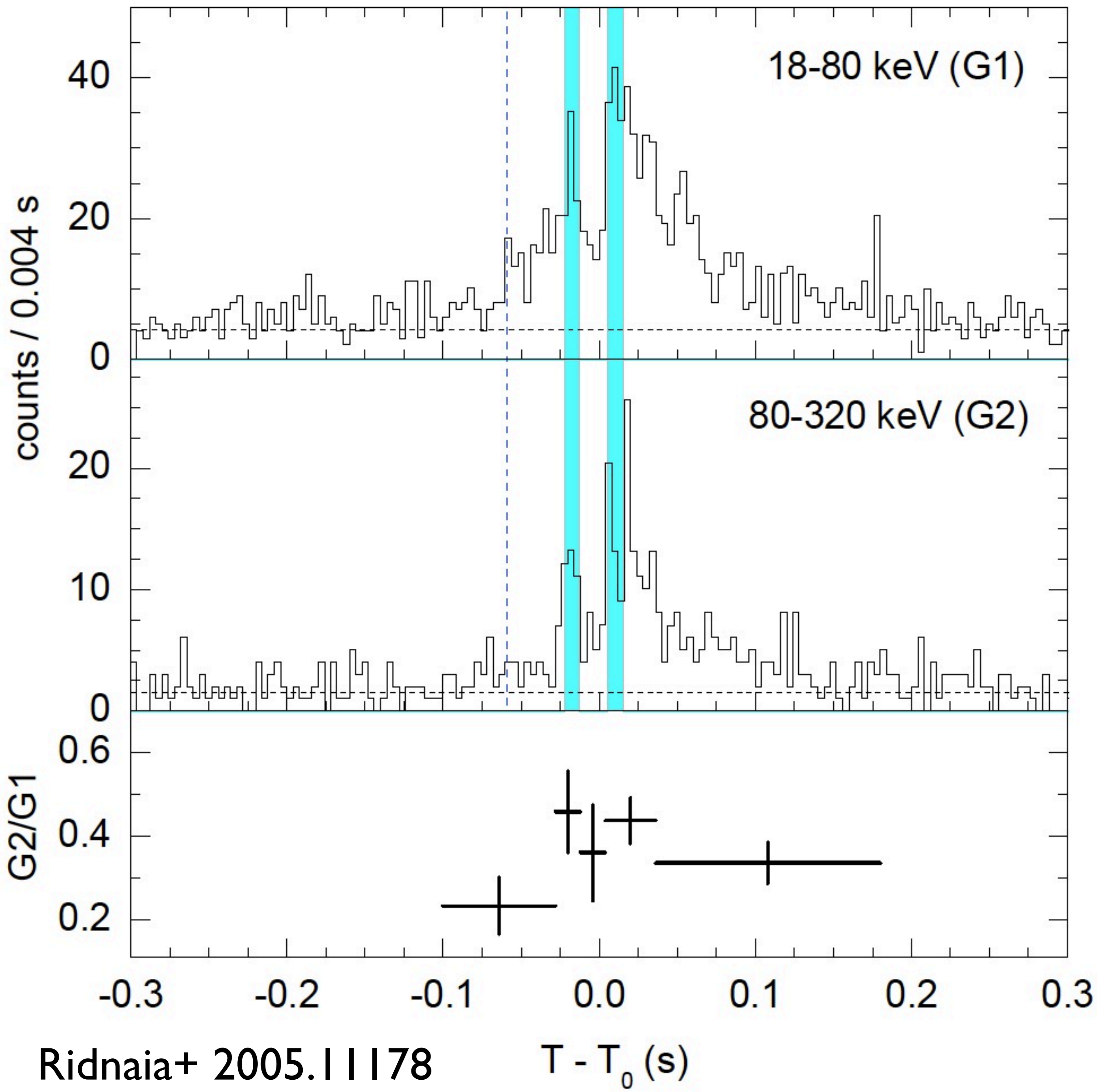

T_0=14:34:24.447 UT
(geocentric time)

Ridnaia+ 2005.11178

AGILE

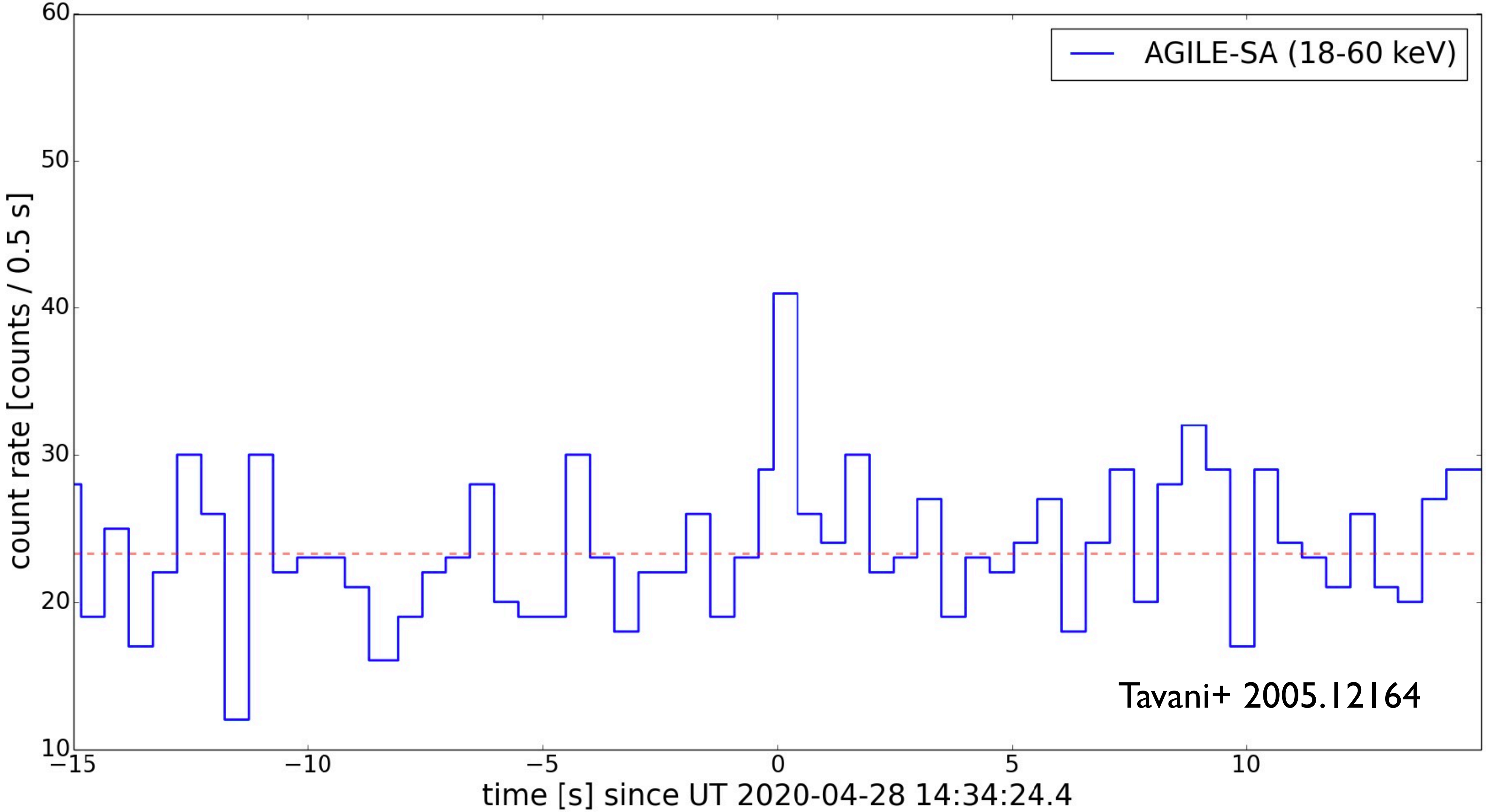

18-60 keV (Super-AGILE), ~0.5 sec, cutoff ~80 keV (No AC signal), ~8.1e39 erg @12 kpc at 121 deg off-axis angle, S/N=3.8σ, post-trial 2.9σ

FRB 190520

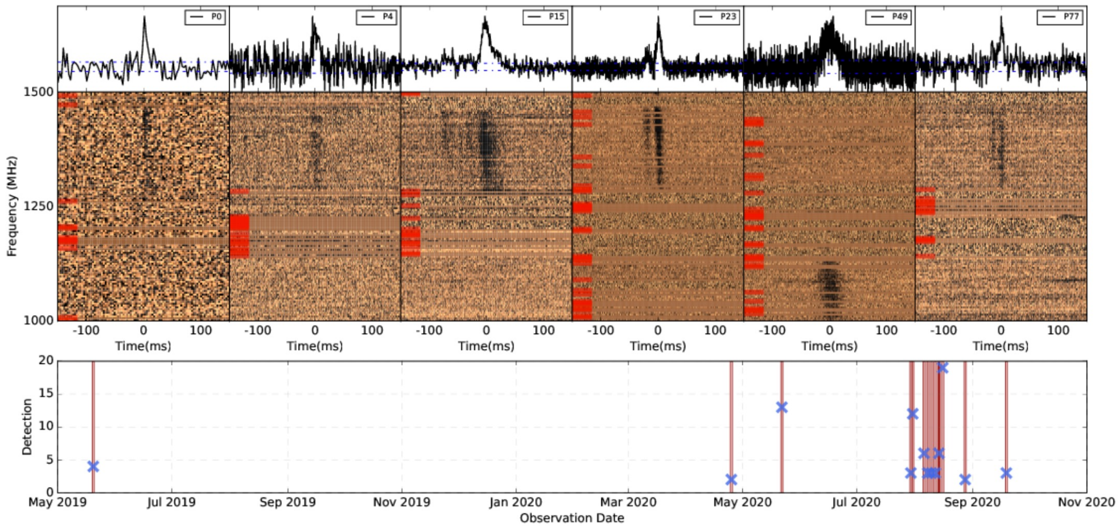

Niu+ 21

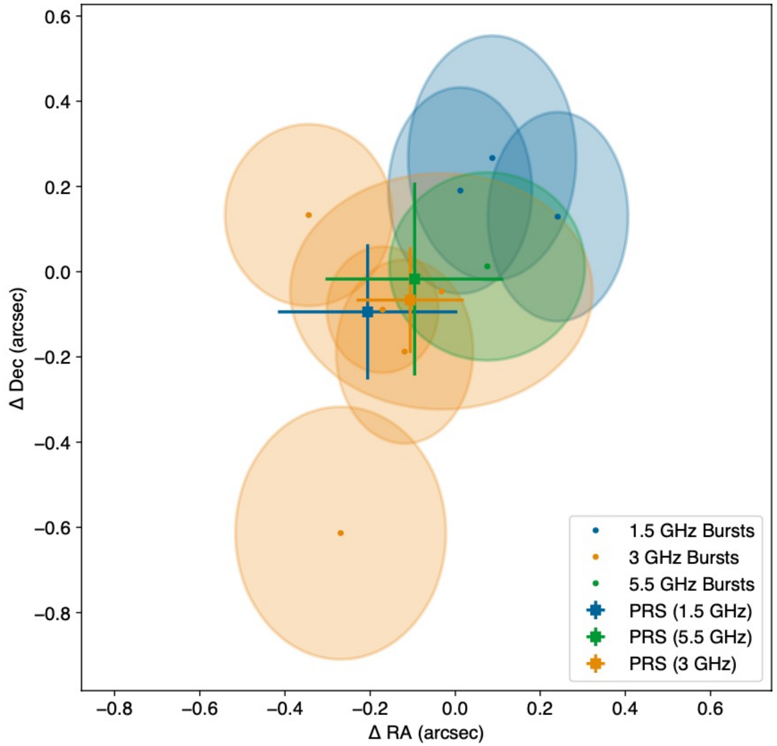

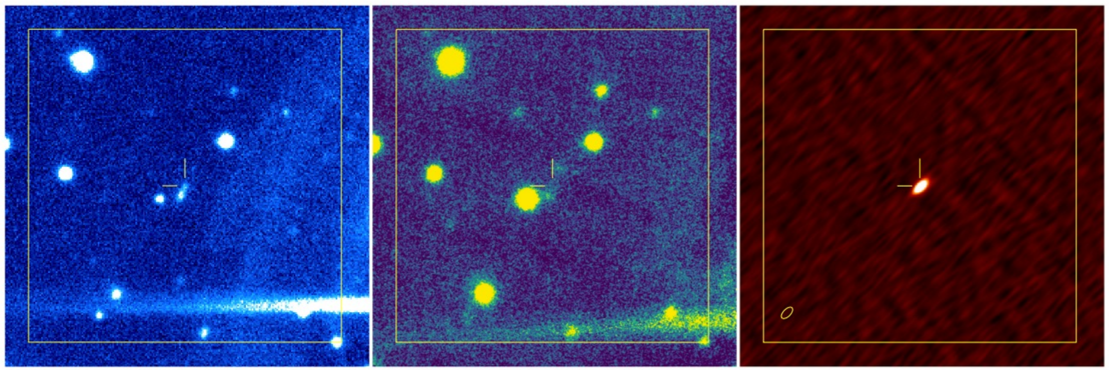

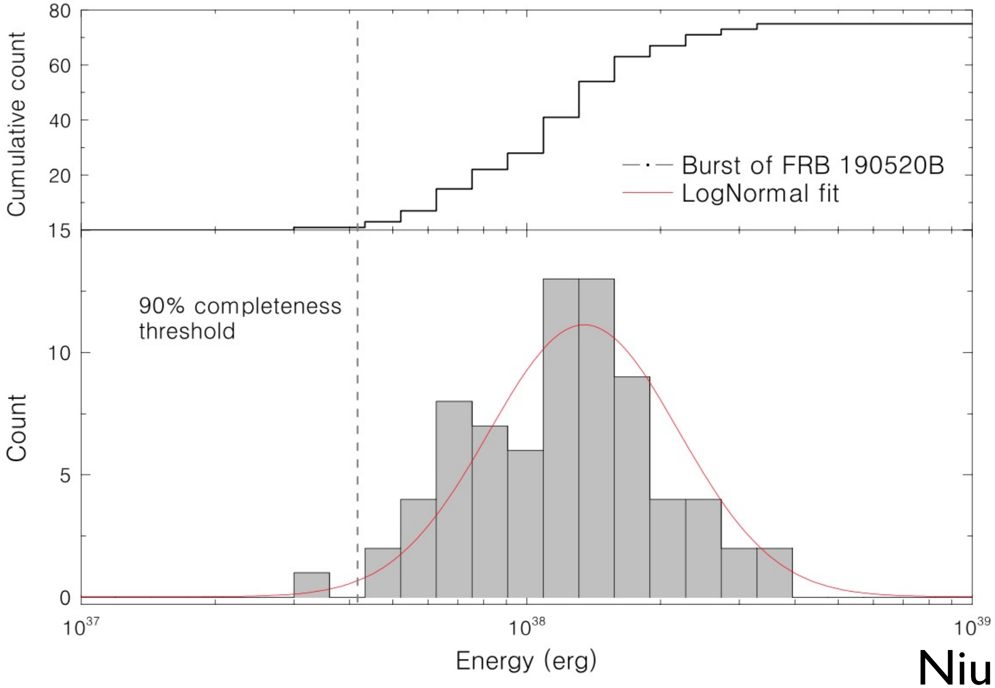
Cumulative count
Burst of FRB 190520B
LogNormal fit
90% completeness threshold
Count
Energy (erg)

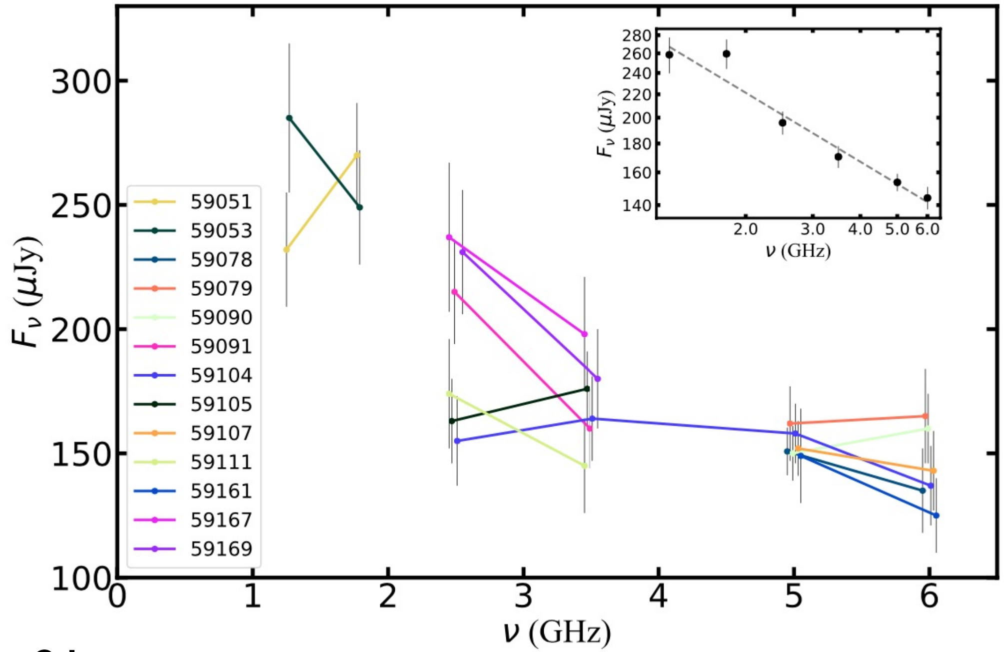
59051
59053
59078
59079
59090
59091
59104
59105
59107
59111
59161
59167
59169
F_ν (μJy)
ν (GHz)

Niu+ 21

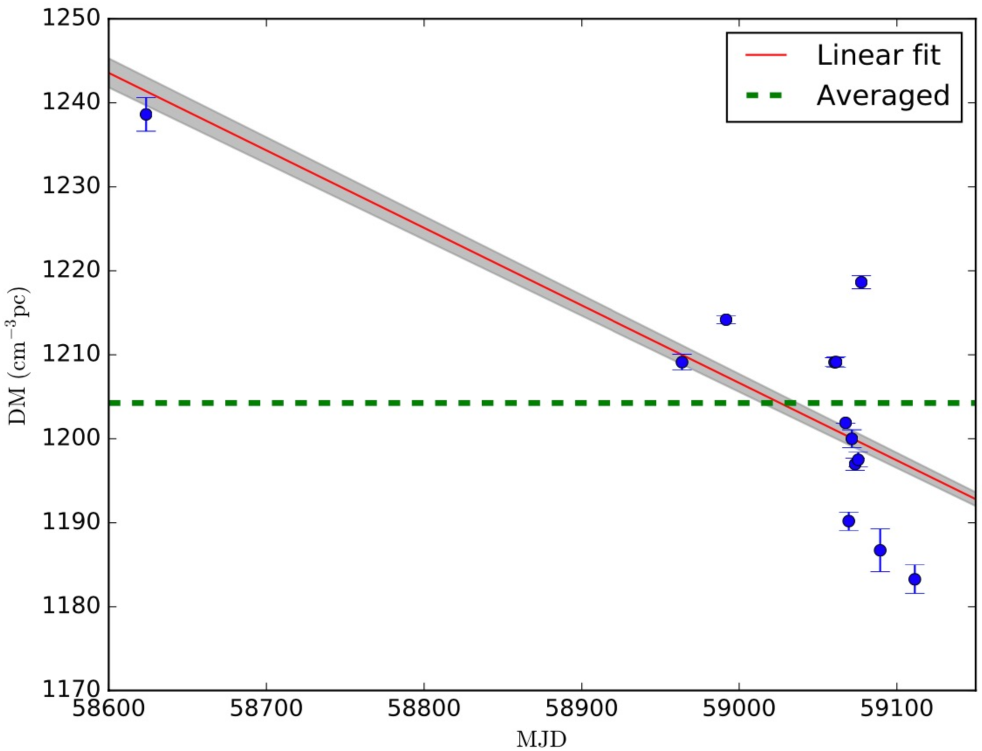
Linear fit
Averaged
DM (cm^{-3}pc)
MJD

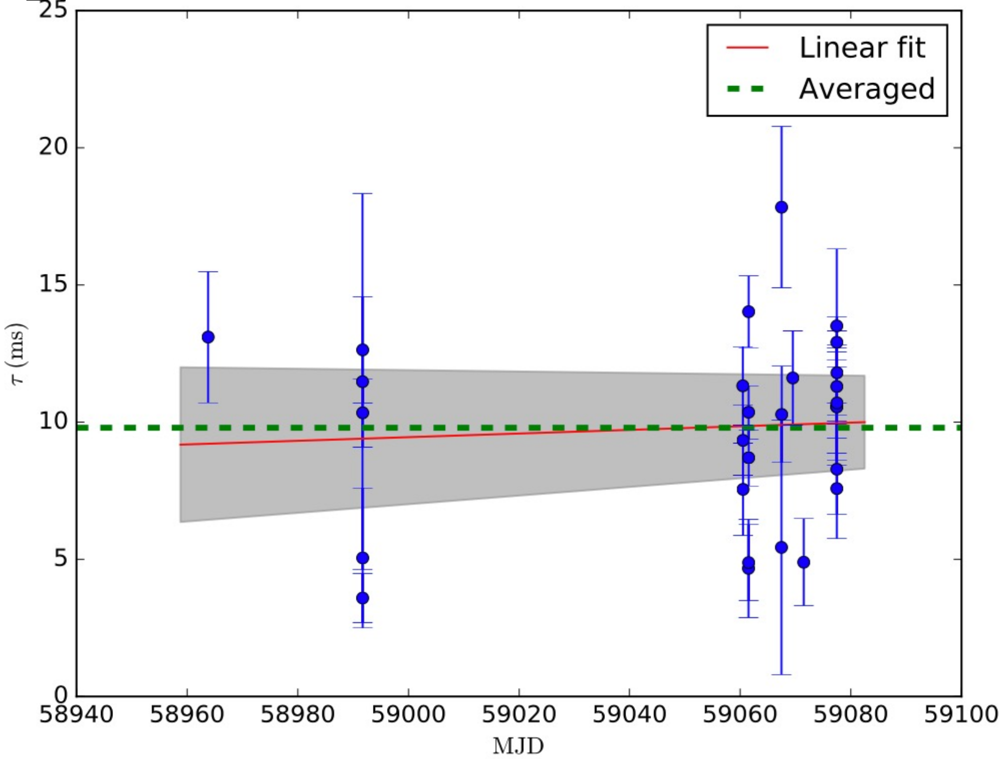
Linear fit
Averaged
τ (ms)
MJD

Current DM Range

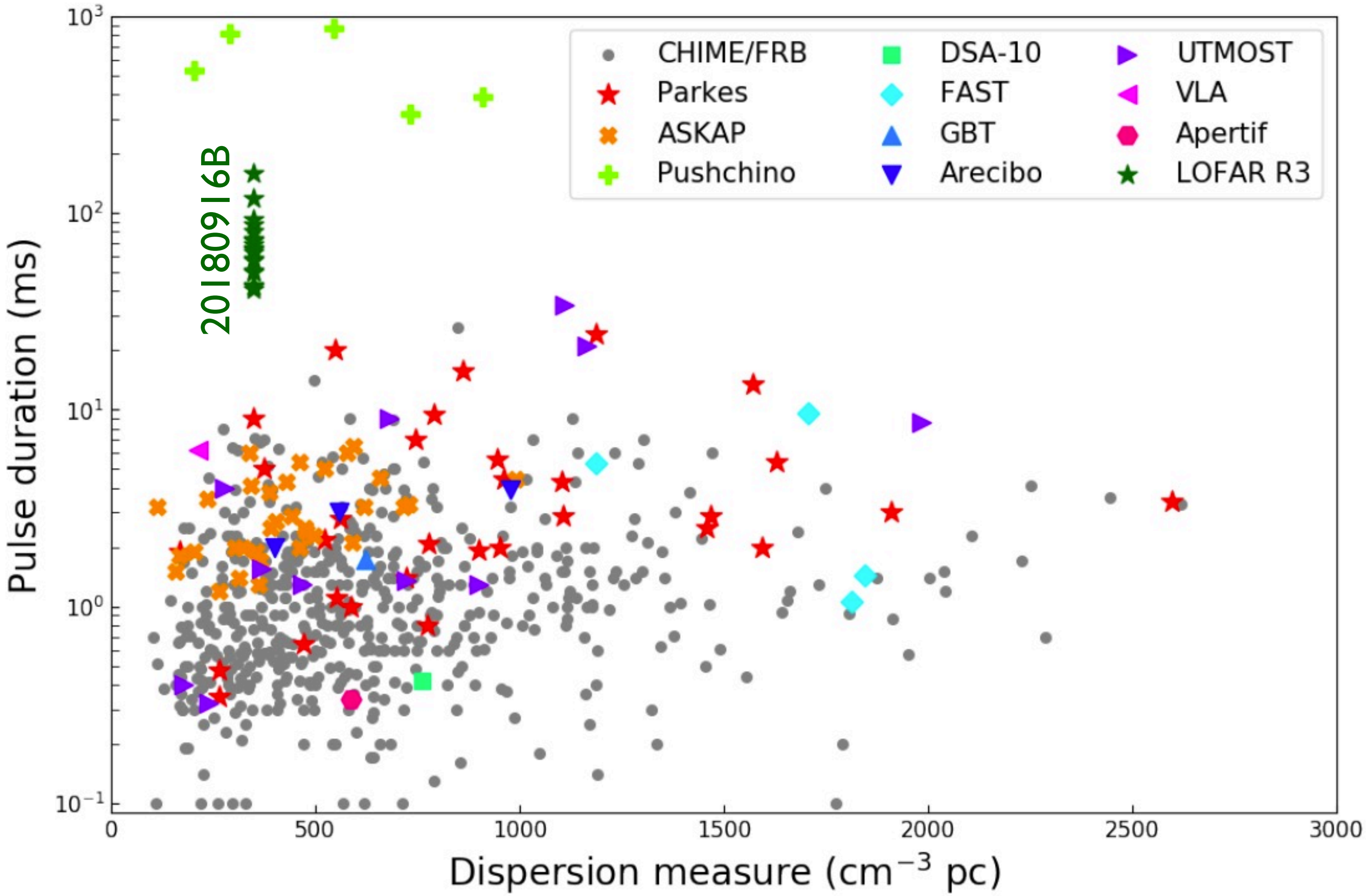

(c) Width vs. DM

Petroff+ 21

Missing Baryon

Fukugita, Hogan & Peebles 98

TABLE 3

THE BARYON BUDGET

Component	Central	Maximum	Minimum	Grade[a]
		Observed at $z \approx 0$		
1. Stars in spheroids	$0.0026\ h_{70}^{-1}$	$0.0043\ h_{70}^{-1}$	$0.0014\ h_{70}^{-1}$	A
2. Stars in disks	$0.00086\ h_{70}^{-1}$	$0.00129\ h_{70}^{-1}$	$0.00051\ h_{70}^{-1}$	A−
3. Stars in irregulars	$0.000069\ h_{70}^{-1}$	$0.000116\ h_{70}^{-1}$	$0.000033\ h_{70}^{-1}$	B
4. Neutral atomic gas	$0.00033\ h_{70}^{-1}$	$0.00041\ h_{70}^{-1}$	$0.00025\ h_{70}^{-1}$	A
5. Molecular gas	$0.00030\ h_{70}^{-1}$	$0.00037\ h_{70}^{-1}$	$0.00023\ h_{70}^{-1}$	A−
6. Plasma in clusters	$0.0026\ h_{70}^{-1.5}$	$0.0044\ h_{70}^{-1.5}$	$0.0014\ h_{70}^{-1.5}$	A
7a. Warm plasma in groups	$0.0056\ h_{70}^{-1.5}$	$0.0115\ h_{70}^{-1.5}$	$0.0029\ h_{70}^{-1.5}$	B
7b. Cool plasma	$0.002\ h_{70}^{-1}$	$0.003\ h_{70}^{-1}$	$0.0007\ h_{70}^{-1}$	C
7′. Plasma in groups	$0.014\ h_{70}^{-1}$	$0.030\ h_{70}^{-1}$	$0.0072\ h_{70}^{-1}$	B
8. Sum (at $h = 70$ and $z \simeq 0$)......	0.021	0.041	0.007	...
		Gas components at $z \approx 3$		
9. Damped absorbers	$0.0015\ h_{70}^{-1}$	$0.0027\ h_{70}^{-1}$	$0.0007\ h_{70}^{-1}$	A−
10. Lyα forest clouds	$0.04\ h_{70}^{-1.5}$	$0.05\ h_{70}^{-1.5}$	$0.01\ h_{70}^{-1.5}$	B
11. Intercloud gas (He II)	...	$0.01\ h_{70}^{-1.5}$	$0.0001\ h_{70}^{-1}$	B
		Abundances of:		
12. Deuterium	$0.04\ h_{70}^{-2}$	$0.054\ h_{70}^{-2}$	$0.013\ h_{70}^{-2}$	A
13. Helium	$0.010\ h_{70}^{-2}$	$0.027\ h_{70}^{-2}$	...	A
14. Nucleosynthesis	$0.020\ h_{70}^{-2}$	$0.027\ h_{70}^{-2}$	$0.013\ h_{70}^{-2}$	...

[a] Confidence of evaluation, from A (robust) to C (highly uncertain).

WHIM

$T \sim 10^{5\text{-}7}$K

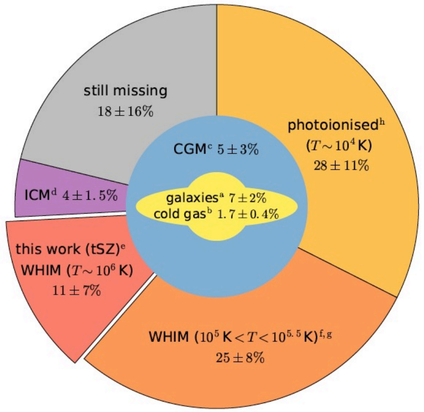

de Graaff+ 19

Locating Missing Baryon

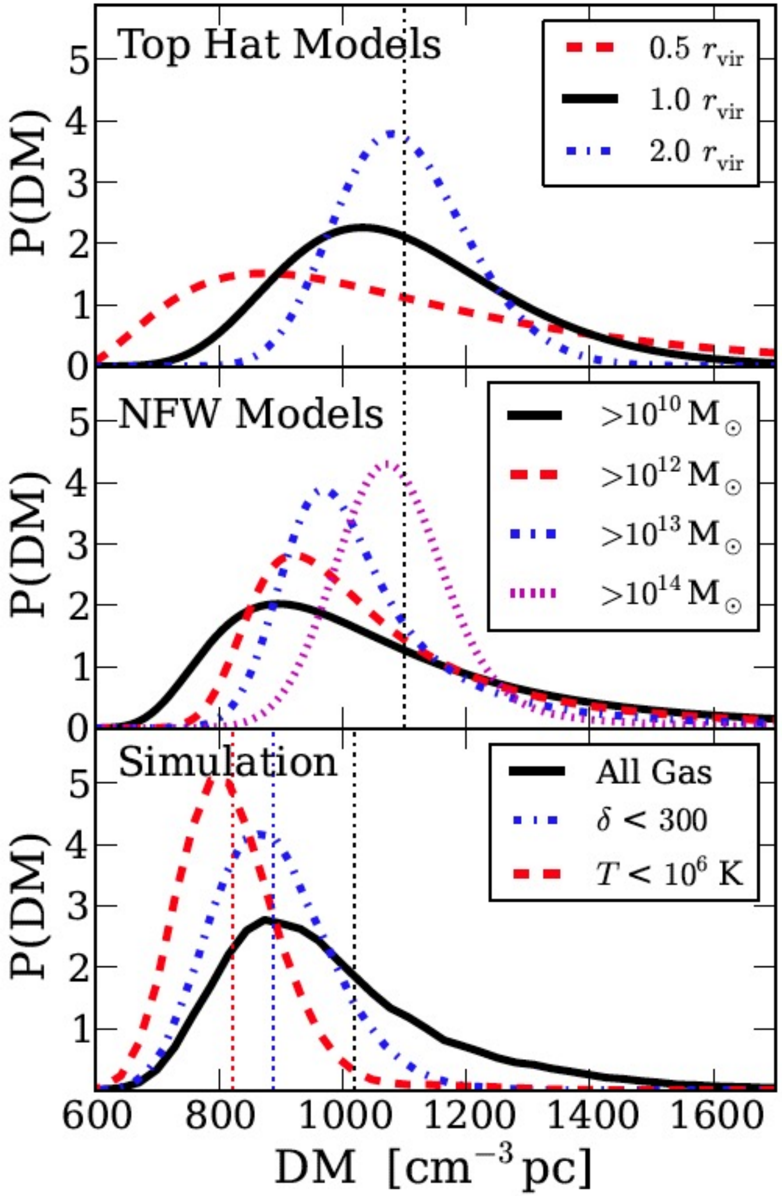

Half of baryon is missing
DM is sensitive its distribution

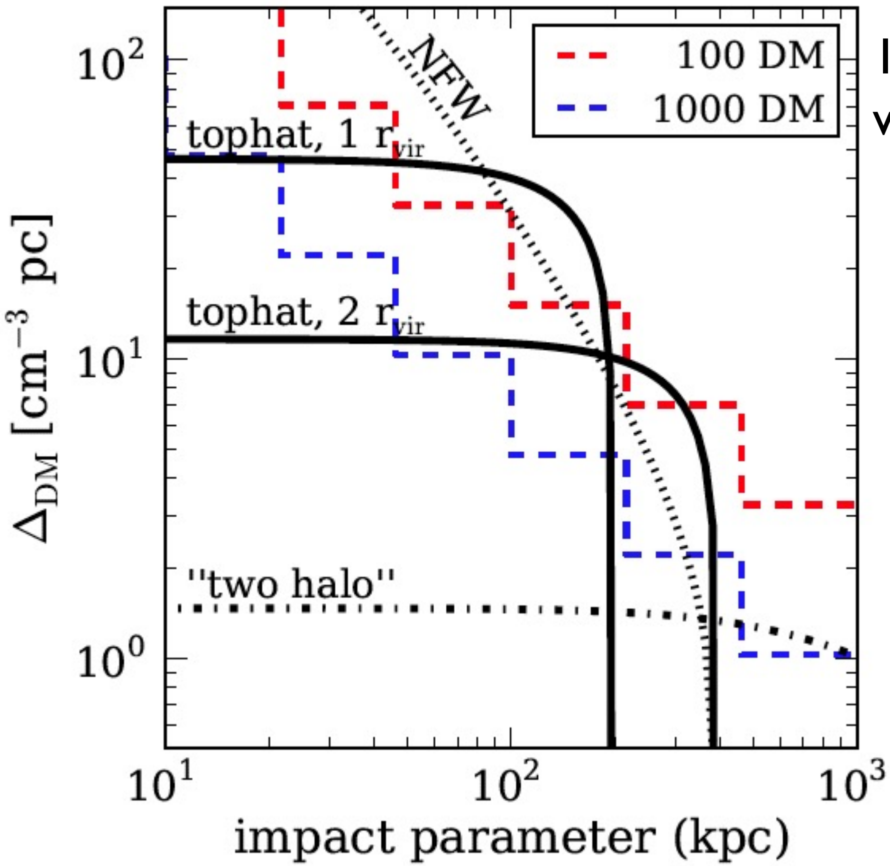

1σ error
w/ stacking

McQuinn 13